

DEVELOPMENT OF A PERFORMANCE-BASED TEST METHOD FOR  
QUANTIFICATION OF CRACKING POTENTIAL IN ASPHALT PAVEMENT  
MATERIALS

BY

AHMAD KHALED EL KHATIB

THESIS

Submitted in partial fulfillment of the requirements  
for the degree of Master of Science in Civil Engineering  
in the Graduate College of the  
University of Illinois at Urbana-Champaign, 2016

Urbana, Illinois

Adviser:

Professor Imad Al-Qadi

## Abstract

With the increasing use of recycled materials in the construction of roadways, it is more critical now than ever to understand the impact that these materials have on pavement behavior and performance. Since recycled materials tend to, in general, behave in a more brittle fashion, a primary area of concern is increased cracking potential. There is a need for a performance-based approach to quantifying the cracking potential of asphalt mixtures, specifically those with high amounts of recycled content. This study aimed to first, characterize the impact of using various proportions of recycled materials in asphalt mixtures, and second, develop a testing protocol to quantify their cracking potential in a way that is scientifically meaningful and economically practical, while ensuring correlation to independent testing. A characterization of varying amounts of recycled content displayed a general trend of increased susceptibility to cracking as recycled content increased. It was determined that low-temperature testing was not capable of sufficiently distinguishing between these various materials. A practical test method, the Illinois Flexibility Index Test (I-FIT), was developed, and found to appropriately distinguish between variations in mix design and characteristics. The I-FIT method is a modification of the semicircle bending beam (SCB) test; the modification includes the testing temperature, the loading rate, and the analysis of test data to calculate a developed parameter titled the Flexibility Index.

## Acknowledgments

I would like to express the deepest and sincerest gratitude and appreciation to Khaled El Khatib and Sahar Moursi, two parents who tirelessly sacrificed comfort, dreams, and aspirations to see this finished product. I am anything I am because of their love and dedication to give their children a better life than theirs. No colleague or friend can express love and sacrifice in the same way a parent does for their child. I thank my father who left behind a promising career in accounting and a familiar life overseas for odd jobs here in America to give his kin a better life. I thank my mother who has dedicated every moment of her existence to the happiness of her children. In her perseverance and defiance of all challenges that face her, in her pursuit of higher education as a working mother, and in her commitment to a lifetime of education, I find my inspiration. I thank the both of them for taking every hardship head on together, hand in hand, always with dignity and grace.

I would also like to express gratitude to my advisor and mentor, Professor Imad Al-Qadi, for his guidance and support. I hold him in the highest regard, both professionally and personally, for the way he conducts himself. There are often shortcuts and questionable paths that one encounters in their career, but Professor Al-Qadi has always taught by example to take the path of honor and integrity. I am fortunate to benefit from the mentorship of an individual who has climbed so high up the ladder of accomplishment. There have been fewer times in my journey of life that I have learned so much about myself and others than during my time as his student and for that I will always be grateful.

As Professor Al-Qadi provided guidance, Dr. Hasan Ozer provided daily feedback and assistance. I am thankful to have had a mentor in him so available for any issue that arose, always handling everything with patience and poise. Dr. Ozer elevated my intellect and challenged me to think about the research in different ways. From him I learned to be methodical and meticulous. Efficient and strategic. He is to be given credit for creating a nurturing yet engaging environment at the Illinois Center for Transportation where students are encouraged to maximize their potential.

I'd also like to thank my wife, in whom I found comfort during long and sleepless nights. Always, she is there to cheer me on. Her continued support was my fuel through the last moments of this race.

Last, but not least, my siblings, in whom I always found companionship. My dearest sister, generous with both her time and compassion, and my brother, from whom I learned to pursue my passions fully.

# Contents

1.	Introduction .....	1
1.1	Background.....	1
1.2	Research Need .....	3
1.3	Objective and Scope .....	3
1.4	Impact of Work.....	4
2.	Literature Review .....	5
2.1	Characterization Tests of Asphalt Concrete with Recycled Content .....	5
2.1.1	Complex Modulus.....	5
2.1.2	Permanent Deformation .....	6
2.1.3	Fatigue Cracking .....	7
2.1.4	Thermal Cracking.....	9
2.2	Summary .....	13
3.	Mix Designs and Material Preparations .....	15
3.1	Asphalt Mixtures .....	15
3.1.1	Laboratory Designed Mixes .....	15
3.1.2	Plant-Produced Mixes .....	18
3.2	Research Methodology .....	19
4.	Experimental Program.....	21
4.1	Complex Modulus.....	21
4.2	Push-Pull.....	21
4.3	Semi-Circular Bending Beam .....	22
4.3.1	Classical Semi-Circular Bending Beam Test (SCB).....	22
4.3.2	Variable Rate Semi-Circular Bending Beam Test (VR-SCB).....	23
4.4	Disc-Compact Tension Test (DCT).....	24
4.5	Texas Overlay Test.....	24
5.	Results and Analysis .....	26
5.1	Push-Pull.....	26
5.2	Low-Temperature SCB.....	27
5.3	Low-Temperature DCT .....	29

5.4 Texas Overlay .....	30
5.5 Variable Rate SCB .....	31
5.5.1 Rate Effect.....	33
5.5.2 Secondary Considerations.....	37
5.6 Summary .....	43
6. Development of Flexibility Index.....	45
6.1 Candidate Parameters.....	45
6.2 Correlation to Crack Velocity.....	48
6.3 Implementation of Selected Index.....	51
6.4 Summary .....	53
7. Conclusions and Recommendations .....	54
References.....	56
Appendix A: Laboratory Mix Designs .....	59
Appendix B: Plant Mix Designs.....	72
Appendix C: IL-SCB Results .....	81

# 1. Introduction

## 1.1 Background

There is a global push for the inclusion of more “green” construction practices. One common approach in the pavement community is the reuse of construction materials. Incorporation of recycled content into new mixtures results in reduced demand for virgin aggregate and binder. The cost savings associated with this reduction are often paired with reduced material transportation and waste disposal costs, resulting in potentially significant reduction of construction cost.

Recycled content in hot-mix asphalt (HMA) can be broken down into components such as Reclaimed Asphalt Pavement (RAP), Recycled Asphalt Shingles (RAS), steel slag, and crumb rubber. In the state of Illinois, recycled content is being used in increasing quantities. From the year 2012 to 2013, Illinois has seen a 43% increase in recycled tonnage used. The state of Illinois used 1,731,296 tons of reclaimed and recycled materials in 2013, approximately four times as much as that in 2009. The use of RAS in AC paving increased 221% from 2012 to 2013. This surge in the use of recycled content originated in the 1970’s during the Arab oil embargo, where oil prices (and consequently asphalt binder prices) increased significantly. To mitigate this rise in material cost, the National Cooperative Highway Research Program (NCHRP) began to conduct and publish research regarding the use of recycled content in AC. The publication of *Recycling Materials for Highways* in 1978, followed by *Guidelines for Recycling Pavement Materials* in 1980 among many other publications aimed to guide agencies in the inclusion of recycled content in their AC design (Copeland, 2011).

This motivation to rely on sustainable, recycled sources was supported by the availability of these materials. Approximately 71.9 million tons of RAP was used in the construction of AC in the year 2014, translating to a 28% increase from 2009, an an 8% increase from 2013 (Hansen & Copeland, 2014). Every year in the United States, approximately 11 million tons of asphalt shingles are created as waste. The majority of this waste is generated by shingles removed from roofing for replacement. It is estimated that RAS in the form of waste compromise approximately 8% of the building-related waste stream and 10% of construction-generated waste (“Asphalt Shingles Manufacturing & Waste Management in the Northeast Fact Sheet,” 2012). It is estimated that in 2014, an approximate 2 million tons of shingles were used in pavement construction, a 20% increase from the 1.6 million tons used in 2013 (Hansen & Copeland, 2014).

Recycled Asphalt Pavement, as the name indicates, is milled directly from existing pavements. Recycled shingles come from two primary sources: tear-off from roofing and discarded material from shingle manufacturing. Recycled asphalt pavement can display significant material variability. Processing of recycled asphalt pavement includes an initial screening to separate material into more consistent sizes. Typically, the objective is to separate materials into coarse and fine piles. If needed, there is often additional crushing in order to increase consistency in size (Copeland, 2011). Recycled asphalt shingles in the form of manufacturing salvage are taken from the manufacturer source to a processing facility and ground to appropriate sizes. Quality control for this source of RAS consists of gradation testing and asphalt content determination. In the case of tear-off shingles, they must first be inspected for asbestos at an inspection rate of two samples per 250 tons of material. Upon testing negative for asbestos, the RAS is then cleaned to reduce unusable material content to 0.5%. At this point, the same process for manufacturer-salvaged RAS is followed which consists of grinding material down to a specified gradation and performing washed-gradation and asphalt content checks every 250 tons. Because of differences in the handling process as well as differences in gradations and binder contents, manufacturer-salvaged shingles and tear-off shingles must be processed and stored separately until they are ready for use in pavement applications (Lippert and Brownlee, 2012).

The availability of RAP and RAS can be converted into significant material cost savings. Considering the 71.9 million tons of RAP used in pavement construction in 2014 and assuming an average 5% liquid asphalt content in the RAP sources, this translates into roughly 3.6 million tons of asphalt liquid saved. Additionally, this RAP translates into an approximate 68 million tons of virgin aggregate saved. The 2 million tons of RAS used in 2014 translate into 400,000 tons of asphalt liquid and 982,000 tons of virgin aggregate saved, assuming an average liquid content of 20% in RAS sources. These material savings from both RAP and RAS result in roughly \$2.8 billions of savings (Hansen & Copeland, 2014).

A more comprehensive approach to the evaluation of cost savings, Life Cycle Cost Analysis (LCCA), takes into account both initial cost of construction as well as agency and user costs (such as maintenance and rehabilitation) for the duration of the pavement's life. A comparison of virgin mixtures with mixtures containing 30% and 40% RAP indicated a total savings of 19% and 30-36%, respectively.

In a LCCA case study performed by Qazi (2014), a 1.6-km lane pavement section at the intersection of Lincoln Avenue and I-74 in Urbana, IL was examined. Binder courses of varying amounts of RAP (0%, 30%, 40%, and 50%) were used. LCA analysis was performed using *RealCost 2.5*, the FHWA's LCCA software. Table 2 presents a breakdown of agency cost:

**Table 1: Agency cost breakdown of AC with increasing amount of RAP, assuming a consistent performance**

	Mix with 0% RAP	Mix with 30% RAP	Mix with 40% RAP	Mix with 50% RAP
<b>Initial construction cost/km</b>	\$360,595	\$325,613	\$313,953	\$302,292
<b>Maintenance cost/km</b>	\$127,501	\$127,501	\$127,501	\$127,501
<b>Total agency cost/km</b>	\$488,096	\$453,114	\$441,454	\$429,793

Table 2 shows a reduction in the initial construction cost as the amount of RAP increases in the pavement. Assuming maintenance cost is constant (which is most likely not the case), implying that all pavements are performing at the same level, the initial construction cost comprises approximately 70-74% of the total agency cost (Aurangzeb, 2014).

## 1.2 Research Need

As the usage of RAP and RAS is increased in the state of Illinois, throughout the United States, and worldwide, there is concern that the inclusion of adding recycled content may impact mixture performance. In order to ensure that using more sustainable materials does not impact AC performance, there must be an effort to characterize the effect that recycled content has on AC performance. To quantify the effect on AC performance, a testing protocol must be developed. Current practices are expensive, time consuming, and it is suspected that they do not sufficiently and accurately characterize the impact of additional recycled content in asphaltic mixtures. Thus, there is a need to further develop a more optimal testing protocol that accurately characterizes a material's resistance to the primary failure distresses in asphalt pavements.

## 1.3 Objective and Scope

The objective of this study is to investigate the impact of recycled content on asphalt mixture behavior culminating in the development of a testing protocol to predict the performance of AC in the field. The final product is intended to be a testing specification that will be implemented in the state of Illinois in order to predict the cracking potential of various asphalt mixtures with minimal disturbance to contractors and industry professionals. In line with this objective, an expansive experimental program was executed using a variety of asphalt mixtures prepared in the lab, asphalt plants, and field that cover a wide spectrum of asphalt mixture properties



## 1.4 Impact of Work

Given the aforementioned trends towards the increased usage of recycled materials, especially RAS and RAP, understanding the affect that these materials have on asphalt mixture behavior is desired. The significant potential for cost savings in the use of RAS and RAP has already been known. On top of this, there are environmental benefits to reusing these materials in place of virgin materials. However, the impact of these materials on asphalt mixture performance is still not clear. This study aims to provide the information and tools to maximize the responsible usage of recycled content in asphaltic mixtures by delivering the following:

1. An investigation of the current efforts to characterize asphalt mixtures with recycled content and an exploration of their effectiveness.
2. An identification of the shortcomings of relevant and current asphalt material characterization practices and a development of a testing protocol to identify cracking potential that addresses and improves upon these shortcomings.
3. An extensive exploration of adding recycled content to asphalt mixtures and the impact that this addition has on mixture properties through a detailed experimental program.
4. Design laboratory mixtures with high amounts of recycled content and making recommendations to improve the development of similar mix designs.

## 2. Literature Review

This chapter discusses a summary of literature compiled from the studies conducted to characterize laboratory performance of asphalt mixtures with recycled content. This chapter aims at introducing conventional test methods used in characterization of asphalt mixtures commonly used for evaluating the effect of RAP and RAS while discussing significant outcome and changes in the performance characteristics with RAP and RAS.

### 2.1 Characterization Tests of Asphalt Concrete with Recycled Content

#### 2.1.1 Complex Modulus

A primary input into the Mechanistic Empirical Pavement Design Guide (MEPDG), complex modulus, is becoming increasingly recommended for characterization of asphaltic mixtures due to its effectiveness in comparing different mixtures (Witczak et al. 2002; Carpenter 2007; Vavrik et al. 2008; Ye et al. 2009; Braham et al. 2011; Ozer et al. 2012).

Complex modulus testing is conducted in accordance with AASHTO TP62-03. Specimens are tested under temperature and frequency sweeps under stress-controlled loading. Testing is conducted on cylindrical specimens of 100 mm (3.94-in) diameter (cored from a 150 mm [5.9 in] diameter cylinder) and 150-mm (5.91-in) height. Microstrain values are limited between 50 to 150 microstrains. Strain readings are collected using strain gauges placed around the specimen's circumference. Testing is conducted at temperatures of  $-10^{\circ}\text{C}$  ( $14^{\circ}\text{F}$ ),  $4^{\circ}\text{C}$  ( $39^{\circ}\text{F}$ ),  $21^{\circ}\text{C}$  ( $70^{\circ}\text{F}$ ),  $37^{\circ}\text{C}$  ( $99^{\circ}\text{F}$ ), and  $55^{\circ}\text{C}$  ( $131^{\circ}\text{F}$ ) and frequencies of 25, 10, 5, 1, 0.5, and 0.1 Hz. Obtained modulus values can then be used to produce a complex modulus master curve.

Research shows that the addition of RAS and RAP significantly impacts the complex modulus of asphalt materials. Ozer et al. (2012) evaluated plant mixtures with varying amounts of RAP and RAS and found that modulus increases with increasing RAS content at high testing temperatures and low frequencies. Higher RAS mixtures also exhibited flatter master curve slopes, an indication of deteriorating relaxation properties.

Additional research conducted by Swamy et al. (2011) and Al-Qadi et al. (2012) showed that the addition of RAP to asphalt mixtures increases complex modulus. Asphalt mixtures with varying amounts of RAP from 0% to 50% were tested and AC with higher RAP displayed higher complex modulus, indicating the presence of aged asphalt binder.

### 2.1.2 Permanent Deformation

There are two primary performance characterization tests that are used to indicate a mixture's susceptibility to permanent deformation or rutting: the Hamburg Wheel Track test (WTT) (AASHTO T324-11) or the uniaxial flow test (AASHTO TP 79). Loading in both test setups is intended to simulate permanent deformation accumulation as a result of cyclic loading.

The Hamburg WTT, also used to characterize material resistance to moisture damage, is conducted by repeatedly running a steel wheel in a linear path over AC specimens. The steel wheel is of a 203.2-mm (8.0-in) diameter and a 47.0-mm (1.85-in) width and loads specimens with a loading of  $705.0 \pm 4.5$  N ( $158.0 \pm 1.0$  lb). Wheel speed is 0.305 m/s (1 ft/sec) and the specimen experiences  $52 \pm 2$  passes/min. Specimens are fixed with gypsum into molds and tested in a water bath at a temperature of 50°C (122°F) using the procedure dictated by AASHTO T324-11.

Al-Qadi et al. (2012) showed, testing a variety of N90 asphalt mixtures between 0% and 50% RAP under the WTT, that the addition of RAP increased resistance to rutting. These results were supported by findings of Xiao et al. (2007), which were drawn from testing of rubberized asphalt mixtures including RAP under a loaded wheel tester.

The uniaxial flow test is run on a cylindrical asphalt specimen of 100-mm (3.94-in) diameter (cored from a 150-mm [5.91-in] diameter cylinder) and 150 mm (5.91-in) height. Haversine loading is applied for 0.1 sec and the specimen is allowed for rest for 0.9 sec. Strain is measured at the end of every rest period by measuring axial deformation from attached strain gauges. The flow number, the primary parameter of interest in this test, is considered to be the minimum rate of change in the axial strain for the duration of the test.

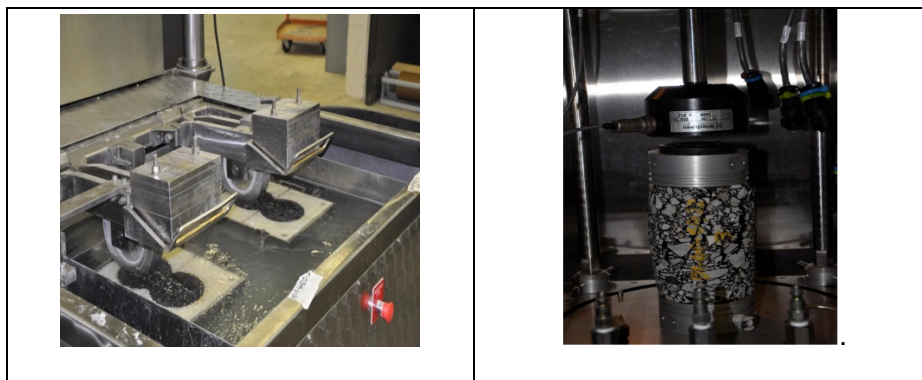


Figure 1. Laboratory tests used in rutting evaluation of asphalt mixtures: Hamburg wheel tracker (left) and flow number test (right)

Apegyei et al. (2011) tested asphalt mixtures with varying amounts of RAP under the flow number test setup. Mixtures tested were designed with 0% to 25% RAP. Researchers found that the addition of RAP to mixtures decreased the rutting resistance. However, this finding may have been due to the binder grade bumping in mixtures with higher RAP content. This suspicion is supported by findings of Andy et al. (2010), where various mixtures of varying levels of both RAP and RAS were prepared and placed in field. Field performance and lab performance data was collected, indicating an increase in flow number or, indirectly, in rutting or permanent deformation resistance with higher amounts of recycled content (RAP and RAS).

### **2.1.3 Fatigue Cracking**

Fatigue cracking is a primary concern with the use of recycled content in asphaltic mixtures. It is suspected that the addition of recycled content may have adverse impacts on the fatigue performance of asphalt mixtures. This hypothesis suggests that high stiffness and poor relaxation properties of mixes with RAP and RAS can cause faster crack initiation and propagation.

The Texas Overlay Test (TOL) is a fatigue test intended to indicate the reflective cracking potential of asphalt mixtures. Developed by Robert Lytton in the 1970s, this test is anteceded to simulate the opening and closing of joints or cracks in order to determine crack initiation and propagation potential (Zhou 2005). Specimens are subject to displacement-controlled cyclic loading at 25°C (77°F) with opening displacements of 0.635 mm (0.025 in) and loading frequencies of 1 Hz. The primary parameter of interest is the number of cycles to failure.

The push-pull test is used to characterize fatigue cracking resistance of various materials. Developed by Kim and colleagues at North Carolina State University, the test loads specimens with similar geometry to the aforementioned complex modulus test in cyclic tension and compression. Testing is conducted at 21°C (70 °F). Specimens are fixed to steel plates at the top and bottom as shown in Figure 2. Loading is applied at a frequency of 10 Hz. Strain levels are varied from 200 to 300 microstrains. Three axial Linear Variable Displacement Transducers (LVDTs) are placed 120° apart around the radius of the specimen. Various criteria such as a 50% reduction in modulus have been used to determine specimen failure. Crack initiation is desired towards the midway point of specimen height. The primary parameter of interest is cycles experienced until failure (Kim et al., 2008).

McDaniel et al. (2011) tested asphalt mixtures with 0%, 15%, 25%, and 40% RAP content under the push-pull configuration and concluded that RAP content significantly improves AC fatigue life. In

contrast, Ozer et al. (2012) tested AC with RAS content varying from 2.5% to 7% under the same push-pull setup and concluded that the addition of RAS significantly decreased the AC fatigue life. Slight improvement in the fatigue life of these AC mixtures was observed with the use of a softer binder.

The Flexural Beam Fatigue test is a 4-point bending test used to simulate the fatigue performance of asphalt pavements under repeated traffic loading. A rectangular asphalt specimen of dimensions 15 mm x 2 mm x 2.5 mm (380 in x 50 in x 63 in) is subjected to repeated loading between with a loading frequency of 0.1 Hz to 10 Hz at a fixed microstrain level. The specimen is clamped at 4 points along its length. Primary parameters of interest are cycles to failure (which usually occurs at the middle of the beam), dissipated energy due to mechanical loading and damage accumulation.

Aurangzeb et al. (2012) concluded that the addition of RAP to mixtures improves fatigue life when tested under the Flexural Beam Fatigue setup. Mixtures tested with RAP content ranged from 0% to 50%. The same trend was observed by Tabaković et al. (2010) when testing asphalt mixtures with RAP content ranging from 10% to 30%. However, Xiao et al. (2013) and Williams et al. (2011) tested asphalt mixtures with varying amounts of recycled content and could not discern an obvious trend in fatigue life with the increase of recycled content.

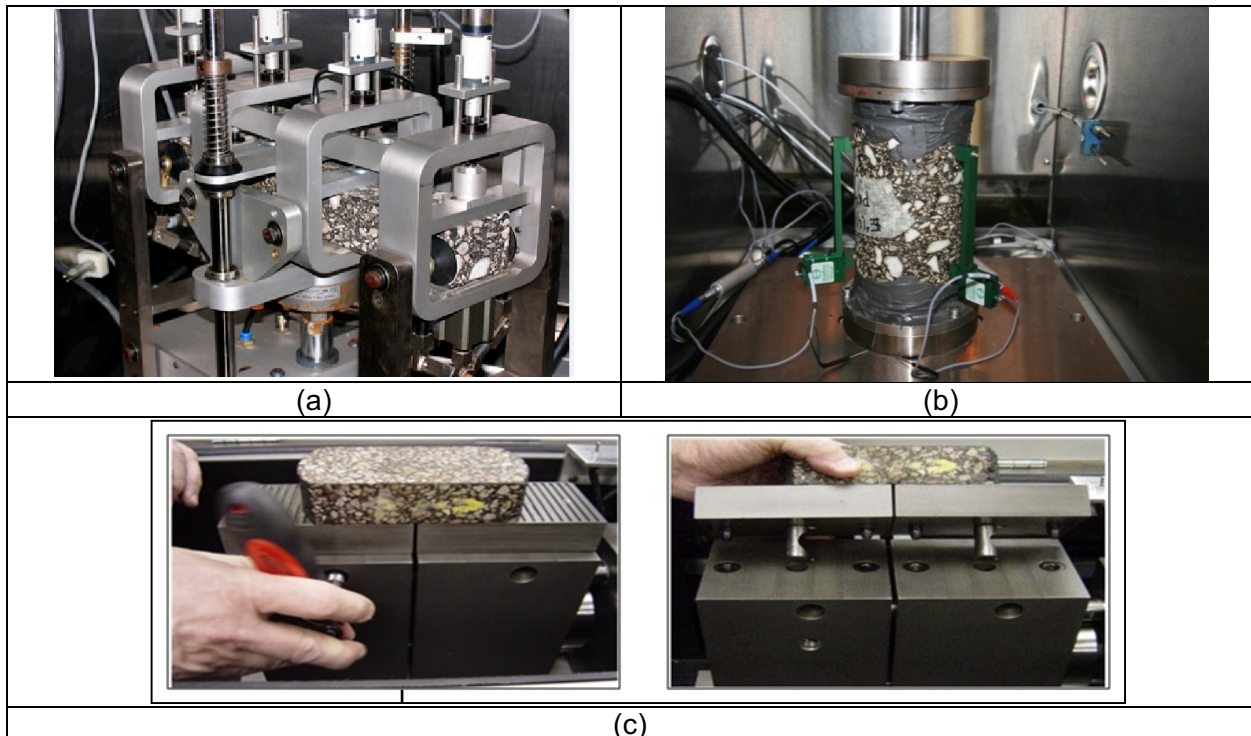
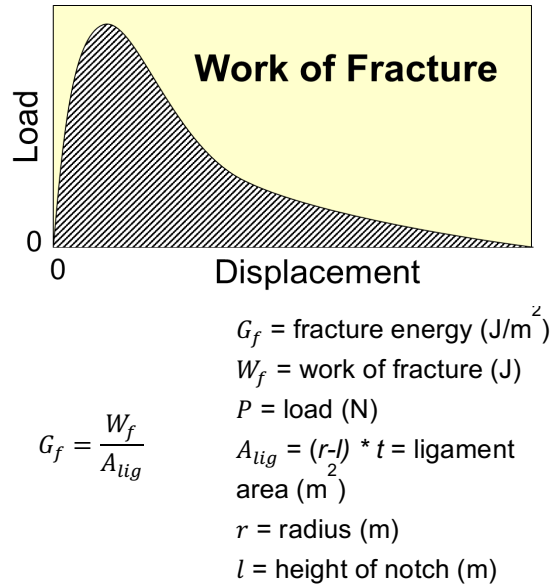
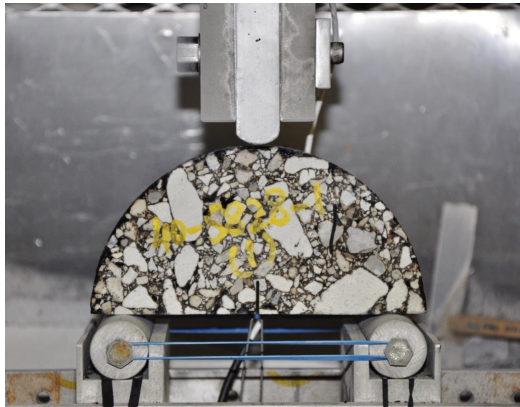


Figure 2. Test setups commonly used for fatigue performance evaluation of asphalt mixtures: (a) Four-point beam fatigue apparatus; (b) Push-Pull test; (c) Texas overlay tester

#### 2.1.4 Thermal Cracking

The replacement of virgin binder with oxidized recycled binder is believed to significantly increase thermal cracking potential in asphalt materials. Marasteanu's Semi-Circular Bending Beam test (SCB) and the Disc-Compact Tension test (DCT) are commonly used tests used to characterize thermal cracking potential of asphalt materials.

The classical SCB test method is a 3-point bending test typically run at low temperatures (PG lower limit + 10°). Specimens are of a 75-mm (3-in) radius and a 50-mm (2-in) thickness. A 1.5 mm (0.06 in) notch is machined in the bottom center of the specimen, extending upwards 15 mm (0.6 in). The primary parameters extracted from this test are the fracture energy (Gf) and peak load. The fracture energy is defined as the amount of energy required to propagate a crack for a unit area and is typically expressed in joules per meter squared. Displacements are obtained by recording the crack mouth opening displacement (CMOD) using a clip-gauge extensometer or an extensometer measuring the load-line displacement. Stable crack growth conditions are ensured during the test. The SCB fixture is illustrated in Figure 3 along with a typical outcome of an SCB test and fracture energy calculation method. In general, the SCB is a simple, low-cost test that easily can be performed on the cylindrical samples obtained from standard cores prepared in the Superpave Gyrotory Compactor (SGC) or taken from the field. The test method is published in an AASHTO provisional specification (AASHTO TP 105-13). This test method requires a displacement control in two phases after the application of a 0.3 + 0.02 kN (67.5 + 4.5 lb) sitting load: first, the specimen is loaded to a load of 1 + 0.1 kN (224.8 + 22.5 lb) in stroke displacement control at a displacement rate of 0.06 mm/min (.00004 in/sec), and second, the test switches to CMOD displacement control and the specimen is loaded at a displacement rate of 0.03 mm/min (0.00002 in/sec) to failure, which is defined as a drop to 0.5 kN or a specified CMOD opening.



**Figure 3. Semi-circular bending beam test fixture and typical outcome from this test to calculate fracture energy**

Research conducted by Li et al. (2008) and Cascione et al. (2010) using the SCB test concluded that fracture energy decreases with the increase in recycled content, whether RAS or RAP. However, Cascione et al. (2010) also showed that mixtures with both RAP and RAS display higher fracture energy than mixtures with exclusively RAS.

Researchers at Louisiana State University tested 11 field-sampled mixtures under the Hamburg Wheel Track test and Louisiana SCB test method. Mixtures tested varied in PG binder grade and included grades of PG64-22, PG70-22M, PG76-22M, and PG82-22CRM (crumb-rubber modified). Experimental results indicated an increase in rutting resistance with an increase in PG grading. Additionally, the calculated J-integral of AC mixtures increased as the binder stiffness increased, indicating an increase in fracture resistance according to the Louisiana SCB method with the exception of the PG82-22 crumb rubber modified binder. It was concluded that the polymer modification of asphalt binder, such as with the PG76-22M binder improved rutting resistance and J-integral values (Cooper, et al., 2014).

Researchers at California State University conducted fatigue beam tests and Louisiana SCB tests on two AC mixtures at 20°C (68°F) under both dry and wet conditions. The AC mixture's PG grade was varied from PG64-10 to PG58-22. It was concluded that the softer binder (PG58-22) displayed a lower J-integral value. Specimens tested under the wet condition resulted in lower J-integral values than those tested under the dry condition. Fatigue beam test results indicated that the softer PG58-22 binder performed better than the PG64-10 binder. As with the Louisiana SCB test results, specimens

conditioned to the wet condition displayed lower fatigue life than those tested under the dry condition. In regards to correlation between the Louisiana SCB method and the fatigue beam test results, the correlation was at  $R^2$  value of 60% (Saadeh and Eljairi, 2011).

In another study, two AC mixtures with varying binder content (4.4% and 5.4%) were tested under a single-notch length SCB test method at a displacement rate of 1 mm/min (0.0007 in/sec). Specimens were tested at a temperature of 10°C (50°F), 0°C (32°F), and -10°C (14°F). Under this experimental matrix, it was observed that strength decreased as the percent of binder content increased. Furthermore, maximum strain increased with an increase in binder content, indicating an increased resistance to cracking. Generally, fracture energy increased with an increase in binder content and decreased with a decrease in temperature. Mixture strength increased with a decrease in temperature and finally, maximum strain decreased with a decrease in temperature (Biligiri, et al., 2012).

An experimental matrix of 29 AC mixtures was conducted with the intention to explore any potential for correlation to field performance using Louisiana SCB and Indirect Tensile test (IDT). Results from the Louisiana SCB correlated to Toughness Index results with an  $R^2$  value of 32%. In general, J-integral values were higher for AC than warm-mix asphalt. The effect of aging was found to have a statistically significant impact on the Louisiana SCB J-integral method with inconsistent trends. However, the effect on tensile strength and Toughness Index was found to be consistent the aging had a statistically significant impact on tensile strength of asphalt mixtures. The J-integral parameter was found to be insensitive to small variations in RAP content with inconsistent trends resulting from an increase in RAP. In terms of field performance correlation, researchers found the correlation between cracking rates calculated from field surveying and the J-integral, was at  $R^2$  value of 58%.

Kansas State University conducted a study on various mixtures that increased the RAP percentage from 20% to 30% to 40% and varied between three different RAP sources. Specimens were tested under the Louisiana SCB test method at 25°C (77°F). It was found that as the RAP percentage increased, mixture strength increased. On the other hand, as the RAP content increased, ram displacement at maximum load both decreased and increased. Furthermore, it was found that the variation of RAP sources had a significant impact on the cracking resistance of asphalt mixtures (Ahmed, et al., 2015).

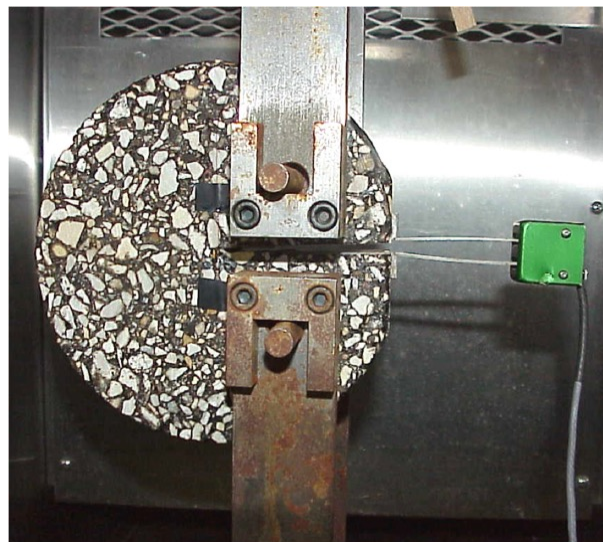
In a recent study, researchers examined various candidate tests for characterization of fracture resistance of asphalt materials. Test candidates were the IDT test, the Overlay Test, the SCB test, and the DCT test. The Texas overlay Test was used as the benchmark test method. Three mixtures were



evaluated, ranked by researchers in order of crack resistance as “Marginal”, “Good”, and “Very Good”. The IDT test, using an index titled the “FE Index” was determined to be the most promising test method serve as a surrogate cracking test (Walubita et al., 2014).

Similar to the SCB test, the DCT is conducted by propagating a crack through a notched specimen under displacement-controlled tensile loading. Arms are inserted into dual openings cored into the circular specimen and these openings are pulled apart at a rate of 1.00 mm/min (0.0007 in/sec) measured from the CMOD displacement. Unlike the SCB, loading is applied in the vertical direction while the crack propagates horizontally into the specimen. Data is collected in the same method as that of the SCB and the primary parameters of interest are identical ( $G_f$ , peak load, etc.) The DCT test setup is shown in the Figure 4.

Findings were presented by Behnia et al. (2012), who tested asphalt mixtures with 0% and 50% RAP under the DCT test and found that fracture energy decreases with the increase in RAP content.



**Figure 4. DCT specimen loaded in testing fixture with CMOD clip gauge for displacement readings**

The IDT is also used to characterize fracture properties of asphalt mixtures (Roque et al. 2004). The 150 mm (6 in) diameter gyratory specimens are cut into thickness of 25.4 mm (1 in). A circular hole with 8 mm (0.3 in) diameter at the center of the specimen is drilled for cracks to initiate and propagate. The typical IDT setup requires a servo hydraulic closed-loop testing machine capable of axial compression.

The specimen is typically loaded diametrically in compression and this indirectly induces horizontal tensile stresses in the middle zone of the specimen that ultimately causes cracking. For the evaluation of the tensile properties of the AC, the permanent deformation under the loading strip is undesirable (Huang et al., 2005). Therefore, the compressive load is distributed using loading strips, which are curved at the interface to fit the radius of curvature of the specimen. Typical test temperatures range from -20°C (-4°F) (Buttlar et al., 1996) to 25°C (77°F) (Huang et al., 2005). The data captured during IDT testing include time, applied load and horizontal and vertical specimen deformation.

McDaniel et al. (2012) tested asphalt mixtures with 0% and 40% RAP content under the IDT test. Even with binder grade bumping to accommodate for the addition of 40% RAP, it was concluded that strength and stiffness increase with the addition of recycled content.

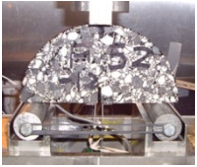

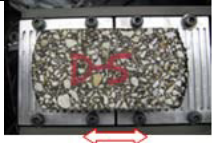

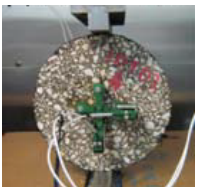
## 2.2 Summary

A brief summary was presented of standard and non-standard asphalt mixture test methods used commonly in characterizing the materials, including the effects of RAP and RAS. Table 2 presents a summary of cracking test methods introduced in this chapter along with advantages and disadvantages with respect to the objectives of this study. After exploration of the conventional fracture tests presented in Table 2, a set of criteria was formulated to define the philosophy behind the selection of a suitable test:

- Meaningful spread of
- Feasibility and cost effectiveness
- Correlation to independent tests
- Correlation to field performance

Semi-circular bending (SCB) and Disc-compact tension (DCT) test were further considered. The parameter extracted from these tests, the fracture energy, is a fundamental fracture property and was thus believed to have potential in characterizing fracture resistance. These two methods both involve simple specimen preparation. However, the SCB test can be implemented practically on relatively inexpensive equipment and requires simple operation, as opposed to the DCT method. For this reason, the SCB was selected as a candidate test method. This was the basis for the research approach moving forward. Alternate tests, such as the DCT, were still explored, and additional tests like the complex modulus, push-pull and the Texas overlay tests were included for comparison.

**Table 2: Laboratory Cracking Test Methods (Al-Qadi et al., 2015)**

Test Type	Purpose	Specimen Dimensions	Specimen Preparation	Test Output	Pros/Cons
<p><b>Semi-circular bending (SCB)</b></p> 	Cracking resistance	6 in (Ø) 3 in (H) 2 in (T)	Notching required = 0.6 in; External LVDTs optional	Fracture energy from load-displacement curve, peak load, critical displacement	<i>Inexpensive device;</i> <i>Relatively easy specimen fabrication;</i> <i>Easily-obtained field specimens;</i> <i>Two specimens per core or slice;</i> <i>Simple three-point bending load representing field bending</i> Smaller ligament area
<p><b>Disc-compact tension (DCT)</b></p> 	Cracking resistance	6 in (Ø) 5.7 in (H) 2 in (T)	Notching required = 2.46 in; Extensometer required	Fracture energy from load-displacement curve, peak load, critical displacement	<i>Direct tensile mode;</i> <i>Easily-obtained field specimens;</i> Possible breakage close to loading holes at intermediate-temperature application; Moderately expensive device
<p><b>Texas overlay (TOL)</b></p> 	Cracking (reflective) potential	6 in (L) 3 in (W) 1.5 in (T)	Gluing required; curing time needed; External LVDTs optional	Number of cycles used as measure of crack resistance	<i>Cyclic loading application;</i> High variability; No fundamental property related; Moderately expensive device
<p><b>Direct tension (DT)</b></p> 	Tensile strength, cracking resistance, & ductility potential	4 in (Ø) 4 in (H)	Gluing required; ≥ curing time; External LVDTs required	Tensile strain at max load used as indicator of ductility & cracking resistance potential	<i>Simple stress state;</i> Possibility of load eccentricity because of end fixtures; Difficult to obtain field specimens; Closed-loop displacement control is difficult; High variability; Moderately expensive device
<p><b>Indirect tension test (IDT)</b></p> 	Tensile strength (indirect)	6 in (Ø) 2 in (T)	External LVDTs required	Max horizontal strain at max load & strength used as indicator of ductility & cracking resistance potential	<i>Relatively easy specimen fabrication;</i> <i>Easily-obtained field specimens;</i> <i>Tensile strength potentially related to cracking resistance</i> No fundamental property related

### 3. Mix Designs and Material Preparations

Based on the objectives of the study and the literature survey, an experimental program was designed. The experimental program contains AC mixture level testing of laboratory produced laboratory compacted, plant-produced and laboratory compacted and field cores with varying degrees of RAP and RAS. The following is a discussion of the mixtures used in this study, as well as the testing program and methods used to characterize them.

#### 3.1 Asphalt Mixtures

In this study, 11 laboratory designed mixes, 16 plant mixes and field cores from nine districts of Illinois taken from different sections were used in various levels of testing program. Discussion in this report will exclude the field core work, to be presented in a separate publication. The mixtures used were selected to provide a wide scope of exploration and the following sections discuss each category of mixtures.

##### 3.1.1 Laboratory Designed Mixes

The laboratory design mixes were designed to evaluate the effect of ABR on fracture and other critical performance related properties. The volumetrics are a critical component in determining the behavior of asphalt materials. Since the laboratory mixtures developed were a primary source of conclusions, strict control over their volumetric properties was exercised. Different mixtures were prepared by changing one variable at a time in an attempt to isolate the effect of specific parameters. The results and conclusions drawn from this study were primarily based on results of laboratory mixtures testing and validation using results derived from plant mixtures and field cores. Therefore, these mixes play a significant role in understanding the effect of different fracture parameters with higher accuracy and better control.

A matrix for laboratory mixes was developed as shown Table 3 below. The approach to selecting these mixtures and their designs was done to understand the effect of different asphalt binder replacement (ABR) content with combinations of RAP and RAS, RAS sources, RAP sources, and binder grade bumping. These AC mixtures are referred to using the convention of “L#”, where # is a placeholder for the mixture number.

**Table 3: Laboratory Designed Mixture Characteristics**

Mix ID	Mix Name	Binder Grade	RAP (%)	RAS (%)	ABR (%)	AC (%)	VMA (%)
--------	----------	--------------	---------	---------	---------	--------	---------

**Table 3 (cont.)**

<b>L3</b>	N90 0 CG	70-22	-	-	-	6.0	15.3
<b>L4</b>	N90 0 CG	64-22	-	-	-	6.0	15.3
<b>L5</b>	N90 30 CG S1 <sup>3</sup>	70-22	-	7	29.8	6.0	15.3
<b>L6</b>	N90 30 CG S1 <sup>3</sup>	58-28	-	7	29.8	6.0	15.3
<b>L7</b>	N90 20 CG S1 <sup>3</sup>	58-28	-	5	21.2	6.0	15.3
<b>L8</b>	N90 10 CG S1 <sup>3</sup>	64-22	-	2.5	10.5	6.0	15.3
<b>L9</b>	N90 30 CG S2 <sup>4</sup> AS <sup>1</sup>	58-28	11	5	30.5	6.0	15.2
<b>L10</b>	N90 60 CG S2 <sup>4</sup> AS <sup>1</sup>	52-34	40	7	60.8	6.1	15.2
<b>L11</b>	N90 0 CG AS <sup>1</sup>	64-22	-	-	-	6.0	15.3
<b>L12</b>	N90 30 CG S2 <sup>4</sup> AS <sup>1</sup>	58-28	-	7	30.6	6.0	15.2
<b>L13</b>	N90 30 CG S1 <sup>3</sup> AS <sup>1</sup>	58-28	-	7	29.8	6.0	15.3

<sup>1</sup> AS indicate mixture with 1% Anti-strip added to virgin binder

<sup>2</sup> These mixtures have different RAS sources but similar mix design

<sup>3</sup> RAS Source (S1)

<sup>4</sup> RAS Source (S2)

### 3.1.1.1 Design Philosophy

The AC mixes were designed as per Illinois modified AASHTO M 323 specifications. Target design air voids were 4.0% for all mixes while keeping VMA and total binder content constant. The total binder used in each of the mixes was kept constant to 6% (including both virgin and binder from ABR) to evaluate the effect of ABR, save for a few AC mixtures where total binder content was increased by 0.1% to maintain VMA. Due to limited variety in aggregate available for design, there were instances where the dust-AC ratio had to be violated as a result of increased fines contribution from recycled materials. The viscosity of 0.17+0.02 Pa-s is used to determine the mixing temperature and 0.28+0.03 Pa-s for compaction temperature. Viscosity determination was based on AASHTO T 316.

### 3.1.1.2 Materials Used

Different levels of ABR necessitated the usage of various kinds of binders. The binders used include PG70-22 SBS, PG64-22, PG58-28 and PG52-34.

TABLE 5 below shows the details of the aggregate materials used in the mix designs:

**Table 4: Type and Source of Aggregate Stockpiles used in the Mix Designs**

<b>Material ID</b>	<b>032CM16</b>	<b>038FM20</b>	<b>037FM02</b>	<b>004MF01</b>
<b>Producer Name (on Mix Design)</b>	Quarry Materials	Quarry Materials	Quarry Materials	Hanson (Thornton)
<b>Producer Number (on Mix Design)</b>	2298-06	2298-06	2298-06	
<b>Plant Location</b>	Hodgkins, IL	Hodgkins, IL	Hodgkins, IL	Thornton, IL
<b>Source No.:</b>	50312-78	50312-78	50970-02	50312-04
<b>Source Name:</b>	Vulcan	Vulcan	Thelan	Hanson
<b>Source Location:</b>	McCook	McCook	Antioch	Thornton, IL
<b>Type of Material</b>	Dolomite	Crushed Dolomite Sand	Natural Sand	Mineral Filler

Laboratory AC mixtures incorporated the use of RAS sampled from Southwind RAS LLC. RAS materials were acquired on different dates during the duration of the project and were identified as Source 1 and Source 2. The aggregate and binder was extracted from samples for both sources. The gradations and binder content were checked for similarity. The differences between both sources was considered during the mix design process to ensure that the target asphalt binder replacement was met. The RAP used in laboratory designed mixtures was sampled from District 5 (Open Road Paving in Urbana). The company provided two gradations of 12.5-mm (1/2-in) nominal maximum aggregate size (NMAS) RAP, +3/8 (+9.5 mm) and -3/8 in (-9.5 mm).

Virgin aggregates were batched separate from the RAS products. A modification was introduced in the form of heating the RAP with virgin aggregated with the binder at mixing temperature, then heating RAS separately at 110°C (230°F) for 30 min. All components were then dry mixed and returned to the oven for another 30 min at mixing temperature. Finally, the virgin binder was then mixed in with the rest of the components.

### *3.1.1.3 Standard Mix Design Approval Tests*

Hamburg Wheel Track testing and tensile strength ratio (TSR) were used as part of the mix design evaluation. The results for the tests are shown below in Table 5 and Table 6. After evaluating TSR results, it was recommended to retest with the addition of anti-stripping agents. After an antistripping dosage of 0.75% was added, TSR retest values were acceptable.

**Table 5: Hamburg Test Results**

Mix ID	Mix Name	Rut Depth (mm)	Total Passes at Achieved Rut Depth	Minimum Passes	Result
L3	N90 CM 4 CG	12.5	11520	7500	Pass
L7	N90 20 CG	12.5	7000	5000	Pass
L9	N90 30 CG AS S2	6.1	20000	5000	Pass
L10	N90 60 CG AS S2	3.1	20000	5000	Pass
L12	N90 30 CG AS S2	5.0	20000	5000	Pass

**Table 6: TSR Test Results**

Mix ID	Mix Name	Dry Strength (psi)	Wet Strength (psi)	TSR	Minimum TSR	Result
L4	N90 CM 4 CG	120	93	0.77	0.85	Fail
L7	N90 20 CG	123	70	0.57		Fail
L11	N90 0 CG AS	108	101	0.94		Pass
L9	N90 30 CG AS S2	128	114	0.89		Pass
L10	N90 60 CG AS S2	140	143	1.02		Pass

### 3.1.2 Plant-Produced Mixes

A total of 16 plant-produced AC mixes were sampled, with various mix design characteristics that allowed researchers to explore the effect of both ABR content and N-design. These mixes have distinct mix design characteristics such as binder content, VMA, and N-design. Major design characteristics of these mixes are shown in Table 8. These AC mixes are referred as “P#” hereafter.

**Table 7: Plant Produced Mix Design Characteristics**

Mix ID	Mix Name	Binder Grade	RAP (%)	RAS (%)	ABR (%)	AC (%)	VMA (%)
P1 <sup>1</sup>	N50 SC <sup>3</sup>	52-28	50	3.5	60	6.7	15.0
P2 <sup>1</sup>	N50 SC <sup>3</sup>	58-28	27	-	29	5.8	14.7
P3	N70 BC <sup>4</sup>	58-28	26	-	29	4.8	13.4
P4	N30 BC <sup>4</sup>	58-28	46.5	-	37	4.8	13.6
P5	N70 SC <sup>3</sup>	64-22	10	-	6	6.1	15.8

**Table 7 (cont.)**

<b>P6</b>	N90 SC <sup>3</sup>	76-22	10	-	6	5.6	14.1
<b>P7</b>	N50 SC <sup>3</sup>	64-22	-	-	-	5.9	16.7
<b>P8</b>	N50-50	58-28	42	4	49	5.5	13.0
<b>P9</b>	N50-60	52-28	42	6	59	5.6	13.0
<b>P10</b>	N70-25	58-28	29	-	25	6	14.5
<b>P11</b>	N70-50	58-28	30	5	48	6	14.5
<b>P12</b>	N80-25	70-28	8	5	26	6.1	16.1
<b>P13</b>	N80-50	70-28	10	8	50	6	15.8
<b>P14<sup>1</sup></b>	N50-Joliet	58-28	30	-	34	5.4	15.3
<b>P15<sup>1,2</sup></b>	N50-Sandeno	52-28	52	4	60	6.7	15.1
<b>P16<sup>1,2</sup></b>	N50-K5	52-28	53	5	57	6.5	14.9

<sup>1</sup> Indicates AC containing steel slag

<sup>2</sup> Indicates AC containing recycled concrete aggregate (RCA)

<sup>3</sup> SC indicates a surface course AC, placed at the top-most layer of the pavement and exposed to traffic

<sup>4</sup> BC indicates a base course AC, placed directly below the surface course

### 3.2 Research Methodology

The research methodology is designed to develop a reliable, yet practical, test method based on fracture mechanics principles. This thesis addresses the following components of the research methodology:

- Assessment of plant and lab AC mixtures for modulus, fatigue, and fracture characterization at various temperatures and loading rates
- Development of a database of AC mixtures with different N-design, NMAAS, RAP and/or RAS content, and binder type
- Correlation to field performance with field core testing
- Theoretical development and numerical models based on fracture mechanics principles

Figure 5 illustrates the broad experimental approach developed. This study focusses on the “**Mixture Characterization**” and “**Theoretical Development**” components.





## 4. Experimental Program

### 4.1 Complex Modulus

Complex modulus testing is conducted in accordance with AASHTO TP79-15. Specimens are fabricated by coring asphalt cylinders into a diameter of 100 (3.9 in.) to 104 mm (4.1 in.) and a height of 147.5 mm (5.8 in.) to 152.5 mm (6.0 in.). Targeted void content is  $7 \pm 0.5\%$ . Axial displacement is measured using three extensometers with a 70 mm gauge placed  $120^\circ$  apart. Specimens are tested under temperature and frequency sweeps under stress-controlled loading. Microstrain values between 50 to 75 microstrains were targeted. Temperatures used are  $-10^\circ\text{C}$  ( $14^\circ\text{F}$ ),  $4^\circ\text{C}$  ( $39^\circ\text{F}$ ),  $21^\circ\text{C}$  ( $70^\circ\text{F}$ ),  $37^\circ\text{C}$  ( $99^\circ\text{F}$ ), and  $55^\circ\text{C}$  ( $131^\circ\text{F}$ ) and frequencies of 25, 10, 5, 1, 0.5, and 0.1 Hz. Data extracted from this temperature and frequency sweep was used to prepare complex modulus master curves using a reference temperature of  $21^\circ\text{C}$  ( $70^\circ\text{F}$ ).



Figure 6. Complex modulus set up with three axial extensometers mounted on the asphalt mixture specimen

### 4.2 Push-Pull

Tests were conducted on the Universal Testing Machine (UTM-100), a servo hydraulic load frame (Figure 7). Testing was conducted at  $21^\circ\text{C}$  and specimens were loaded at a frequency of 10 Hz. Strain levels were varied from 200 to 300 microstrains. Three axial LVDT's are located  $120^\circ$  apart around the radius of the specimen. Various criteria such as a 50% reduction in modulus have been used to determine specimen failure. Specimens are fixed to the top and bottom steel plates using Devcon 10110 epoxy. Before application of loading, specimens undergo a fingerprint modulus test to

approximate the complex modulus of the material for accurate load application. The specimen is then allowed to rest for 15 min and loading is applied at a rate of 10 Hz until failure.



Figure 7. Push-Pull fixture setup with extensometers and specimen fixed to top and bottom plates

## 4.3 Semi-Circular Bending Beam

### 4.3.1 Classical Semi-Circular Bending Beam Test (SCB)

The classical SCB test method is a 3-point bending test typically run at low temperatures (PG lower limit + 10°) in accordance with AASHTO TP-105-13. Temperature control was ensured with temperature gauges and specimens were not tested if found to be further than 1° from the target temperature. The primary parameter extracted from this test is the fracture energy (Gf). The fracture energy is defined as the amount of energy required to propagate a crack for a unit area and is typically expressed in joules per meter squared. Displacements are obtained by recording the CMOD using a clip-gauge extensometer or an extensometer measuring the load-line displacement. Stable crack growth conditions are ensured during the test. The SCB fixture is illustrated in the figure below along with a typical outcome of an SCB test and fracture energy calculation method. In general, the SCB is a simple, low-cost test that easily can be performed on the cylindrical samples obtained from standard cores prepared in the Superpave Gyrotory Compactor (SGC) or taken from the field. This test method requires a displacement control in two phases after the application of a 0.2 kN (45 lbf) sitting load: first, the specimen is loaded to a load of 1 kN (225 lbf) in stroke displacement control at a displacement rate of 0.06 mm/min (.00004 in/sec), and second, the test switches to CMOD control and the specimen is loaded at a displacement rate of 0.03 mm/min (.00002 in/sec) to failure, which is defined as a drop to 0.5 kN (112 lbf) or a specified CMOD opening.

The classical SCB tests conducted in this study are displacement-controlled through the use of a CMOD gauge. The specified displacement rate used was 0.7 mm/min (0.0005 in/sec). Load readings are plotted versus the horizontal CMOD displacement readings and a curve like that shown in Figure 3 is obtained. The area under this curve is calculated as the work of fracture. This area is then normalized by the ligament area of each specimen to obtain the fracture energy in units of  $J/m^2$ .

#### 4.3.2 Variable Rate Semi-Circular Bending Beam Test (VR-SCB)

The Variable Rate Semi-Circular Bending Beam (VR-SCB) test is a modification of the above mentioned classical SCB test. Specimen geometry and testing fixture setup are identical, save for the addition of an LVDT. This LVDT is used for displacement control instead of the CMOD in this test method as shown in Figure 9. The primary motivation to modify the SCB test method to use load-line displacement control is for development of a practical test method and fixture that can be conducted with commonly available loading frames in the labs of DOT, consultants, or contractors.



Figure 8. Semi-circular bending beam test fixture with an LVDT added for load-line displacement control

Tests in this setup are conducted at a temperature of 25°C (77°F). Fracture tests are conducted with variable load-line displacements rates. Testing the same material at multiple rates allowed the researchers to examine the sensitivity of materials to variation in displacement rates. The use of a higher testing temperature necessitates the use of a faster displacement rate to mitigate the effect of creep and to simulate a lower testing temperature as is presented later. Displacement rates ranging from 6.25 mm/min (0.00410 in/sec) to 50 mm/min (0.03281 in/sec) were used.

#### 4.4 Disc-Compact Tension Test (DCT)

DCT tests were conducted in accordance with ASTM D7313-07a. Specimens were tested in order to evaluate fracture following the same approach as that of the SCB test. 50-mm- (2-in-) thick specimens of 150 mm (6 in.) diameter were prepared and bore holes of 25 mm (1 in) diameter were machined into the specimen to allow for the use of loading rods. Specimens were conditioned and tested at a temperature of -12°C using the temperature control methods discussed for the aforementioned SCB testing. The DCT test loads specimens in tension in order to propagate a crack initiating at a machined notch in the specimen. Like the SCB test, a load versus displacement curve is extracted from the test and fracture energy is calculated using the same procedure. Displacement values are taken from a CMOD clip gauge as in the classical SCB test setup. The DCT test setup and loading fixture is shown in Figure 9.

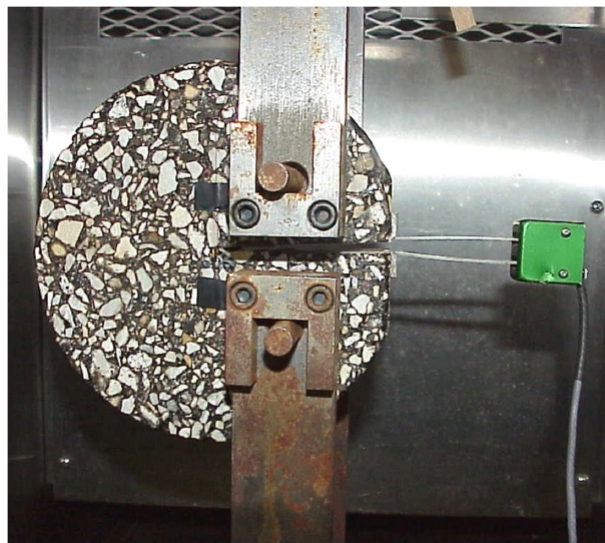


Figure 9. DCT specimen loaded in testing fixture with CMOD clip gauge for displacement readings

#### 4.5 Texas Overlay Test

The Texas overlay Test is a displacement-controlled cyclic test run at  $25^{\circ}\text{C} \pm 0.5^{\circ}\text{C}$ . Specimens are repeatedly displaced in tension to a displacement of 0.06 cm (0.025 in) at 1 Hz. The test is considered complete when there is a 93% reduction in the first cycle's recorded maximum load or when 1,200 cycles are reached. The primary parameter extracted from this test is the number of cycles to failure.

Test specimens were cut from gyratory compacted pills and glued to an aluminum plate. Figure 10 illustrates specimen geometry and a manufactured AC mixture specimen.

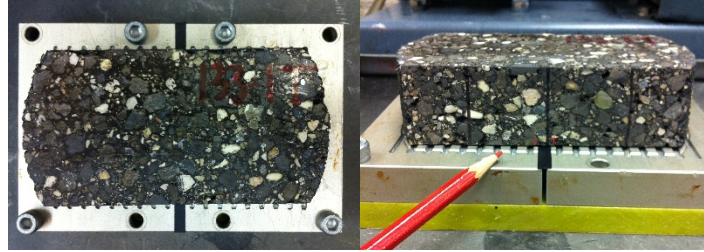


Figure 10. Texas overlay test setup illustrating specimen glued to an aluminum plate and underlying assembly with a joint opening and closing at a specified rate of displacement

## 5. Results and Analysis

Preliminary characterization of mixtures was conducted to explore the effect of recycled content on AC mixture behavior. Because of limitations on time, material, and resources, testing was conducted strategically, following an experimental matrix that provided the most insight into the effect of binder replacement on asphalt mixture behavior. Table 8 shows the experimental matrix for various tests conducted on several AC mixtures.

**Table 8: Experimental Matrix of Mixtures Tested Under Various Methods**

<b>Test Method</b>	<b>Mixtures Tested</b>
Push-Pull	P8 to P15 and L3, L6, L7
Texas Overlay (TEX-248-F)	P1 to P7
Low-Temperature SCB (AASHTO TP105-13)	P1 to P15, L3 to L7 and L9 to L13
Low-Temperature DCT (ASTM D7313 - 13)	P8 to P15

### 5.1 Push-Pull

Strain-controlled fatigue tests were conducted for selected plant and laboratory produced mixes. Push-pull tests were conducted at 20°C (68°F) and 200 and 300 microstrains. The following were taken as failure criteria:

- 50% reduction in the initial complex modulus
- Sudden change in the phase angle
- Sudden change in the dissipated strain energy ( $W_N$ ) representing failure localization
- Sudden change in the energy ratio (R) defined by the ratio of initial dissipated energy and dissipated energy at the  $N^{\text{th}}$  cycle
- Abrupt change in the dissipated energy ratio (DER)

After conducting laboratory fatigue tests, the outputs were put into an excel template to calculate the number of cycles to failure for each failure parameters. The number of cycles to failure for the respective mixtures using the studied parameters are provided in Table 9 and Table 10.

**Table 9: Number of Cycles to Failure Using Different Fatigue Parameters for Plant Mixtures (Based on 200 Microstrain Tests)**

Mix	50% E*	Phase Angle	W <sub>N</sub>	R	DER
P14	11324	17666	17820	17820	18125
P15	6640	17160	16000	16252	-
P8	3221	13172	13000	13000	13100
P9	1260	2330	2350	2350	-
P10	8526	17234	17163	17163	-
P11	823	1432	1497	1525	1510
P12	3122	17122	17012	16952	-
P13	362	683	665	672	650

**Table 10: Number of Cycles to Failure Using Different Fatigue Parameters for Lab Mixtures**

Mix	50% E*	Phase Angle	W <sub>N</sub>	R	DER
L4	15980	15980	12250	12223	12764
L7	19720	20567	9076	9224	10143
L6	14122	12375	10453	11589	10032

According to the results presented in Tables 10 and 11, the following observations can be made. As ABR level increased, there was a reduction in the fatigue life. This was observed for N50, N70, and N80 AC mixtures. As ABR increased due to the addition of RAS, this trend was not manifested, although this may be a result of the binder bumping in these AC mixtures. Unfortunately, the push-pull test displays high variability. Furthermore, specimen preparation and testing are long and complex procedures. Because of these factors, the push-pull test was ruled out as the test method of choice.

## 5.2 Low-Temperature SCB

The low-temperature SCB test was conducted at -12°C (10°F) and using CMOD control. The results for plant-produced AC mixtures are shown in Figure 11 and Figure 13. Fracture energy values for the 15 plant mixes tested ranged between 436 and 689 J/m<sup>2</sup>. In general, low-temperature fracture energy tests produced a very tight range of fracture energy even though these mixes have distinctive mix design characteristics, including N-design, binder type and content, ABR level, and aggregate gradation and sources. A similar spread in fracture energy values was observed when other low-temperature fracture tests were conducted.



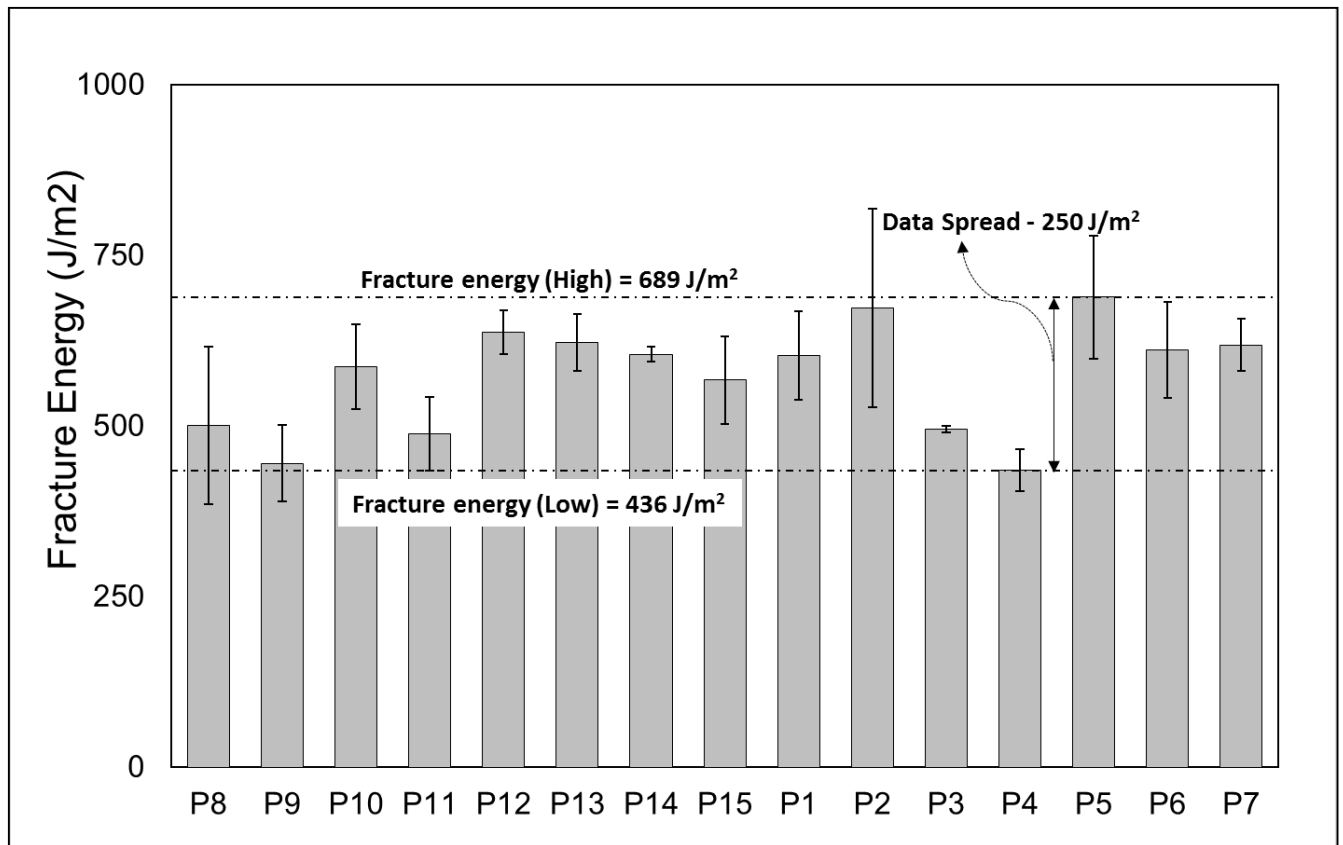


Figure 11. -12°C SCB plant mixture results for fracture testing in CMOD control.

Figure 11 presents the low-temperature SCB test results for the laboratory produced AC mixtures. Similar to the plant-produced AC mixtures, fracture energy values are in a relatively tight range. These results do not display a clear relationship between fracture energy and the addition of recycled content. L3, L4, and L11 are control AC mixtures with 0% ABR, displaying approximately the same fracture energy. There is no significant difference between the control AC mixtures and AC mixes with 20 and 30% ABR. It only appears that the mix with 60% ABR (L10) had the lowest fracture energy even though with relatively high standard deviation.

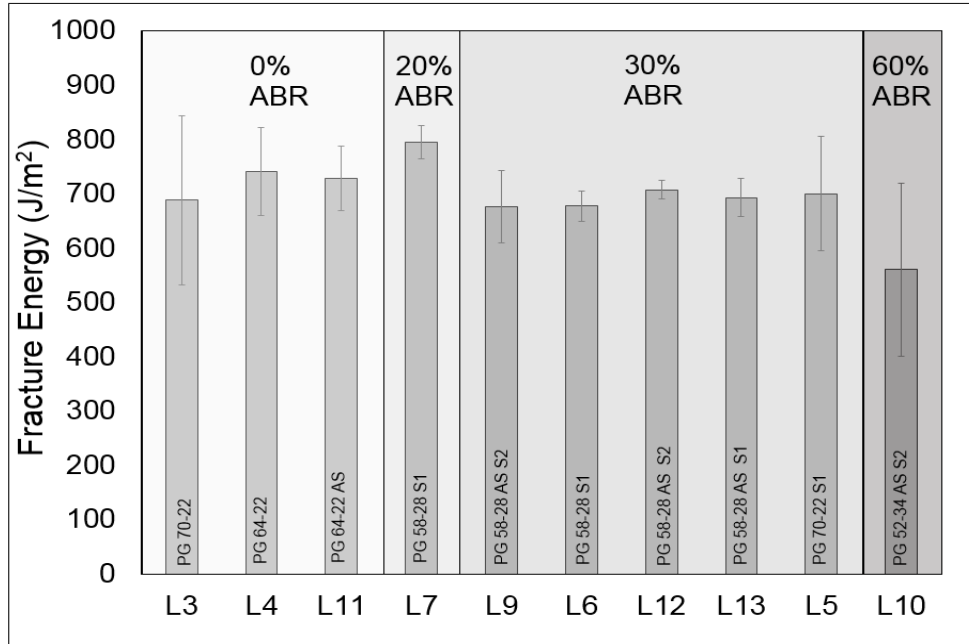


Figure 12. -12°C SCB lab mixture results for fracture testing in CMOD control.

### 5.3 Low-Temperature DCT

Results from the low-temperature DCT testing at -12°C (10°F) are shown in Figure 13. Again, there are inconsistent trends in this data, and no clear relationship between the fracture energy and the amount of recycled content and AC mixture characteristics is observed. For example, P8 and P9 display a trend of decreasing fracture energy with increasing ABR but, on the other hand, P12 and P13 contradict this trend. The fracture energy values in the DCT test setup display a range of 83 J/m<sup>2</sup>. With a range of results this tight, variability becomes a concern. Potentially, inherent variability of results overshadows behavioral distinctions between very different AC materials.

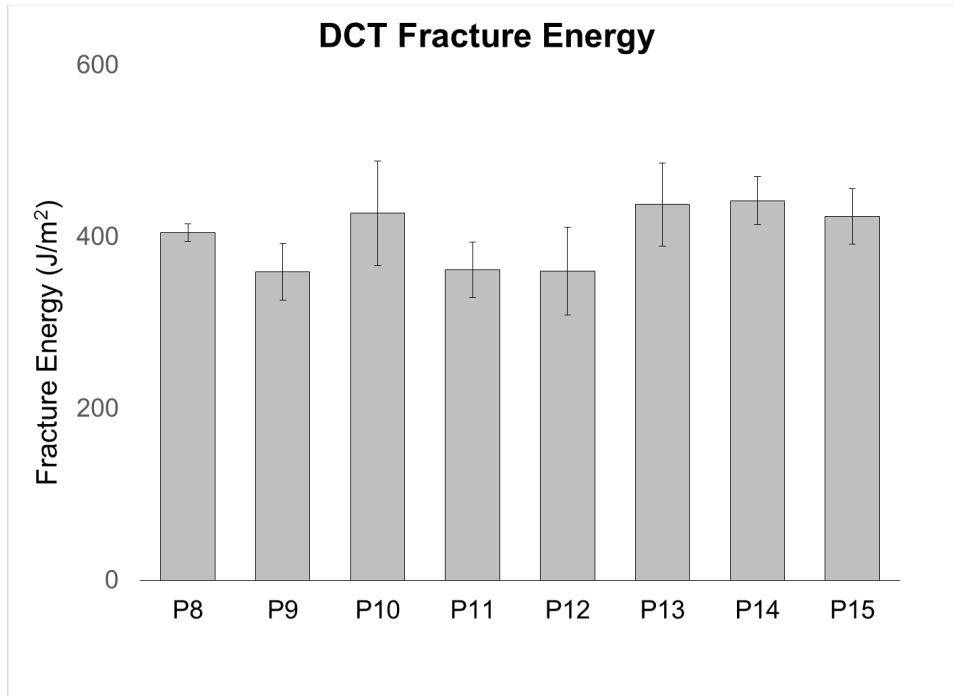


Figure 13. -12°C DCT lab mixture results for fracture testing in CMOD control.

## 5.4 Texas Overlay

Texas overlay test results are shown in Figure 15 with number of cycles to failure and initial load at the beginning of the test. P6 and P7 are the better performing AC mixtures in terms of cycles to failure while P2 and P5 are in the lower end of the performance spectrum. There is a clear trend between the peak load and cycles to failure that a mixture experiences. P7, an excellent performing mixture, has the lowest peak load value while P6, another excellent performer, displays the highest peak load value.

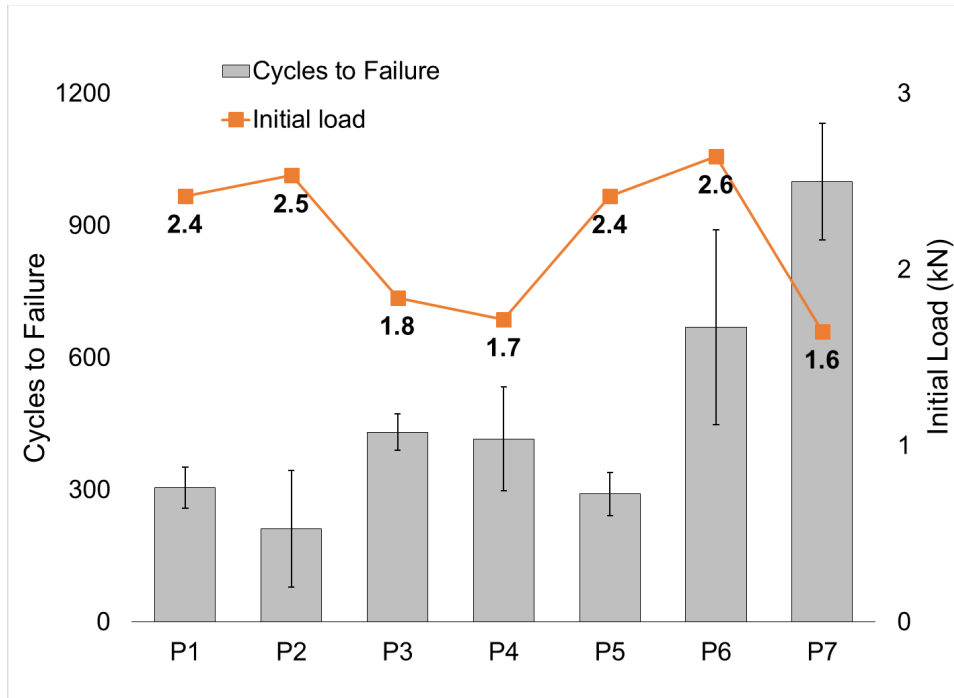


Figure 14. Texas overlay results for plant mixtures at -12°C.

## 5.5 Variable Rate SCB

Based on the results from the tests conducted at different temperatures and rates, it was shown that intermediate-temperature testing at 25°C (77°F) provides an opportunity for accomplishing the objectives of the study, i.e., development of a practical and reliable test method to distinguish AC mixture's cracking resistance. Further details on identifying the optimized temperature, 25°C (77°F) for testing can be found at (Khan, 2015) This study focused on testing at this temperature with varying rates to determine the optimum rate that would result in a meaningful separation with acceptable repeatability. This section presents the results conducted at 25°C (77°F) and varying rates for a set of plant and laboratory AC mixtures.

The intermediate-temperature semi-circular bending beam test is a modification of the low-temperature SCB test. Specimen geometry and testing fixture setup are identical. An LVDT was added to the fixture. This LVDT is used for displacement control instead of the CMOD in this test method as shown in Figure 3. The procedure to calculate the fracture energy is identical to that of the low-temperature SCB test, except for the use of LVDT displacement values instead of CMOD displacement values. Based on the aforementioned results and discussions, displacement rates of 6.25 mm/min (0.00410 in/sec), 25 mm/min (0.01640 in/sec), and 50 mm/min (0.03280 in/sec) were explored.

Typical results from the intermediate-temperature testing are shown in Figure 15 through Figure 17. The figures illustrate the effect of rate and ABR using a low and high rate of testing, respectively. The results are shown from the two laboratory AC mixtures with no ABR and 30% ABR. The lower displacement rate of 6.25 mm/min (0.00410 in/sec) produced more ductile behavior, displaying lower peak load and a softer post-peak tail. The higher displacement rate of 50 mm/min (0.03280 in/sec) produced a load-displacement curve which was visibly more brittle, displaying higher peak loads and sharper post-peak unloading. Similar results were obtained for the AC mix that contains 30% ABR (LX). However, in this case, it is clear that the response is much more brittle with increasing peak loads and a reduction in the displacement to initiate and complete crack propagation.

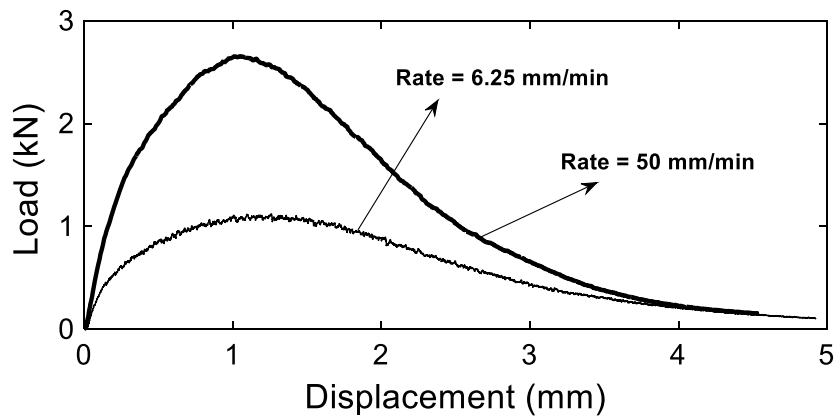


Figure 15. Typical load-displacement curve for a control mixture with 0% ABR at 25°C.

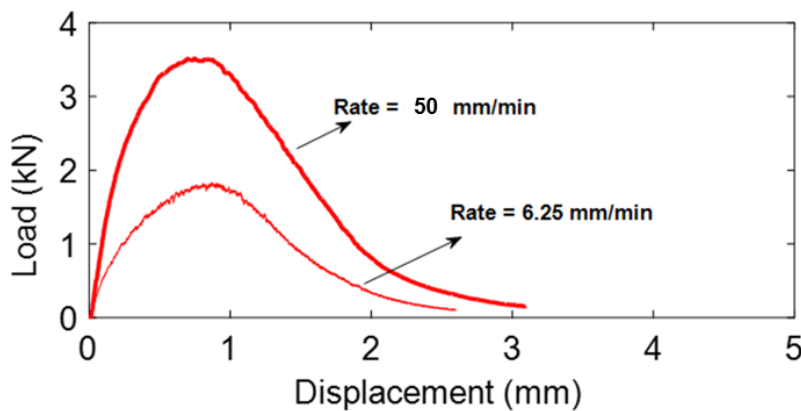


Figure 16. Typical load-displacement curve for a control mixture with 30% ABR at 25°C.

Figure 17 illustrates typical results for some of the laboratory AC mixtures with varying ABR and binder grade. These tests were conducted at 50 mm/min (0.03280 in/sec). The separation between the AC

mixtures is evident from the load-displacement curve patterns. As ABR increases, the curves appear to become more brittle with increasing peak, smaller displacement range, and higher slope in the post after the peak.

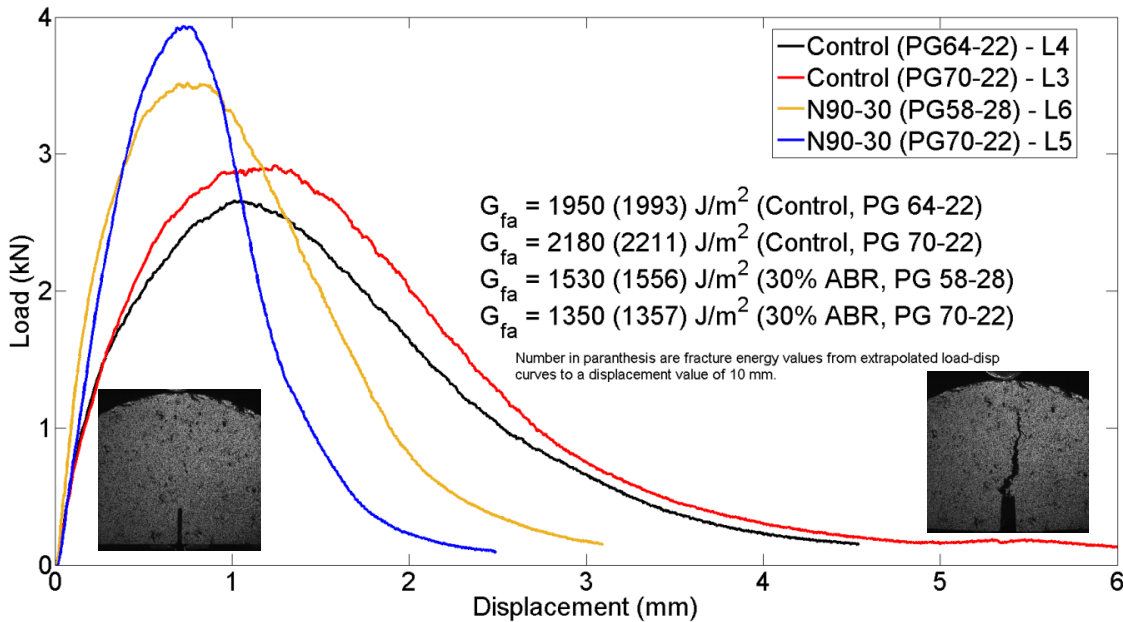


Figure 17. Typical load-displacement curves for lab AC mixes (L3 to L6) and corresponding fracture energy calculated at cut-off displacement (short) and extrapolated (long) from the SCB tests conducted at 50 mm/min (0.03280 in/sec) loading rate and 25°C.

Typical load-displacement curves illustrate a point where intermediate-temperature testing has a potential for separating mixes with changes in the mix design characteristics. Therefore, the rest of this chapter presents the results from the tests conducted at this temperature with varying rates.

### 5.5.1 Rate Effect

#### 5.5.1.1 Results at 50 mm/min

Figure 18 shows the intermediate-temperature SCB fracture energy results for the plant mixtures tested at 50 mm/min (0.03280 in/sec). The range of fracture energy varied from 877 to 2148  $J/m^2$  for the tests conducted at 50 mm/min (0.03280 in/sec). A greater range of fracture energy values at the intermediate temperature of 25°C (77°F) provides a potential better distinction between AC mixes. Fracture energy appeared to decrease consistently with increasing ABR. This trend can be observed when comparing P8 and P9, where P9 has significantly higher ABR content. The same comparison can be made between P10 and P11 and between P12 and P13. Fracture energy values in this testing setup ranged from 877  $J/m^2$  to 2148  $J/m^2$ . This results in a fracture energy value range of 1271  $J/m^2$ , as compared with the previous 253  $J/m^2$  observed under classical low-temperature SCB testing.

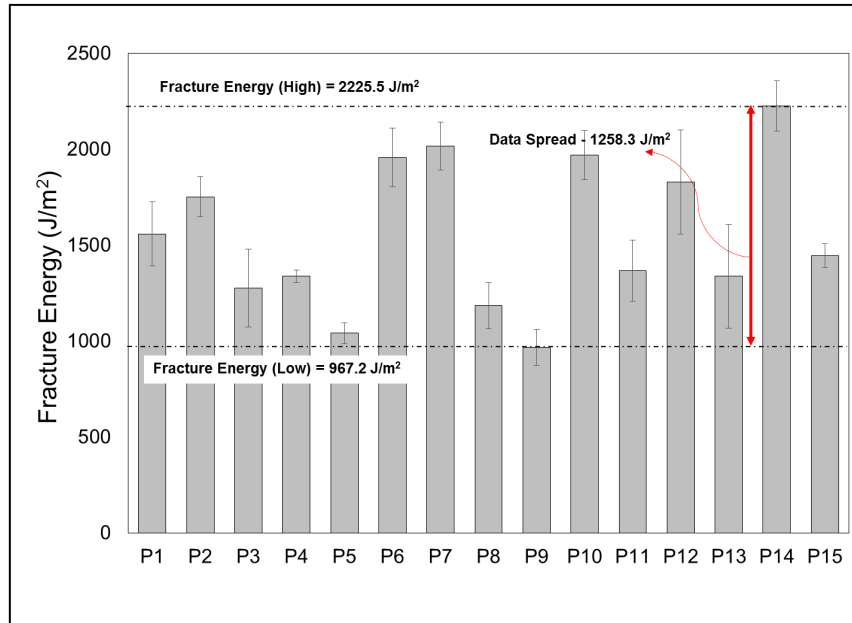


Figure 18: Intermediate-temperature (25°C) SCB results for plant mixtures tested at 50 mm/min displacement rate.

Figure 18 presents the fracture energy results for laboratory AC mixtures tested at 50 mm/min (0.03280 in/sec). The effect of increasing ABR on the fracture is clearly evident for AC mixtures prepared by changing the ABR content only, while keeping all other AC mix design properties the same. L3 and L4 are identical AC mixtures, except for the use of a softer binder in L4, which resulted in a decrease in fracture energy. However, this trend is reversed for the two AC mixtures with 7% RAS, L5 and L6, as softer binder is used in L6. However, when holding all AC mix design parameters constant and changing the percentage of RAS used, as in the case of L3 and L5, there was a dramatic drop in fracture energy as RAS content increased. The drop in fracture energy continued as ABR increased up to 60%. Fracture energy values ranged from 1399 J/m<sup>2</sup> to 2205 J/m<sup>2</sup>, resulting in a fracture energy range of 806 J/m<sup>2</sup>. This can be compared with the corresponding fracture energy range of 117 J/m<sup>2</sup> for the classical low-temperature SCB test setup for the same AC mixtures or 83 J/m<sup>2</sup> for the DCT.

Figure 19 and Figure 20 present the results for a low-rate (6.25 mm/sec (0.00410 in/sec)) fracture test. Low-rate fracture tests did not display a clear trend with increasing ABR for plant or laboratory AC mixtures. In general, it was observed that the fracture energy values at higher loading rates produced higher fracture energy for all AC mixes at 25 °C.

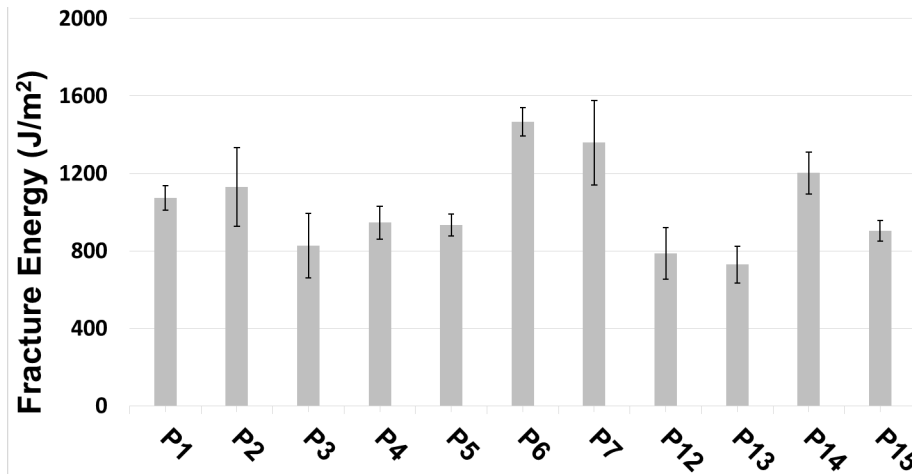


Figure 19: Intermediate-temperature (25°C) SCB results for plant AC mixtures tested at 6.25 mm/min (0.00410 in/sec) displacement rate.

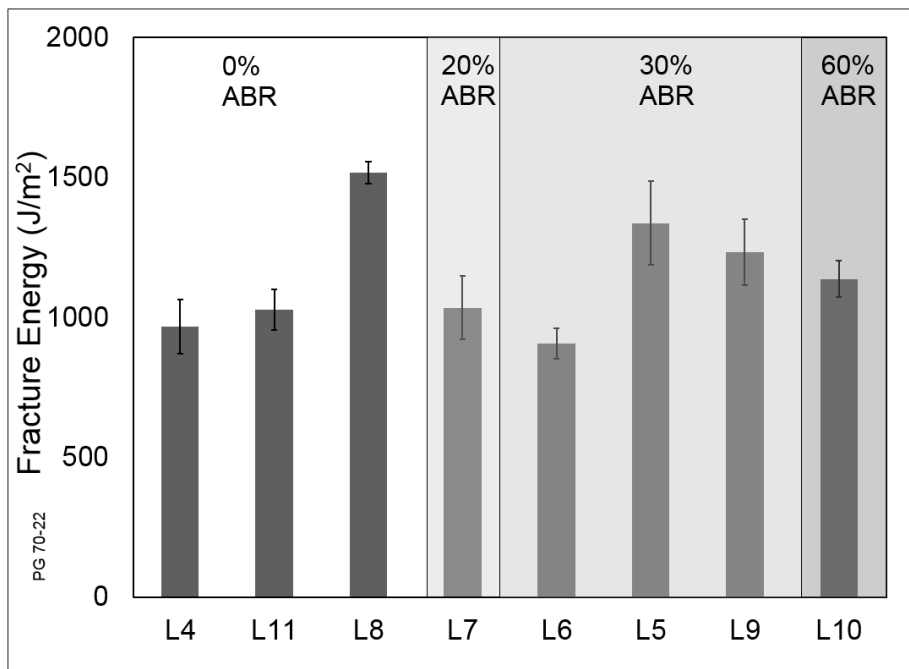


Figure 20: Intermediate-temperature (25°C) SCB results for lab AC mixtures tested at 6.25 mm/min (0.00410 in/sec) displacement rate.

Table 11: Summary of SCB Fracture Test Results Conducted at Intermediate Temperature (25°C) at Two Various Loading Rates

Mix #	Intermediate-Temperature SCB (25°C) @ 6.25 mm/min				Intermediate-Temperature SCB (25°C) @ 50 mm/min			
	$G_{fa}$ (J/m <sup>2</sup> )	COV, %	$f_t$ (MPa)	COV, %	$G_{fa}$ (J/m <sup>2</sup> )	COV, %	$f_t$ (MPa)	COV, %



**Table 11 (cont.)**

P1	1073	6%	0.29	14%	1568	12%	0.49	4%
P2	1131	18%	0.31	2%	1629	13%	0.53	2%
P3	827	20%	0.32	8%	1201	19%	0.48	7%
P4	946	9%	0.25	4%	1314	6%	0.52	10%
P5	933	6%	0.39	2%	952	10%	0.65	2%
P6	1466	5%	0.41	3%	1891	9%	0.64	6%
P7	1359	16%	0.25	10%	1948	6%	0.47	9%
P8	-- <sup>3</sup>	--	--	--	1130	15%	0.48	11%
P9	--	--	--	--	877	17%	0.39	9%
P10	--	--	--	--	1858	6%	0.40	5%
P11	--	--	--	--	1290	14%	0.57	11%
P12	787	17%	0.23	1%	1629	16%	0.41	14%
P13	729	13%	0.31	6%	1133	27%	0.43	7%
P14	1202	9%	0.29	8%	2193	7%	0.51	3%
P15	904	6%	0.23	5%	1417	6%	0.51	7%
L3	--	--	--	--	2205	5%	0.37	2%
L4	1010	3%	0.16	7%	1775	10%	0.32	20%
L5	--	--	--	--	1399	6%	0.48	8%
L6	1029	22%	0.24	4%	1769	11%	0.57	27%
L7	1028	11%	0.17	2%	1722	5%	0.36	5%
L8	1518	10%	0.28	8%	2043	7%	0.51	2%

<sup>2</sup> Tensile strength ( $f_t$ ) is calculated using the equation:  $f_t = P/2rt$  (P: load, r: radius, t: thickness)

<sup>3</sup> Limited data available for some mixes insufficient material.

In light of the larger and more meaningful data spread presented by the intermediate-temperature SCB test method, its correlation to qualitative fatigue tests, and applicability, it was concluded that this test method can be used to distinguish AC mixes for their cracking potential. However, further analysis of SCB test results can further improve the test's reliability and prediction accuracy.

#### *5.5.1.2 Correlation to Fatigue Testing and Statistical Analysis to Discriminate Performance*

Among the criteria considered in the selection of the SCB test method and parameters is correlation to other independent tests and engineering intuition. In order to check if this criterion is satisfied, a group of AC mixes was selected to compare fatigue performance using the TOL and SCB fracture test results. Statistical analysis was conducted to evaluate the capability of each test and establish an independent ranking. The results, shown in Table 13, indicate a positive correlation between intermediate-temperature (25°C) SCB fracture tests and TOL in identifying the material demonstrating the best and worst performance (A and B). Because of the spread in test data, the SCB fracture test resulted in three

groups (A, B and C) with statistically significant differences when loaded at 6.25 mm/min (0.00410 in/sec) and four groups (A, B, C and D) when loaded at 50 mm/min (0.03280 in/sec).

**Table 12: Summary of Statistical Ranking Results for the Texas Overlay and Two SCB Tests at a Significance Level of 0.10.**

Mix #	RAP/RAS (%)	Texas Overlay		SCB at 25°C and 6.25 mm/min		SCB @ 25°C and 50 mm/min	
		Grouping <sup>1</sup> @ $\alpha=0.10^*$	Cycles to Failure	Grouping @ $\alpha=0.10$	Avg. $G_{fa}$ (J/m <sup>2</sup> )	Grouping @ $\alpha=0.10$	Avg. $G_{fa}$ (J/m <sup>2</sup> )
P1	50/3.5	B	305	B/C	1073	B/C	1473
P2	27/0	B	212	A/B/C	1131	A/B/C	1576
P3	26/0	B	431	C	827	C/D	1209
P4	46.5/0	B	416	C	946	C/D	1314
P5	10/0	B	291	C	933	D	952
P6	10/0	A	669	A	1466	A/B	1852
P7	0/0	A	1000	A/B	1359	A	1948

<sup>1</sup> \*  $\alpha=0.10$ , means the rejection region comprises 10% of the sampling distribution

Table 12 shows that the intermediate-temperature SCB test method and the Texas overlay test are correlated at their performance extremes. P6 and P7, the better performing AC mixtures, are placed in the higher subsets in both testing methods. Additionally, the lower performing AC mixtures, such as P5, are consistently placed in the lower performance subsets in both test methods. However, this correlation is lost in the middle of the performance spectrum, where both test methods have different classification of AC mixtures.

## 5.5.2 Secondary Considerations

In the development of the test method, the following additional considerations are taken into account:

- Robustness of fixture and compliance to record actual specimen deformations
- Specimen conditioning method
- Repeatability of the selected displacement rate

### 5.5.2.1 Machine Compliance and Fixture

The displacement measurements used for the SCB fracture tests conducted in this project are different from the method described in the specification AASHTO TP 105-13 for computation of fracture energy. The specification recommends measurement of displacements with two LLD gauges attached to gauge points located on the front and back of the specimen, while the gauges are aligned with the notch and placed 44.5 mm (1.8 in.) from the bottom of the specimen; this measurement is referred to as “AASHTO

displacement.” Our displacement measurements consist of a measurement of the loading head displacement relative to the load frame with LLD gauges; it is referred to as “loading head displacement.”

The digital image correlation (DIC) technique was used to compare the two methods by measuring the displacement of DIC gauges at the surface of the specimen. These DIC gauges are zones at the surface of the specimen where the displacement is averaged. The DIC gauge measuring the AASHTO displacement is positioned where the gauge point should be for this method, while the DIC gauge for the loading head displacements is positioned right under the loading head, as shown in Figure 21. The displacements measured through DIC were used to obtain the load-displacement curves and compare it to the load displacement obtained directly from the machine, as shown in Figure 21.

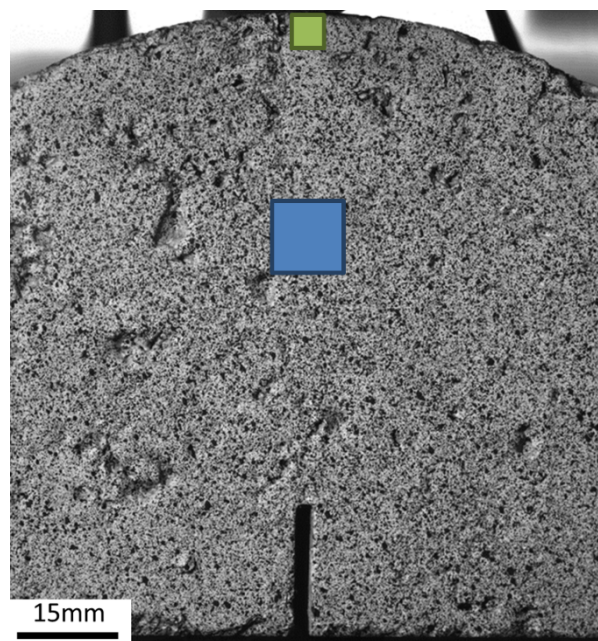


Figure 21: Location of the DIC gauges on the SCB specimen. Green box = Loading head displacement, blue box = AASHTO displacement.

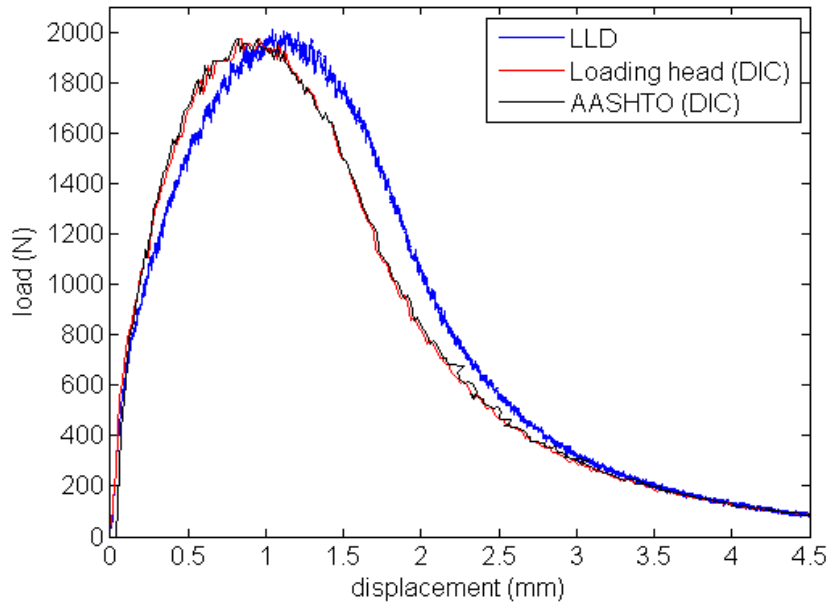


Figure 22: Comparison of load - displacement measurements: Blue = Loading head displacement measured by the load frame, red = DIC loading head measurements, black = DIC AASHTO measurements.

The curves in Figure 22 show that the two measurements with DIC are almost exactly the same. There are minor differences from the measurements recorded with the load frame; this is probably due to the compliance of the machine. These results show that our method gives similar results to the AASHTO method. The advantage is that, unlike the AASHTO method, the loading head displacement method does not require gauge points to be placed on the crack path and thus avoids measurement complications.

#### 5.5.2.2 Selection of Temperature Conditioning Method

Even at the proposed 25°C, there is still a need for a conditioning method to ensure consistent testing temperature. A study was conducted to examine various methods of temperature conditioning. Three methods were explored:

- Water bath conditioning
- Oven conditioning
- Chamber conditioning

Water bath conditioning was conducted in accordance with AASHTO T283. Specimens were submerged in a water bath at a specified temperature of 25°C (77°F) for 2 hrs and were then tested under the intermediate-temperature SCB fracture test.

Oven conditioning was conducted by placing specimens in trays into AC mixing ovens set to a temperature of 25°C (77°F). Specimens were monitored with temperature gauges until temperature gauges reached the desired temperature of 25°C (77°F) and then tested under the intermediate SCB fracture test.

Test chamber conditioning was conducted by conditioning the specimens in the Interlaken environmental chamber. The temperature of the test chamber was set to 25°C (77°F) and specimens were conditioned until a temperature gauge reached a temperature of 25°C (77°F). Specimens were then tested under the intermediate-temperature SCB test method.

Test results are shown in Figure 23. Visually, no significant differences were noticed between the three different conditioning methods. Most of the load-displacement curves fall on top of each other and those that deviate can be attributed to test variability.

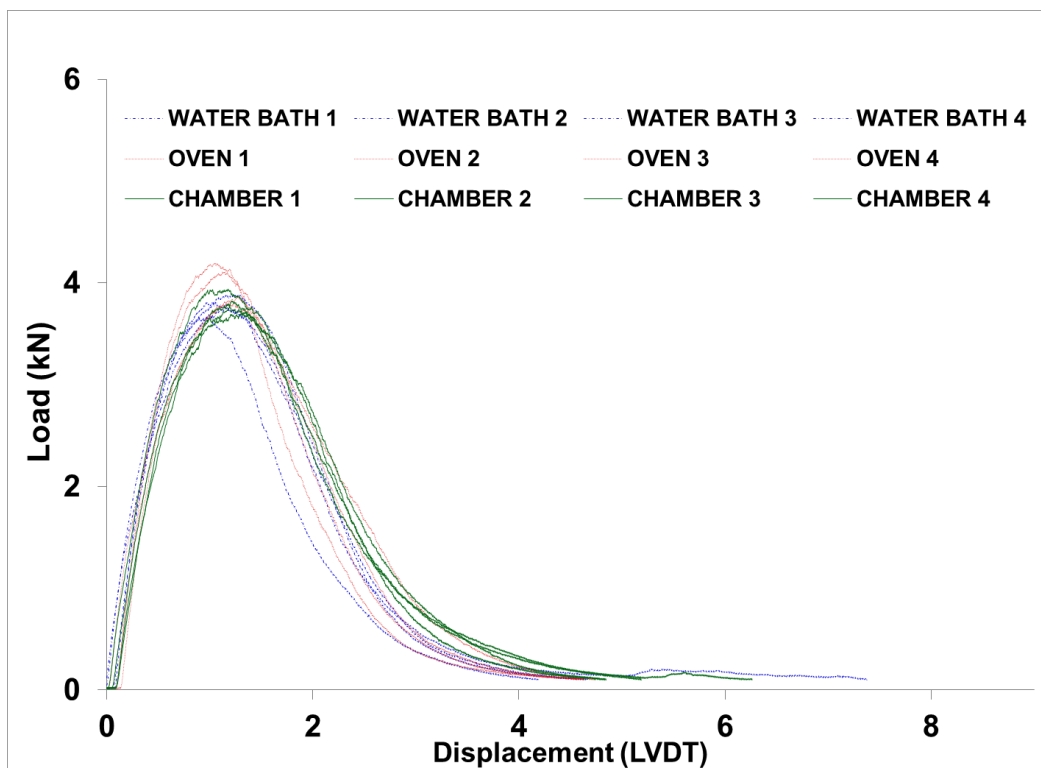


Figure 23: Load-displacement curves for specimens tested after three different conditioning methods.

Table 13 shows that all three conditioning methods are not significantly different from each other. Examining the coefficient of variation (COV) between methods, it can be noted that the parameter with the highest coefficient of variation is the slope of inflection in the fracture energy curve tail. All other

parameters display lower COV values between the various methods, indicating that one is free to use whichever method is most practical.

**Table 13: Statistical Summary for Various Temperature Conditioning Methods Explored Prior to Intermediate-Temperature SCB Testing**

Conditioning Method	Replicate ID	COV Fracture Energy (%)	COV Strength (%)	COV Intercept (%)	COV Slope (%)
<b>WATER BATH</b>	T4-B-1	7.82	13.33	8.13	9.85
	T4-B-2				
	T4-T-1				
	T4-T-2				
<b>OVEN</b>	T2-B-1	4.76	6.23	14.26	30.53
	T2-B-2				
	T2-T-1				
	T2-T-2				
<b>CHAMBER</b>	T1-B-1	3.31	2.37	5.44	12.98
	T1-B-2				
	T1-T-1				
	T1-T-2				
<b>Inter-Method</b>		6.54	19.29	11.16	21.49

### 5.5.2.3 Selection of Temperature Conditioning Method

Based on multi-temperature and rate testing, it was concluded that 25°C (77°F) is the testing temperature consistent with the objectives of the study. The second question to answer was the selection of displacement rate. Selection of a specific displacement rate must accomplish the following:

- Minimized variability and maximized repeatability
- Feasibility of running on a standard, commonly available load frame
- Accommodation of a wide spectrum of materials
- Proper distinction between different mixtures
- Minimized testing time

As the final objective was to run the developed test on a standard load frame, any displacement rate selected must be accommodated by the load frame. Standard tensile strength ratio (TSR) load frames operate at 50 mm/min (0.03280 in/sec). Thus, it should not be an issue to find equipment for running the intermediate-temperature SCB.

Minimized variability and maximized repeatability are critical for specimen to specimen comparison as well as lab to lab comparison. This criterion can be measured using each displacement rate’s average COV. LVDT- based fracture energy COV values were calculated for each AC mixture under each displacement rate. Fracture energy was used because this is the most basic parameter to be calculated from a displacement-controlled fracture test. The average of all individual mixture COV’s was then taken, as shown in Table 14.

**Table 14: Average Values of Coefficient of Variation of LVDT Fracture Energy at the Various Displacement Rates Tested at 25° C**

<b>Displacement Rate (mm/min)</b>	<b>Average LVDT Fracture Energy Coefficient of Variation</b>
<b>6.25</b>	11.3%
<b>25</b>	8.6%
<b>50</b>	9.2%

It can be seen from Table 14 that the COV among the rates are similar. Therefore, one can conclude that there is no drastic difference between the different rates in terms of repeatability.

During testing, the selected displacement must not cause the material to fail catastrophically. Previous testing shows that the higher the displacement rate, the more brittle the material behaves. A displacement rate that is too high can cause catastrophic failure. Since some materials are more brittle than others, the selected rate must provide a soft enough failure to allow even these brittle materials to fail in a stable manner. At a testing temperature of 25°C (77°F), the highest displacement rate of 50 mm/min (0.03280 in/sec) did not cause overly brittle failure for even the brittle materials in the wide

variety of AC mixtures used in this study. At the same time, the test should also allow crack initiation and propagation. Sometimes for low displacement rates, cracks may never initiate for some ductile materials exhibiting excessive creep and relaxation.

The selected displacement rate must properly distinguish between various AC mixtures since this is the ultimate objective of the testing specification. Based on the results presented in the previous section, higher loading rates provided a more consistent separation of AC mixes. This examination confirms that the higher displacement rate of 50 mm/min (0.03280 in/sec) produces a higher data spread between different AC mixtures. Additionally, the selected displacement rate must be as fast as possible to ensure reasonable testing times and to avoid excessive creep and relaxation during application of the load. A higher displacement rate would better protect against this concern. It was clear that out of the two tested displacement rates, the 50 mm/min (0.03280 in/sec) displacement rate is best suited for the purposes of this study.

- It displays an excellent level of repeatability when compared with other displacement rates.
- It can easily be run on most standard load frame.
- It does not cause catastrophic failure in brittle AC mixtures at the 25° C testing condition.
- It provides the most distinction between different AC mixtures.
- It is the fastest of both rates.

## 5.6 Summary

Having determined that low-temperature fracture testing is insufficient for distinguishing between AC mixtures, a testing temperature was explored. It was found that 25°C (77°F) is capable of distinguishing between AC mixtures with different mix design properties. Next, multiple displacement rates were explored at 25°C (77°F). From this observations, the following was concluded:

- Comparison of the LVDT displacement readings and the AASHTO TP 105-13 displacement collection method showed sufficient similarity between readings.
- Examination of laboratory AC mixtures revealed intermediate-temperature testing can better detect the deterioration of a AC mixture from its parent mixture than low-temperature testing can.
- Shifting testing temperature to 25°C (77°F) resulted in a significantly higher range of results as compared with the low-temperature testing, indicating that this temperature can better distinguish between different AC mixtures.



- At 25°C (77°F), generally, AC mixtures with higher amounts of ABR resulted in a decrease in fracture energy, with some noticeable exceptions.
- Increasing the displacement rate of testing resulted in an increase in the fracture energy. However, no catastrophic failure was experienced as a result of the increased displacement rate.
- A displacement rate of 50 mm/min (0.03280 in/sec) was selected to target acceptable variability, maximize distinction between AC mixtures, accommodate common load frames, and expedite testing time.
- The intermediate-temperature SCB, when correlated to the Texas overlay test, showed correlation between the excellent performing AC mixtures and the poor performing AC mixtures.

## 6. Development of Flexibility Index

The SCB test was conducted at an intermediate temperature and a displacement rate of 50 mm/min (0.03280 in/sec), however, there were instances when fracture energy was not sufficient as a sole parameter for distinguishing between AC mixtures.

Figure 24 illustrates a comparison of two AC mixes (control with no recycled materials and the same mix derived from the control with 30% ABR using 7% RAS) tested at 50 mm/min (0.03280 in/sec) and 25°C (77°F). Although the fracture energy values of the two AC mixes were the same, the mixes had distinctive load-displacement characteristics. Hence, it was evident that fracture energy should not be used alone to discriminate between the two AC mixes. This could be attributed to the nature of the fracture energy parameter. Depending directly on the geometry of the load-displacement curve, the fracture energy is a function of the strength and ductility of the material. If the material displays a high peak load, this may compensate for the lack of ductility in the post-peak region of the load-displacement curve, which might explain why, in earlier results, more brittle AC mixtures with higher amounts of recycled content displayed higher fracture energy values.

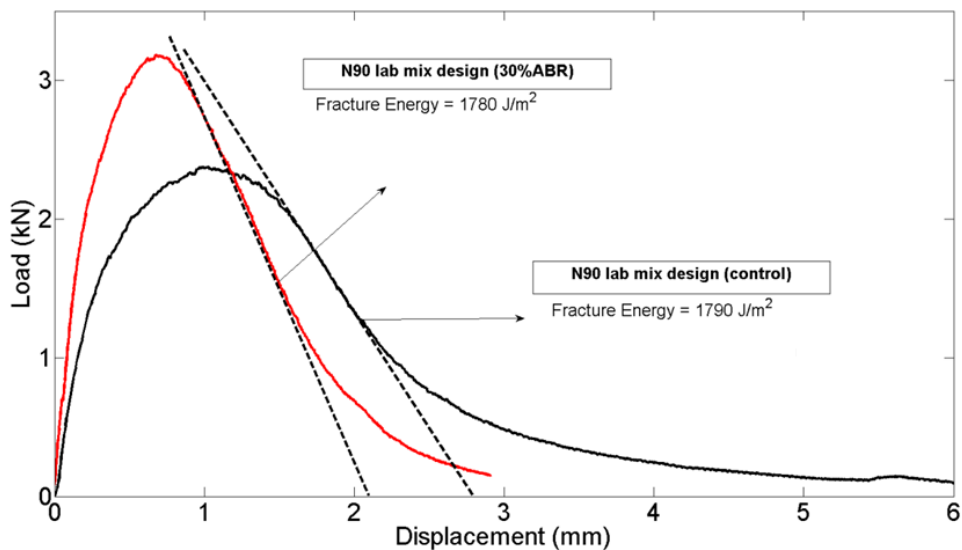


Figure 24: Major characteristics derived from load-displacement curves from SCB tests conducted at 25 °C (77°F) and at 50 mm/min (0.03280 in/sec) displacement rate illustrating the potential effects of ABR.

### 6.1 Candidate Parameters

There is a need to develop a parameter in order to be able to consistently distinguish between AC mixtures. An index parameter that can describe the fundamental fracture processes and overall

patterns of load-displacement curves, shown in Figure 25, is needed to discriminate the cracking potential of AC mixes. The primary underlying mechanism causing the changes in the load-displacement curve in a fracture test is attributed to the size of the fracture process zone where microcracking or void formation takes place; the fracture process zone is determined by the inhomogeneities in the microstructure (maximum aggregate size, distribution of aggregates, matrix volume, and properties). In general, the size of this zone is correlated to the brittleness of material and strongly governs fracture behavior. As the zone grows, the load-displacement curve becomes “bulkier,” thus reflecting an increase in fracture energy. Therefore, the process zone and, consequently, any index parameter derived from it, might have an impact on the speed of crack propagation. As the material becomes more brittle, the speed of crack propagation increases. Therefore, the parameters that may have an influence on the formation of the fracture process zone were considered in the development of the index.

From the load and displacement history recorded from the SCB test, the following parameters of interest were extracted:

- Fracture energy (GF)
- Peak load ( $P_{max}$ )
- Critical displacement ( $w_1$ )
- Displacement at the peak load ( $w_0$ )
- Slope at inflection point ( $m$ )

Fracture energy was calculated by finding the area under the load-displacement curve. Critical displacement-related parameters were calculated using the following procedure: the inflection point was determined on the curve after the peak point; the tangential slope was drawn at the inflection point; the intersection of the tangential slope with the x-axis yielded the critical displacement value. The critical displacement and slope represent the ability of the mix to resist crack propagation; the higher the value of critical displacement, the less brittle the AC mix.

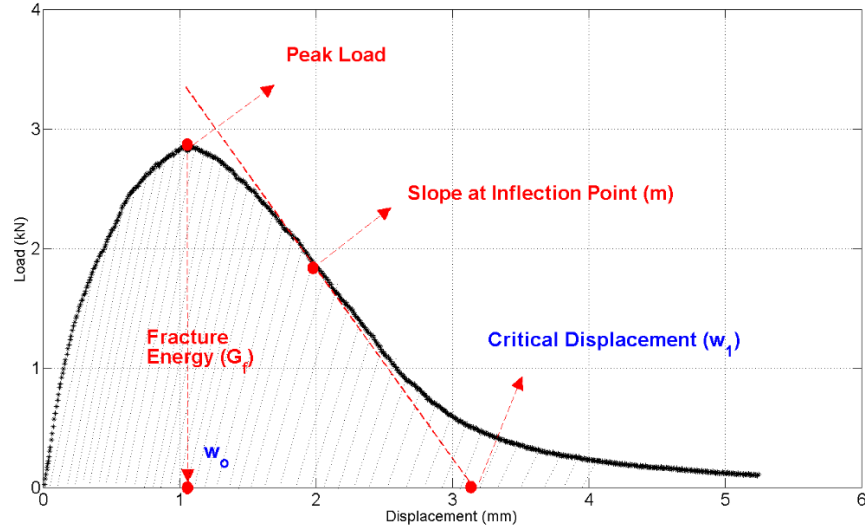


Figure 25: A typical outcome of the SCB test illustrating the parameters derived from the load-displacement curve including peak load (will be related to tensile strength), critical displacement, slope at inflection point, displacement at peak load, and fracture energy.

Empirical correlations between candidate indices and the speed of crack propagation (or approximate crack propagation velocity) were obtained from the SCB experiments. The form of the index parameter was inspired by the rate of crack growth definition provided by Bazant and Prat (1988) for concrete materials for the purpose of explaining the effect of temperature and humidity on crack growth at a reference temperature.

$$\dot{a} = v_c \left( \frac{G}{G_f} \right)^{n/2} \quad (4)$$

where  $v_c$  is a constant;  $G$  is energy release rate ( $G = K_I^2/E$  with  $K_I$  is stress intensity factor); and  $n$  is a factor.

$$\dot{a} = v_c \frac{1}{(EG_f)^{n/2}} (K_I)^{n/2} \quad (5)$$

The stress intensity factor is related to the geometry and loading, which is assumed constant for the SCB geometry; the other factors are proportional to the material properties that can accelerate or decelerate crack growth. As fracture energy and modulus decrease or stress intensity increases, crack growth accelerates. An empirical correlation between brittleness (inverse of flexibility) and crack

growth was used to formulate the index parameter. Equation 5, including a function for the Flexibility Index (FI), is simplified as follows:

$$\dot{a} = \frac{1}{FI_o} (K_I)^{n/2} \quad (6)$$

where three versions of FI considered in this study are:

$$FI_I = G_{fa} / abs(m) \quad (7a)$$

$$FI_{II} = G_{fa} E / (abs(m) f_t^2) \quad (7b)$$

$$FI_{III} = G_{fa} \quad (7c)$$

The FI could be a parameter of process zone size (correlated to characteristic length given in Equations 2 and 3) or other combinations with good correlation to crack growth speed. In this study, because the test specimen geometry was kept constant, the stress intensity factor was also considered constant up to crack initiation, as long as the changes in the crack front stress field were not dramatic between different materials.

## 6.2 Correlation to Crack Velocity

An approximate crack velocity was used as proxy to the speed of crack propagation in Equation 6. The approximate crack velocity was calculated directly from the experimental data by assuming constant crack propagation speed. A comparison of the approximate crack velocity to the true velocity profile was performed using the CCD system, as shown in Figure 26. The true crack velocity was calculated by tracking the crack position while it propagated for the first 20-25 mm (0.8-1.0 in.) from its original position. It was observed that the true crack velocity obtained at the crack front increased with time and with crack propagation. Among the materials compared (L4 and L5), acceleration of the crack was more significant as the material became more brittle. Constant velocity profiles obtained directly from the specimen loading were considered as a first-order approximation to true crack profile Figure 26(b). As expected, deviation from the true velocity profile became more significant for brittle materials with nonlinear crack velocity profiles, as demonstrated in the case of L5 (N90-30). The approximate crack velocity doubled in more brittle material (L5) and was therefore considered in this study to correlate with the proposed index parameters.

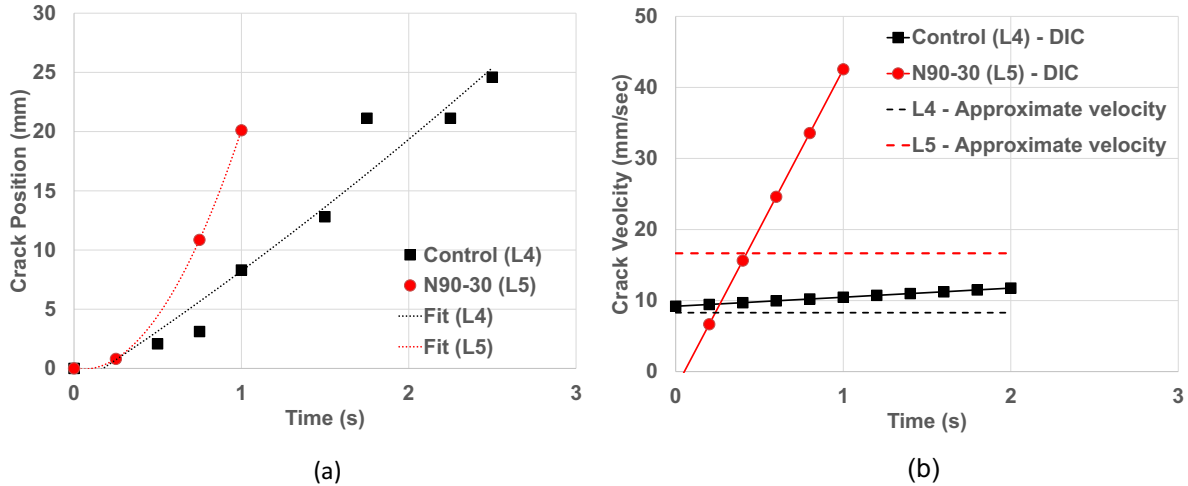


Figure 26: A comparison of true crack profile of crack velocity (obtained from the DIC system) with the approximate crack velocity for tests conducted at 25°C (77°F) and 50 mm/min (0.03280 in/sec) and two different specimen (L4 and L5): (a) Crack position obtained from the DIC system and polynomial fit, and (b) true crack velocity obtained from crack position from DIC and approximate crack velocity directly obtained from the experimental data.

An empirical correlation between the approximate crack velocity and candidate FI parameters is shown in Figure 27. Among the parameters derived from the load-displacement curve, post-peak slope ( $m$ ) appears to be the most sensitive to changes in testing conditions (loading rate and temperature) and material characteristics reflecting changes in crack growth speed. Therefore, correlation was improved when the slope ( $m$ ) was used to define the FI.

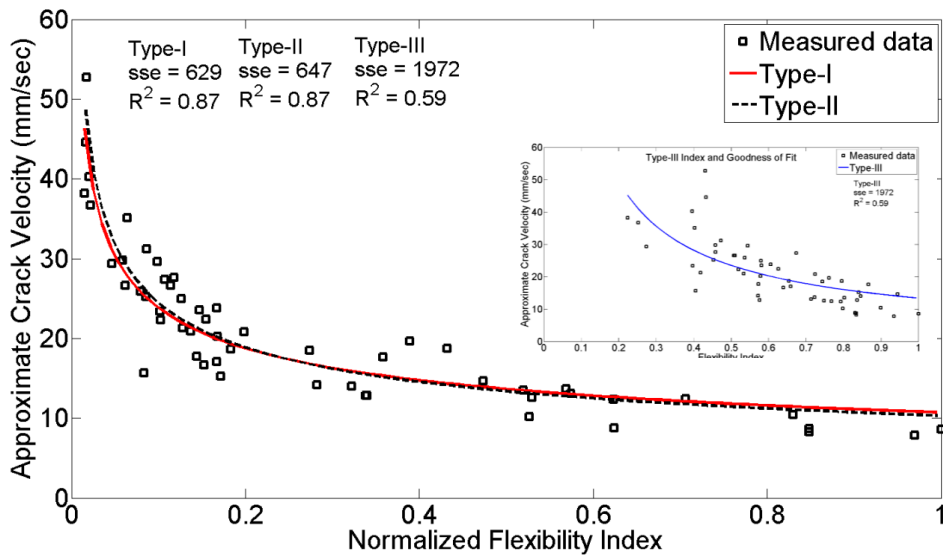


Figure 27: Correlation between normalized FI parameters (Types I, II, and, III corresponding to Equations 7a through 7c, respectively) and approximate crack velocity derived from SCB tests conducted at 25°C (77°F) and 50 mm/min (0.03280 in/sec).

The form of the FI with fracture energy and post-peak slope (Type I in Figure 27) was chosen as the final form because of its simplicity and good correlation to crack propagation growth. The final form of the proposed FI is presented in Equation 8. Coefficient A is a calibration coefficient for unit conversions and possibly field aging shift. A is equal to 0.01 for plant and lab compacted mixes in this study. However, this value may change for field specimens when aging and field compaction are considered.

$$FI = A \times \frac{G_{fa}}{abs(m)} \quad (8)$$

The FI values for the lab design AC mixes are shown in Figure 28 by normalizing the index with respect to the control AC with PG70-22. Changes in behavior from the control AC mix with a polymer-modified binder to the AC mix with different levels of RAS and normal grade binder are captured through the FI values. For example, when L4 was modified to L8 with the addition of 2.5% RAS, the FI captured this modification with a decrease in FI indicating brittleness. When L7 was modified to L6 with the addition of another 2.5% RAS, the FI also captured the change. The evolution of the FI with critical changes in the mix design characteristics was consistent and reflected the brittleness of the material observed in the load-displacement curves as well as the increase in crack propagation speed. Therefore, there exists a strong inverse correlation between crack velocity and FI, unlike fracture energy, which, for example, ranked L6, L7, and L8 similar to, or even better than, L4 although the latter exhibited slower crack propagation speeds.

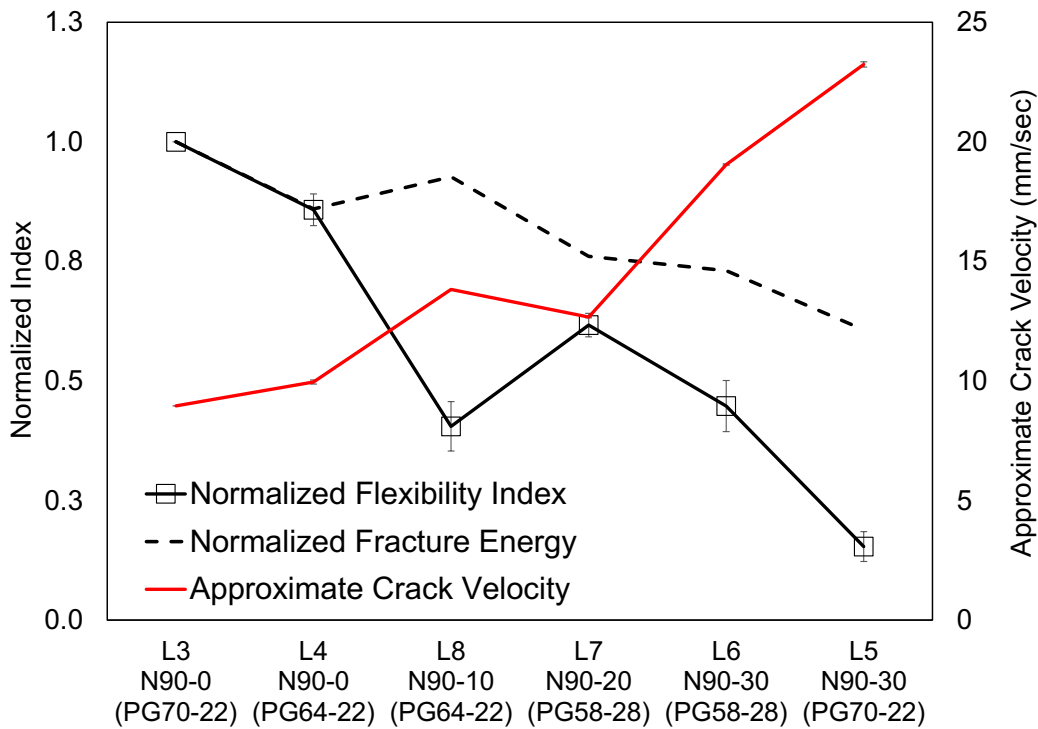


Figure 28: Normalized FI for lab design mixes (L3 to L7) calculated at 25 °C (77°F) illustrating the reduction in flexibility with changes in AC mix design characteristics and compared with approximate crack velocity and normalized fracture energy.

### 6.3 Implementation of Selected Index

Figure 29 illustrates the results for some of the mixes evaluated using the FI. Mix P7 is free of recycled content and has polymer-modified binder; whereas, Mixes P1 to P4 contain high levels of recycled binder. Mix P5 does not contain significant recycled content, but ranked as the worst performing material in the fatigue and SCB tests. According to the results obtained from these plant AC mixes, the proposed FI ranked mixes consistently and generated greater separation to allow for capturing nuances between AC mixes.



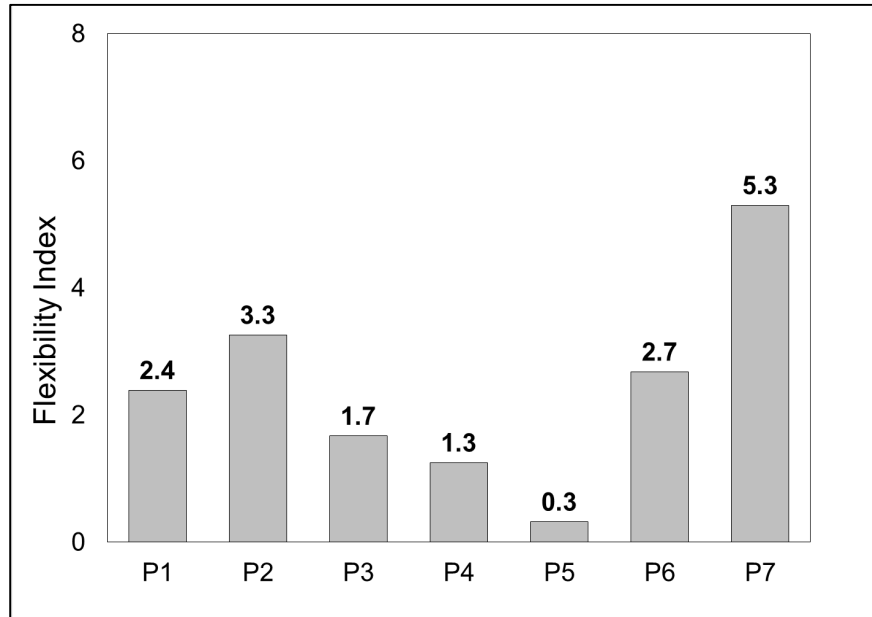


Figure 29: Flexibility Index calculated for selected plant mixes.

The FI values and fracture energy are shown in Figure 30 for all mixes. The values were normalized with respect to the control mix with PG 70-22. The overall pattern with the FI reflected consistent reduction with increasing ABR. The reduction was much more pronounced when compared to fracture energy values obtained at the same temperature. Some key findings from the comparison of FI values for different AC mixes include the following:

- The worst FI values belonged to L5 (N90-30% ABR with PG 70-22) and L10 (N90-60 % ABR with PG 52-34).
- Mixes with similar ABR content, same binder type, but different proportions of RAS (L6, L9, L12, and L13) had similar FI values, indicating that RAS source did not have a significant impact.
- The changes in the binder grade had a clear impact on FI values. Mixes with the same ABR, similar RAS type and content, but stiffer binder such as L5 (N90-30% ABR with PG 70-22) showed significant separation in terms of FI compared with a softer binder L6 (N90-30% ABR with PG 58-22).

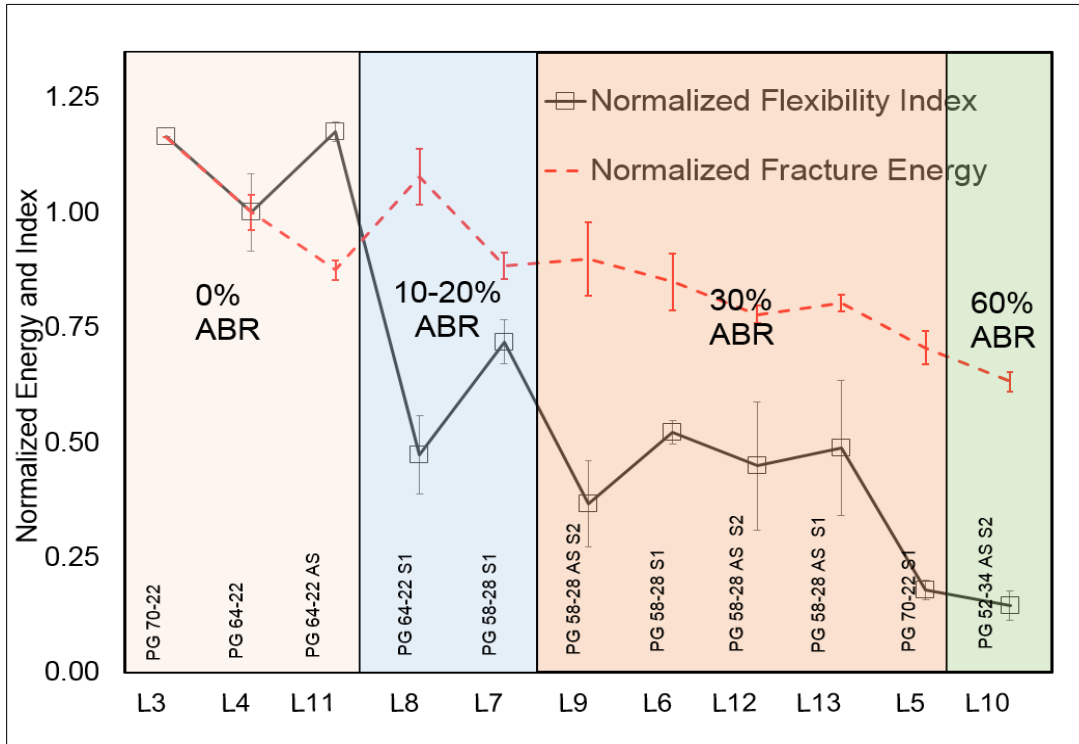


Figure 30. Normalized SCB fracture energy and FI for lab mixes.

## 6.4 Summary

This study introduces a practical test method and develops an index parameter for characterizing the fracture potential of AC mixes. The Flexibility Index is introduced to identify the resistance of AC mixes for development of cracking related damage in the field. Formulation of the FI is consistent with the fundamental fracture mechanics principles and displays strong correlation to the crack velocity determined from experiments to indicate crack propagation. Plant and laboratory AC mixes showed that the FI captures changes in the AC mixtures better than a sole fracture energy parameter. The ranking obtained using the FI was consistent with the changes in AC mix volumetrics and independent test outcomes.

## 7. Conclusions and Recommendations

In this study, a feasible test method was developed having the capability of screening asphalt mixtures cracking potential. The study proposes running the IL-SCB test method at 25°C (77°F) and a displacement rate of 50 mm/min (0.03280 in/sec). The test is referred to as Illinois Flexibility Index Test (I-FIT).

The approach to develop this test method considered plant-produced, lab-produced, and lab-designed AC mixtures. The AC mixes characteristics were valuated under a variety of performance-based tests, including fatigue life, rutting potential, and carious cracking potential tests. The two primary cracking tests evaluated were the disc-compact tension (DCT) test and the semi-circular bending (SCB) test. Various test temperatures and displacement rates were explored, and the most suitable combination was selected, keeping in mind the objective of AC mixture differentiation.

Ultimately, the introduced test method was coupled with an index parameter, the Flexibility Index (FI), to characterize the fracture potential of AC mixes. The FI was derived from the load-displacement response incorporating fracture energy and slope of the load-displacement curve after a crack begins to propagate. The FI correlated very well with the speed of crack propagation in the IL-SCB tests. The Flexibility Index was capable of quantifying the effects of binder grade bumping and ABR levels; as ABR decreased, the Flexibility Index increased.

The following criteria—along with simplicity, repeatability, efficiency, and cost effectiveness—were considered when selecting the test method:

1. *Significant spread in the test output* is needed to develop a threshold and quantify the differences between AC mixtures possessing varying cracking potential. Without a test method that does this, these differences may be hidden by statistical variation. The developed test provides distinction between AC materials that is greater than potential statistical variation.
2. *Applicability and seamless implementation* of the developed method is needed to ensure accessibility to state agencies and contractors and widespread adoption. The developed test method is affordable, simple to run, and time-efficient.
3. *Correlation to independent tests and engineering intuition* is needed. A comparison between intermediate temperature IL-SCB and Texas Overlay results was conducted and results were found to correlate well at the high performance and low performance ends of the cracking potential spectrum.

The findings and observations resulting from this study include the following:

- Results indicate that the Texas Overlay Test is able to roughly distinguish between AC mixtures with varying amounts of ABR content. However, the test variability is relatively high.
- Pronounced differences in mix design characteristics were masked by Low-temperature cracking tests (DCT and low-temperature SCB).
- Fracture testing displayed results that were heavily dependent on the temperature and rate of displacement. Differences between AC materials are most pronounced at selected temperature and loading rate of 25°C (77°F) and 50 mm/min (0.03280 in/sec). Data at these testing conditions displayed consistent and repeatable data while clearly distinguishing between different mix design characteristics.

## References

- Al-Qadi, I., Ozer, H., Lambros, J., El Khatib, A., Singhvi, P., Khan, T., ... Doll, B. (2015). *Testing Protocols to Ensure Performance of High Asphalt Binder Replacement Mixes Using RAP and RAS*. Urbana.
- Al-Qadi, I., Ozer, H., Lambros, J., Lippert, D., El Khatib, A., Khan, T., & Singh, P. (2015). Testing Protocols to Ensure Mix Performance w/ High RAP and RAS. In *Bituminous Conference*. Urbana-Champaign.
- Andy Cascione, R. Christopher Williams, Debra Haugen, Mihai Marastaneu, and J. M. (2010). Performance of Recycled Asphalt Shingles in Hot Mix Asphalt Pooled Fund Study TPS-5(213). *Pooled Fund Study, TPS-5(213)*.
- Apeageyi, A. K., Diefenderfer, B. K., & Diefenderfer, S. D. (2011). Rutting Resistance of Asphalt Concrete Mixtures That Contain Recycled Asphalt Pavement. *Transportation Research Record: Journal of the Transportation Research Board*, 2208(-1), 9–16. <http://doi.org/10.3141/2208-02>
- Behnia, B., Dave, E. V., Ahmed, S., Buttlar, W. G., & Reis, H. (2011). Effects of recycled asphalt pavement amounts on low-temperature cracking performance of asphalt mixtures using acoustic emissions. *Transportation Research Record*, (2208), 64–71. <http://doi.org/10.3141/2208-09>
- Braham, A., Zofka, A., Li, X., & Ni, F. (2012). Exploring the reduction of laboratory testing for the cohesive zone model for asphalt concrete. *International Journal of Pavement Engineering*, 13(4), 350–359. <http://doi.org/10.1080/10298436.2011.595792>
- Carpenter, S. (2007). *Dynamic Modulus Performance of IDOT Mixtures*. Urbana-Champaign.
- Cooper, S., Mohammad, L., Kabir, S., & King, W. (2014). Balanced Asphalt Mixture Design Through Specification Modification. *Transportation Research Record: Journal of the Transportation Research Board*, 2447, 92–100. <http://doi.org/10.3141/2447-10>
- Foxlow, J. J., Daniel, J. S., & Swamy, A. K. (2011). RAP or RAS? The differences in performance of HMA containing reclaimed asphalt pavement and reclaimed asphalt shingles. In *Asphalt Paving Technology: Association of Asphalt Paving Technologists-Proceedings of the Technical Sessions* (Vol. 80, pp. 347–373). Tampa, FL, United states.
- Hansen, K., & Copeland, A. (2014). *Asphalt Pavement Industry Survey on Recycled Materials and Warm-Mix Asphalt Usage*. Lanham.
- Harvey, J., Wu, R., Signore, J., Basheer, I., Holikatti, S., Vacura, P., ... Kluttz, R. (2014). Application of Asphalt Mix Performance-Based Specifications. *Transportation Research Board*.
- Ozer, H., Al-Qadi, I. and A. K. (2012). Laboratory Evaluation of High Asphalt Binder Replacement with Recycled Asphalt Shingles ( RAS ) for a Low N-Design Asphalt Mixture, (June 2012).
- Huang, B., Shu, X., & Tang, Y. (2005). Comparison of Semi-Circular Bending and indirect Tensile strength

tests for HMA mixtures. *Advances in Pavement Engineering*. Retrieved from [http://ascelibrary.org/doi/pdf/10.1061/40776\(155\)14](http://ascelibrary.org/doi/pdf/10.1061/40776(155)14)

Al-Qadi, I., Carpenter, S. H., Pine, W. J., & Trepanier, J. (2012). Impact of High RAP Content on Structural and Performance Properties of Asphalt Mixtures, (12).

Khan, T. (2015). *Displacement Rate and Temperature Effect on Asphalt Concrete Cracking*. University of Illinois at Urbana-Champaign.

Kim, B. Y. R., Baek, C., Underwood, B. S., Subramanian, V., Guddati, M. N., & Lee, K. (2008). Application of Viscoelastic Continuum Damage Model Based Finite Element Analysis to Predict the Fatigue Performance of Asphalt Pavements, *12*(2), 109–120. <http://doi.org/10.1007/s12205-008-0109-x>

Li, X., Marasteanu, M. O., Williams, R. C., & Clyne, T. R. (2008). Effect of Reclaimed asphalt Pavement (Proportion and Type) and Binder Grade on Asphalt Mixtures. *Transportation Research Record*, (2051), 90–97. <http://doi.org/10.3141/2051-11>

Ozer, H., Al-Qadi, I. L., Lambros, J., El-Khatib, A., Singhvi, P., & Doll, B. (2016). Development of the fracture-based flexibility index for asphalt concrete cracking potential using modified semi-circle bending test parameters. *Construction and Building Materials*, *115*, 390–401. <http://doi.org/10.1016/j.conbuildmat.2016.03.144>

Ozer, H., Al-Qadi, I., Singhvi, P., Khan, T., Perez, J., & El Khatib, A. (2016). Fracture Characterization of Asphalt Mixtures with High Recycled Content Using Illinois Semicircular Bending Test Method and Flexibility Index. *Transportation Research Board*, *2*.

Rebecca McDaniel, and R. M. A. (2001). *NCHRP, Recommended Use of Reclaimed Asphalt Pavement in the Superpave Mix Design Method: Technician's Manual*.

Rebecca S. McDaniel, Ayesh Shah, and G. H. (2012). *Investigation of Low and High Temperature Properties of Plant Produced RAP Mixtures*. West Lafayette, IN.

Saadeh, S., & Eljairi, O. (2011). *Development of a Quality Control Test Procedure for Characterizing Fracture Properties of Asphalt Mixtures*.

Tabaković, A., Gibney, A., McNally, C., & Gilchrist, M. (2010). Influence of Recycled Asphalt Pavement on Fatigue Performance of Asphalt Concrete Base Courses. *Journal of Materials in Civil Engineering*, *22*(6), 643–650. [http://doi.org/10.1061/\(ASCE\)MT.1943-5533.0000093](http://doi.org/10.1061/(ASCE)MT.1943-5533.0000093)

Vavrik, W., Carpenter, S., Gillen, S., Behnke, J., & Fred, G. (2008). *Evaluation of Field-Produced Hot Mix Asphalt (HMA) Mixtures With Fractionated Recycled Asphalt Pavement (RAP)*. Champaign.

Walubita, L. F., Faruk, A. N. M., Hu, X., Malunga, R., Teshale, E. Z., & Scullion, T. (2014). The Search for a Practical Laboratory Cracking Test for Evaluating Bituminous ( HMA ) Mixes, 178–185.

- Williams, R. C., Ph, D., Haugen, D. S., Buttlar, W. G., Bentsen, R. A., & Behnke, J. (2011). CHARACTERIZATION OF HOT MIX ASPHALT CONTAINING POST-CONSUMER RECYCLED ASPHALT SHINGLES AND FRACTIONATED RECLAIMED ASPHALT PAVEMENT FINAL REPORT Prepared By : Andrew Cascione Iowa State University Department of Civil , Construction and Environmental Engine, (January).
- Witczak, M. W., Kaloush, K., Pellinen, T., & El-Basyouny, M. (2002). *NCHRP Report 465: Simple Performance Test for Superpave Mix Design*. Tempe.
- Xiao, F., Amirkhanian, S., & Juang, C. H. (2007). Rutting Resistance of Rubberized Asphalt Concrete Pavements Containing Reclaimed Asphalt Pavement Mixtures. *Journal of Materials in Civil Engineering*, 19(6), 475–483. [http://doi.org/10.1061/\(ASCE\)0899-1561\(2007\)19:6\(475\)](http://doi.org/10.1061/(ASCE)0899-1561(2007)19:6(475))
- Zhou, F. and S. T. (2005). *Overlay Tester: A rapid performance related to crack resistance test* (Vol. 7).

## Appendix A: Laboratory Mix Designs

**Table 15 Aggregate Gradations of Material Used in Design of Laboratory Mixes**

Sieve	CM16	FM20	FM22	Mineral Filler	RAP* (3/8 in)	RAP* (-3/8 in)	RAS* Source 1	RAS* Source 2
1 in	100	100	100	100	100	100	100	100
3/4 in	100	100	100	100	99.3	100	100	100
1/2 in	100	100	100	100	90.8	100	100	100
3/8 in	97	100	100	100	78.6	99.3	100	100
No. 4	32	97	100	100	39	71.7	98.5	96.1
8	9	68	94.5	100	26.5	48.6	95.4	93.3
16	7	40	72	100	19.1	32.6	75.9	77.1
30	6	24	49	100	14.8	24.2	50.8	57.1
50	6	15	19.9	100	10.7	17.2	42.9	49.4
100	5	9	4.1	95	7.7	12.7	37.2	43.0
200	4.6	6.7	1.5	90	6	10.1	30.6	34.2
Binder Content	%	—	—	—	4.2	5.1	26.7	27.4

\*Extracted gradation



**Table 16 Mix Design Characteristics of Plant- and Laboratory-Produced Mixes and Testing Program Applied to Each Mix**

Mix ID	Mix Name	Mixture Source	Binder Grade	RAP %	RAS %	ABR %	AC %	VMA %	E*	TOL	-12°C SCB	25°C SCB
P1 <sup>1</sup>	N50 SC <sup>3</sup>	<b>TOL Study</b>	52-28	50	3.5	60	6.7	15		X	X	X
P2 <sup>1</sup>	N50 SC <sup>3</sup>		58-28	27	—	29	5.8	14.7		X	X	X
P3	N70 BC <sup>4</sup>		58-28	26	—	29	4.8	13.4		X	X	X
P4	N30 BC <sup>4</sup>		58-28	46.5	—	37	4.8	13.6		X	X	X
P5	N70 SC <sup>3</sup>		64-22	10	—	6	6.1	15.8		X	X	X
P6	N90 SC <sup>3</sup>		76-22	10	—	6	5.6	14.1		X	X	X
P7	N50 SC <sup>3</sup>		64-22	—	—	—	5.9	16.7		X	X	X
P8	N50-50	<b>Designs by S.T.A.T.E. Testing</b>	58-28	42	4	49	5.5	13	X		X	X
P9	N50-60		52-28	42	6	59	5.6	13	X		X	X
P10	N70-25		58-28	29	—	25	6	14.5	X		X	X
P11	N70-50		58-28	30	5	48	6	14.5	X		X	X
P12	N80-25		70-28	8	5	26	6.1	16.1	X		X	X
P13	N80-50		70-28	10	8	50	6	15.8	X		X	X
P14 <sup>1</sup>	N50-Joliet	<b>Total Recycle Mixes</b>	58-28	30	—	34	5.39	15.3	X		X	X
P15 <sup>1,2</sup>	N50-Sandeno		52-28	52	4	60	6.72	15.1	X		X	X
P16 <sup>1,2</sup>	N50-K5		52-28	53	5	57	6.5	14.9			X	X
L3	N90 0 CG	<b>Laboratory Design Mixtures</b>	<b>70-22</b>	—	—	—	6	15.3	X		X	X
L4	N90 0 CG		<b>64-22</b>	—	—	—	6	15.3	X		X	X
L5	N90 30 CG S1 <sup>7</sup>		<b>70-22</b>	—	7	29.8	6	15.3			X	X
L6	N90 30 CG S1 <sup>7</sup>		<b>58-28</b>	—	7	29.8	6	15.3			X	X
L7	N90 20 CG S1 <sup>7</sup>		<b>58-28</b>	—	5	21.2	6	15.3			X	X
L8	N90 10 CG S1 <sup>7</sup>		<b>64-22</b>	—	2.5	10.5	6	15.3	X		X	X
L9	N90 30 CG S2 <sup>8</sup> AS <sup>5</sup>		<b>58-28</b>	11	5	30.5	6	15.2	X		X	X
L10	N90 60 CG S2 <sup>8</sup> AS <sup>5</sup>		<b>52-34</b>	40	7	60.8	6.1	15.2			X	X
L11	N90 0 CG AS <sup>5</sup>		<b>64-22</b>	—	—	—	6	15.3			X	X
L12	N90 30 CG <sup>6</sup> S2 <sup>8</sup> AS <sup>5</sup>		<b>58-28</b>	—	7	30.6	6	15.2			X	X
L13	N90 30 CG <sup>6</sup> S1 <sup>7</sup> AS <sup>5</sup>		<b>58-28</b>	—	7	29.8	6	15.3			X	X

X = Test was performed for this mix.

<sup>1</sup> AC containing steel slag.

<sup>2</sup> AC containing recycled concrete aggregate (RCA)

<sup>3</sup> Surface course AC, placed at the top-most layer of the pavement and exposed to traffic.

<sup>4</sup> Base course AC, placed directly below the surface course.

<sup>5</sup> AS mixture with 1% anti-strip added to virgin binder.

<sup>7</sup> RAS source (S1)

<sup>6</sup> These mixtures have different RAS sources but similar mix design.

<sup>8</sup> RAS source (S2).

**Table 17 Laboratory Mix Design L3**

<b>AGGREGATE DETAILS</b>						
Agg. Blending %	CM16	FM20	FM02	RAS	MF	Target
		61.5	26.9	11.3	0.0	0.3
% Passing Sieve						
1" (25.0 mm)	100.0	100.0	100.0	100.0	100.0	100.0
3/4" (19.0 mm)	100.0	100.0	100.0	100.0	100.0	100.0
1/2" (12.5 mm)	100.0	100.0	100.0	100.0	100.0	100.0
3/8" (9.5 mm)	97.0	100.0	100.0	99.8	100.0	98.2
No. 4 (4.75 mm)	32.0	97.0	100.0	98.8	100.0	57.4
No. 8 (2.36 mm)	9.0	68.0	94.5	95.4	100.0	34.8
No. 16 (1.18 mm)	7.0	40.0	72.0	75.9	100.0	23.5
No. 30 (600 µm)	6.0	24.0	49.0	50.8	100.0	16.0
No. 50 (300 µm)	6.0	15.0	19.9	42.9	100.0	10.3
No. 100 (150 µm)	5.0	9.0	4.1	37.2	95.0	6.2
No. 200 (75 µm)	4.6	6.7	1.5	30.6	90.0	5.1
Bulk Spec Gravity (Gsb)	2.644	2.691	2.619	2.500	2.900	2.654
Apparent Spec Gravity (Gsa)	2.792	2.796	2.719		2.900	#DIV/0!
Absorption (%)	2.0	1.4	1.4	1.0		1.723

<b>Notes:</b>

<b>BINDER DETAILS</b>	
Binder Type	PG 70 - 22
Specific Gravity, G <sub>b</sub>	1.03

<b>MIXING CONDITIONS</b>	
Mixing Temperature	160 C
Compaction Temperature	150 C
G <sub>mm</sub>	2.491

<b>VOLUMETRICS</b>										
Binder%	Gmb @ N90	Ht @N90 (mm)	VTM	VMA	DP	VFA	% Gmm @ Nini	Gse	Absorbed Asphalt	Effective Asphalt
6%	2.394	115.36	3.9%	15.2%	0.85	74.4%		2.739	1.20%	4.87%
6%	2.399	114.89	3.7%	15.0%	0.85	75.4%		2.739	1.20%	4.87%
6%	2.387	115.78	4.2%	15.5%	0.85	73.0%		2.739	1.20%	4.87%

**Table 18 Laboratory Mix Design L4**

<b>AGGREGATE DETAILS</b>						
Agg. Blending %	CM16	FM20	FM02	RAS	MF	Target
	61.5	26.9	11.3	0.0	0.3	100.0
% Passing Sieve						
1" (25.0 mm)	100.0	100.0	100.0	100.0	100.0	100.0
3/4" (19.0 mm)	100.0	100.0	100.0	100.0	100.0	100.0
1/2" (12.5 mm)	100.0	100.0	100.0	100.0	100.0	100.0
3/8" (9.5 mm)	97.0	100.0	100.0	99.8	100.0	98.2
No. 4 (4.75 mm)	32.0	97.0	100.0	98.8	100.0	57.4
No. 8 (2.36 mm)	9.0	68.0	94.5	95.4	100.0	34.8
No. 16 (1.18 mm)	7.0	40.0	72.0	75.9	100.0	23.5
No. 30 (600 µm)	6.0	24.0	49.0	50.8	100.0	16.0
No. 50 (300 µm)	6.0	15.0	19.9	42.9	100.0	10.3
No. 100 (150 µm)	5.0	9.0	4.1	37.2	95.0	6.2
No. 200 (75 µm)	4.6	6.7	1.5	30.6	90.0	5.1
Bulk Spec Gravity (Gsb)	2.644	2.691	2.619	2.500	2.900	2.654
Apparent Spec Gravity (Gsa)	2.792	2.796	2.719		2.900	#DIV/0!
Absorption (%)	2.0	1.4	1.4	1.0		1.723

<b>Notes:</b>	

<b>BINDER DETAILS</b>	
Binder Type	PG 64-22
Specific Gravity, G <sub>b</sub>	1.03

<b>MIXING CONDITIONS</b>	
Mixing Temperature	150 C
Compaction Temperature	150 C
G <sub>mm</sub>	2.496

<b>VOLUMETRICS</b>										
Binder%	Gmb @ N90	Ht @N90 (mm)	VTM	VMA	DP	VFA	% Gmm @ Nini	Gse	Absorbed Asphalt	Effective Asphalt
6%	2.392	115.36	4.2%	15.3%	0.85	72.7%		2.745	1.29%	4.79%
6%	2.393	114.89	4.1%	15.3%	0.85	72.9%		2.745	1.29%	4.79%

**Table 19 Laboratory Mix Design L5**

<b>AGGREGATE DETAILS</b>						
Agg. Blending %	CM16	FM20	FM02	RAS	MF	Target
	63.5	16.0	12.5	7.0	1.0	100.0
% Passing Sieve						
1" (25.0 mm)	100.0	100.0	100.0	100.0	100.0	100.0
3/4" (19.0 mm)	100.0	100.0	100.0	100.0	100.0	100.0
1/2" (12.5 mm)	100.0	100.0	100.0	100.0	100.0	100.0
3/8" (9.5 mm)	97.0	100.0	100.0	99.8	100.0	98.1
No. 4 (4.75 mm)	32.0	97.0	100.0	98.8	100.0	56.3
No. 8 (2.36 mm)	9.0	68.0	94.5	95.4	100.0	36.1
No. 16 (1.18 mm)	7.0	40.0	72.0	75.9	100.0	26.2
No. 30 (600 µm)	6.0	24.0	49.0	50.8	100.0	18.3
No. 50 (300 µm)	6.0	15.0	19.9	42.9	100.0	12.7
No. 100 (150 µm)	5.0	9.0	4.1	37.2	95.0	8.7
No. 200 (75 µm)	4.6	6.7	1.5	30.6	90.0	7.2
Bulk Spec Gravity (Gsb)	2.644	2.691	2.619	2.500	2.900	2.640
Apparent Spec Gravity (Gsa)	2.792	2.796	2.719		2.900	#DIV/0!
Absorption (%)	2.0	1.4	1.4	1.0		1.692

<b>Notes:</b>	

<b>BINDER DETAILS</b>	
Binder Type	PG 70 - 22
Specific Gravity, G <sub>b</sub>	1.03

<b>MIXING CONDITIONS</b>	
Mixing Temperature	160 C
Compaction Temperature	150 C
G <sub>mm</sub>	2.476

<b>VOLUMETRICS</b>										
Binder%	Gmb @ N90	Ht @N90 (mm)	VTM	VMA	DP	VFA	% Gmm @ Nini	Gse	Absorbed Asphalt	Effective Asphalt
6%	2.381	113.83	3.8%	15.2%	1.20	74.8%		2.720	1.14%	4.92%
6%	2.362	114.65	4.6%	15.9%	1.20	71.0%		2.720	1.14%	4.92%
6%	2.377	113.68	4.0%	15.4%	1.20	74.0%		2.720	1.14%	4.92%

**Table 20 Laboratory Mix Design L6**

<b>AGGREGATE DETAILS</b>						
Agg. Blending %	CM16	FM20	FM02	RAS	MF	Target
		63.5	16.0	12.5	7.0	1.0
% Passing Sieve						
1" (25.0 mm)	100.0	100.0	100.0	100.0	100.0	100.0
3/4" (19.0 mm)	100.0	100.0	100.0	100.0	100.0	100.0
1/2" (12.5 mm)	100.0	100.0	100.0	100.0	100.0	100.0
3/8" (9.5 mm)	97.0	100.0	100.0	99.8	100.0	98.1
No. 4 (4.75 mm)	32.0	97.0	100.0	98.8	100.0	56.3
No. 8 (2.36 mm)	9.0	68.0	94.5	95.4	100.0	36.1
No. 16 (1.18 mm)	7.0	40.0	72.0	75.9	100.0	26.2
No. 30 (600 µm)	6.0	24.0	49.0	50.8	100.0	18.3
No. 50 (300 µm)	6.0	15.0	19.9	42.9	100.0	12.7
No. 100 (150 µm)	5.0	9.0	4.1	37.2	95.0	8.7
No. 200 (75 µm)	4.6	6.7	1.5	30.6	90.0	7.2
Bulk Spec Gravity (Gsb)	2.644	2.691	2.619	2.500	2.900	2.640
Apparent Spec Gravity (Gsa)	2.792	2.796	2.719		2.900	#DIV/0!
Absorption (%)	2.0	1.4	1.4	1.0		1.692

Notes:

<b>BINDER DETAILS</b>	
Binder Type	PG 58 - 28
Specific Gravity, G <sub>b</sub>	1.03

<b>MIXING CONDITIONS</b>	
Mixing Temperature	153C
Compaction Temperature	147C
G <sub>mm</sub>	2.485

<b>VOLUMETRICS</b>										
Binder%	Gmb @ N90	Ht @N90 (mm)	VTM	VMA	DP	VFA	% Gmm @ Nini	Gse	Absorbed Asphalt	Effective Asphalt
6%	2.370	113.88	4.6%	15.6%	1.20	70.4%		2.731	1.31%	4.77%
6%	2.370	113.75	4.6%	15.6%	1.20	70.4%		2.731	1.31%	4.77%

**Table 21 Laboratory Mix Design L7**

<b>AGGREGATE DETAILS</b>						
Agg. Blending %	CM16	FM20	FM02	RAS	MF	Target
		63.5	18.0	13.1	5.0	0.4
% Passing Sieve						
1" (25.0 mm)	100.0	100.0	100.0	100.0	100.0	100.0
3/4" (19.0 mm)	100.0	100.0	100.0	100.0	100.0	100.0
1/2" (12.5 mm)	100.0	100.0	100.0	100.0	100.0	100.0
3/8" (9.5 mm)	97.0	100.0	100.0	99.8	100.0	98.1
No. 4 (4.75 mm)	32.0	97.0	100.0	98.8	100.0	56.2
No. 8 (2.36 mm)	9.0	68.0	94.5	95.4	100.0	35.5
No. 16 (1.18 mm)	7.0	40.0	72.0	75.9	100.0	25.3
No. 30 (600 µm)	6.0	24.0	49.0	50.8	100.0	17.5
No. 50 (300 µm)	6.0	15.0	19.9	42.9	100.0	11.7
No. 100 (150 µm)	5.0	9.0	4.1	37.2	95.0	7.6
No. 200 (75 µm)	4.6	6.7	1.5	30.6	90.0	6.2
Bulk Spec Gravity (Gsb)	2.644	2.691	2.619	2.500	2.900	2.642
Apparent Spec Gravity (Gsa)	2.792	2.796	2.719		2.900	#DIV/0!
Absorption (%)	2.0	1.4	1.4	1.0		1.696

<b>Notes:</b>

<b>BINDER DETAILS</b>	
Binder Type	PG 58-28
Specific Gravity, G <sub>b</sub>	1.03

<b>MIXING CONDITIONS</b>	
Mixing Temperature	153C
Compaction Temperature	147C
G <sub>mm</sub>	2.484

<b>VOLUMETRICS</b>										
Binder%	Gmb @ N90	Ht @N90 (mm)	VTM	VMA	DP	VFA	% Gmm @ Nini	Gse	Absorbed Asphalt	Effective Asphalt
6%	2.388	113.7	3.9%	15.0%	1.04	74.3%		2.730	1.25%	4.82%
6%	2.383	114.18	4.1%	15.2%	1.04	73.3%		2.730	1.25%	4.82%

**Table 22 Laboratory Mix Design L8**

<b>AGGREGATE DETAILS</b>						
Agg. Blending %	CM16	FM20	FM02	RAS	MF	Target
		63.5	18.5	15.5	2.5	0.0
% Passing Sieve						
1" (25.0 mm)	100.0	100.0	100.0	100.0	100.0	100.0
3/4" (19.0 mm)	100.0	100.0	100.0	100.0	100.0	100.0
1/2" (12.5 mm)	100.0	100.0	100.0	100.0	100.0	100.0
3/8" (9.5 mm)	97.0	100.0	100.0	99.8	100.0	98.1
No. 4 (4.75 mm)	32.0	97.0	100.0	98.8	100.0	56.2
No. 8 (2.36 mm)	9.0	68.0	94.5	95.4	100.0	35.3
No. 16 (1.18 mm)	7.0	40.0	72.0	75.9	100.0	24.9
No. 30 (600 µm)	6.0	24.0	49.0	50.8	100.0	17.1
No. 50 (300 µm)	6.0	15.0	19.9	42.9	100.0	10.7
No. 100 (150 µm)	5.0	9.0	4.1	37.2	95.0	6.4
No. 200 (75 µm)	4.6	6.7	1.5	30.6	90.0	5.2
Bulk Spec Gravity (Gsb)	2.644	2.691	2.619	2.500	2.900	2.645
Apparent Spec Gravity (Gsa)	2.792	2.796	2.719		2.900	#DIV/0!
Absorption (%)	2.0	1.4	1.4	1.0		1.708

Notes:

<b>BINDER DETAILS</b>	
Binder Type	PG 64-22
Specific Gravity, G <sub>b</sub>	1.03

<b>MIXING CONDITIONS</b>	
Mixing Temperature	157C
Compaction Temperature	150C
G <sub>mm</sub>	2.488

<b>VOLUMETRICS</b>										
Binder%	Gmb @ N90	Ht @N90 (mm)	VTM	VMA	DP	VFA	% Gmm @ Nini	Gse	Absorbed Asphalt	Effective Asphalt
6%	2.385	114.93	4.1%	15.2%	0.86	72.8%		2.735	1.29%	4.79%
6%	2.380	115.18	4.3%	15.4%	0.86	71.8%		2.735	1.29%	4.79%

**Table 23 Laboratory Mix Design L9**

AGGREGATE DETAILS											
Agg. Blending %	CM16	FM20	FM02	RAP(-3/8)	RAP(+3/8)	RAS	MF	Target			
	56.0	17.8	9.9	7.0	4.0	5.0	0.3	100.0			
% Passing Sieve											
1" (25.0 mm)	100.0	100.0	100.0	100.0	100.0	100.0	100.0	100.0	Pavegrip Antistrip was added to the binder. (1% of total binder weight)		
3/4" (19.0 mm)	100.0	100.0	100.0	100.0	99.3	100.0	100.0	100.0			
1/2" (12.5 mm)	100.0	100.0	100.0	100.0	90.8	100.0	100.0	99.6			
3/8" (9.5 mm)	97.0	100.0	100.0	99.3	78.6	100.0	100.0	97.4			
No. 4 (4.75 mm)	32.0	97.0	100.0	71.7	39.0	97.2	100.0	56.8			
No. 8 (2.36 mm)	9.0	68.0	94.5	48.6	26.5	93.4	100.0	35.9			
No. 16 (1.18 mm)	7.0	40.0	72.0	32.6	19.1	77.1	100.0	25.4	<b>BINDER DETAILS</b>		
No. 30 (600 µm)	6.0	24.0	49.0	24.2	14.8	57.2	100.0	17.9			Binder Type
No. 50 (300 µm)	6.0	15.0	19.9	17.2	10.7	49.7	100.0	12.4	Specific Gravity, G <sub>b</sub>	1.03	
No. 100 (150 µm)	5.0	9.0	4.1	12.7	7.7	43.2	95.0	8.5			
No. 200 (75 µm)	4.6	6.7	1.5	10.1	6.0	34.4	90.0	6.9			
Bulk Spec Gravity (Gsb)	2.644	2.691	2.619	2.641	2.627	2.500	2.900	2.642	<b>MIXING CONDITIONS</b>		
Apparent Spec Gravity (Gsa)	2.792	2.796	2.719		2.900			#DIV/0!	Mixing Temperature	147C	
Absorption (%)	2.0	1.4	1.4	1.0				1.825	Compaction Temperature	143C	
									G <sub>mm</sub>	2.492	
VOLUMETRICS											
Binder%	Gmb @ N90	Ht @N90 (mm)	VTM	VMA	DP	gmm		VFA	Gse	Absorbed Asphalt	Effective Asphalt
6.00%	2.384	112.93	4.4%	15.2%	1.14	2.493		71.3%	2.740	1.40%	4.68%
6.00%	2.383	113.25	4.4%	15.2%	1.14	2.492		71.3%	2.740	1.40%	4.68%



**Table 24 Laboratory Mix Design L10**

AGGREGATE DETAILS											
Agg. Blending %	CM16	FM20	FM02	RAP(-3/8)	RAP(+3/8)	RAS	MF	Target			
	38.0	11.4	3.4	20.0	20.0	7.0	0.2	100.0			
% Passing Sieve											
1" (25.0 mm)	100.0	100.0	100.0	100.0	100.0	100.0	100.0	100.0	Pavegrip Antistrip was added to the binder. (1% of total binder weight)		
3/4" (19.0 mm)	100.0	100.0	100.0	100.0	99.3	100.0	100.0	99.9			
1/2" (12.5 mm)	100.0	100.0	100.0	100.0	90.8	100.0	100.0	98.2			
3/8" (9.5 mm)	97.0	100.0	100.0	99.3	78.6	100.0	100.0	94.4			
No. 4 (4.75 mm)	32.0	97.0	100.0	71.7	39.0	97.2	100.0	55.8			
No. 8 (2.36 mm)	9.0	68.0	94.5	48.6	26.5	93.4	100.0	36.1			
No. 16 (1.18 mm)	7.0	40.0	72.0	32.6	19.1	77.1	100.0	25.6			
No. 30 (600 µm)	6.0	24.0	49.0	24.2	14.8	57.2	100.0	18.7			
BINDER DETAILS											
No. 50 (300 µm)	6.0	15.0	19.9	17.2	10.7	49.7	100.0	13.9	Binder Type	PG 52-34	
No. 100 (150 µm)	5.0	9.0	4.1	12.7	7.7	43.2	95.0	10.4	Specific Gravity, G <sub>b</sub>	1.03	
No. 200 (75 µm)	4.6	6.7	1.5	10.1	6.0	34.4	90.0	8.4			
MIXING CONDITIONS											
Bulk Spec Gravity (Gsb)	2.644	2.691	2.619	2.641	2.627	2.500	2.900	2.634	Mixing Temperature	150C	
Apparent Spec Gravity (Gsa)	2.792	2.796	2.719		2.900			#DIV/0!	Compaction Temperature	144C	
Absorption (%)	2.0	1.4	1.4	1.0				2.017	G <sub>mm</sub>		
VOLUMETRICS											
Binder%	Gmb @ N90	Ht @N90 (mm)	VTM	VMA	DP	Gmm		VFA	Gse	Absorbed Asphalt	Effective Asphalt
6.10%	2.379	111.46	4.5%	15.2%	1.37	2.492		70.2%	2.745	1.58%	4.61%
6.10%	2.386	111.07	4.0%	14.9%	1.37	2.487		72.9%	2.745	1.58%	4.61%
6.10%	2.379	111.6	4.6%	15.2%	1.37	2.494		69.7%	2.745	1.58%	4.61%

**Table 25 Laboratory Mix Design L11**

<b>AGGREGATE DETAILS</b>						
Agg. Blending %	CM16	FM20	FM02	RAS	MF	Target
		61.5	26.9	11.3	0.0	0.3
% Passing Sieve						
1" (25.0 mm)	100.0	100.0	100.0	100.0	100.0	100.0
3/4" (19.0 mm)	100.0	100.0	100.0	100.0	100.0	100.0
1/2" (12.5 mm)	100.0	100.0	100.0	100.0	100.0	100.0
3/8" (9.5 mm)	97.0	100.0	100.0	99.8	100.0	98.2
No. 4 (4.75 mm)	32.0	97.0	100.0	98.8	100.0	57.4
No. 8 (2.36 mm)	9.0	68.0	94.5	95.4	100.0	34.8
No. 16 (1.18 mm)	7.0	40.0	72.0	75.9	100.0	23.5
No. 30 (600 µm)	6.0	24.0	49.0	50.8	100.0	16.0
No. 50 (300 µm)	6.0	15.0	19.9	42.9	100.0	10.3
No. 100 (150 µm)	5.0	9.0	4.1	37.2	95.0	6.2
No. 200 (75 µm)	4.6	6.7	1.5	30.6	90.0	5.1
Bulk Spec Gravity (Gsb)	2.644	2.691	2.619	2.500	2.900	2.654
Apparent Spec Gravity (Gsa)	2.792	2.796	2.719		2.900	#DIV/0!
Absorption (%)	2.0	1.4	1.4	1.0		1.723

**Notes:**

Pavegrip Antistrip was added to the binder. (1% of total binder weight)

<b>BINDER DETAILS</b>	
Binder Type	PG 64-22
Specific Gravity, G <sub>b</sub>	1.03

<b>MIXING CONDITIONS</b>	
Mixing Temperature	150 C
Compaction Temperature	150 C
G <sub>mm</sub>	2.496

<b>VOLUMETRICS</b>										
Binder%	Gmb @ N90	Ht @N90 (mm)	VTM	VMA	DP	VFA	% Gmm @ Nini	Gse	Absorbed Asphalt	Effective Asphalt
6%	2.392	115.36	4.2%	15.3%	0.85	72.7%		2.745	1.29%	4.79%
6%	2.393	114.89	4.1%	15.3%	0.85	72.9%		2.745	1.29%	4.79%

**Table 26 Laboratory Mix Design L12**

<b>AGGREGATE DETAILS</b>									
Agg. Blending %	CM16	FM20	FM02	RAS	MF	Target			
	64.0	15.5	12.5	7.0	1.0	100.0			
% Passing Sieve									
1" (25.0 mm)	100.0	100.0	100.0	100.0	100.0	100.0	Pavegrip Antistrip was added to the binder. (1% of total binder weight)		
3/4" (19.0 mm)	100.0	100.0	100.0	100.0	100.0	100.0			
1/2" (12.5 mm)	100.0	100.0	100.0	100.0	100.0	100.0			
3/8" (9.5 mm)	97.0	100.0	100.0	100.0	100.0	98.1			
No. 4 (4.75 mm)	32.0	97.0	100.0	97.2	100.0	55.8			
No. 8 (2.36 mm)	9.0	68.0	94.5	93.4	100.0	35.6			
No. 16 (1.18 mm)	7.0	40.0	72.0	77.1	100.0	26.1			
No. 30 (600 µm)	6.0	24.0	49.0	57.2	100.0	18.7			
No. 50 (300 µm)	6.0	15.0	19.9	49.7	100.0	13.1			
No. 100 (150 µm)	5.0	9.0	4.1	43.2	95.0	9.1			
No. 200 (75 µm)	4.6	6.7	1.5	34.4	90.0	7.5			
Bulk Spec Gravity (Gsb)	2.644	2.691	2.619	2.500	2.900	2.640			
Apparent Spec Gravity (Gsa)	2.792	2.796	2.719		2.900	#DIV/0!			
Absorption (%)	2.0	1.4	1.4	1.0		1.695			
							<b>BINDER DETAILS</b>		
							Binder Type	PG 64-22	
							Specific Gravity, G <sub>b</sub>	1.03	
							<b>MIXING CONDITIONS</b>		
							Mixing Temperature	153	
							Compaction Temperature	145	
							G <sub>mm</sub>	2.484	
<b>VOLUMETRICS</b>									
Binder%	Gmb @ N90	Ht @N90 (mm)	VTM	VMA	DP	VFA	Gse	Absorbed Asphalt	Effective Asphalt
6%	2.380	113.58	4.2%	15.3%	1.25	72.4%	2.730	1.29%	4.78%
6%	2.382	113.53	4.1%	15.2%	1.25	72.9%	2.730	1.29%	4.78%

**Table 27 Laboratory Mix Design L13**

<b>AGGREGATE DETAILS</b>						
Agg. Blending %	CM16	FM20	FM02	RAS	MF	Target
		63.5	16.0	12.5	7.0	1.0
% Passing Sieve						
1" (25.0 mm)	100.0	100.0	100.0	100.0	100.0	100.0
3/4" (19.0 mm)	100.0	100.0	100.0	100.0	100.0	100.0
1/2" (12.5 mm)	100.0	100.0	100.0	100.0	100.0	100.0
3/8" (9.5 mm)	97.0	100.0	100.0	99.8	100.0	98.1
No. 4 (4.75 mm)	32.0	97.0	100.0	98.8	100.0	56.3
No. 8 (2.36 mm)	9.0	68.0	94.5	95.4	100.0	36.1
No. 16 (1.18 mm)	7.0	40.0	72.0	75.9	100.0	26.2
No. 30 (600 µm)	6.0	24.0	49.0	50.8	100.0	18.3
No. 50 (300 µm)	6.0	15.0	19.9	42.9	100.0	12.7
No. 100 (150 µm)	5.0	9.0	4.1	37.2	95.0	8.7
No. 200 (75 µm)	4.6	6.7	1.5	30.6	90.0	7.2
Bulk Spec Gravity (Gsb)	2.644	2.691	2.619	2.500	2.900	2.640
Apparent Spec Gravity (Gsa)	2.792	2.796	2.719		2.900	#DIV/0!
Absorption (%)	2.0	1.4	1.4	1.0		1.692

**Notes:**

Pavegrip Antistrip was added to the binder. (1% of total binder weight)

<b>BINDER DETAILS</b>	
Binder Type	PG 58 - 28
Specific Gravity, G <sub>b</sub>	1.03

<b>MIXING CONDITIONS</b>	
Mixing Temperature	153C
Compaction Temperature	147C
G <sub>mm</sub>	2.485

<b>VOLUMETRICS</b>										
Binder%	Gmb @ N90	Ht @N90 (mm)	VTM	VMA	DP	VFA	% Gmm @ Nini	Gse	Absorbed Asphalt	Effective Asphalt
6%	2.370	113.88	4.6%	15.6%	1.20	70.4%		2.731	1.31%	4.77%
6%	2.370	113.75	4.6%	15.6%	1.20	70.4%		2.731	1.31%	4.77%

# Appendix B: Plant Mix Designs

## Table 28 Plant Mix 8 (P8)

IDOT Lab Verification No.:  Ver. 9.91-06.15.12 DATE: **October 15 2012**

Producer Number & Name → **4066-06 Rock Road Rockford** ← Plant Location **RR12003**

Material Code Number → **19512R HMA N50 19.0 REC BIND**

Plant Btr #	#5	#4	#3	#2	#1	MF	FRAP #3	FRAP #2	RAS #1	ASPHALT
Size	042CM11	032CM19			037FM01		017CM1204		017FM09	10126
Source (PROD #)	50072-01	50072-01			52010-02		4066-06		6616-04	5627-13
(NAME)	WCC	WCC			WCC		Rock Road		Southwind	BP Amoco
(LDC)	Irene	Irene			Alpert		Irene		So. Beloit	Barlett
(ADD. INFO)							Category 2			59-26
Aggregate Blend:	27.5	12.5	0.0	0.0	14.0	6.0	42.0	0.0	28.7	< AC in RAP
									Plan PG Grade >	PG 59-28
									4.0	100.0

Lab Preparing Design   
 Designing Lab Mtd **RR12003**  
 Designing Lab Name **S.T.A.T.E.**

Agg No.	#5	#4	#3	#2	#1	MF	FRAP #3	FRAP #2	RAS #1	Aggregate Blend	Mixture Comp Spec
1" (25.0mm)	100.0	100.0	100.0	100.0	100.0	100.0	100.0	100.0	100.0	100.0	100
3/4" (18.8mm)	88.0	100.0	100.0	100.0	100.0	100.0	100.0	100.0	100.0	97	82-109
1/2" (12.5mm)	34.0	100.0	100.0	100.0	100.0	100.0	100.0	100.0	100.0	82	50-65
3/8" (9.5mm)	7.0	94.0	100.0	100.0	100.0	100.0	96.5	100.0	100.0	72	
No.4 (4.75mm)	2.0	32.0	100.0	100.0	96.0	100.0	48.0	100.0	97.3	42	24-56
No.8 (2.36mm)	2.0	5.0	100.0	100.0	80.0	100.0	25.7	100.0	92.3	27	20-36
No.16 (1.18mm)	2.0	4.0	100.0	100.0	62.0	100.0	28.2	100.0	79.4	21	10-25
No.30 (60µm)	2.0	4.0	100.0	100.0	40.0	100.0	16.7	100.0	61.7	16	
No.60 (300µm)	2.0	4.0	100.0	100.0	11.0	100.0	13.0	100.0	52.3	10	4-12
No.100 (150µm)	2.0	4.0	100.0	100.0	1.0	100.0	9.3	100.0	44.7	7	3-9
No.200 (75µm)	1.7	3.2	100.0	100.0	0.3	100.0	6.1	100.0	34.0	4.8	3-6

Bulk Sp Gr	2.626	2.612	1.890	1.900	2.828	1.800	2.660	1.800	2.590	2.633	Dust/AC
Absorption, %	2.10	2.60	1.00	1.00	1.30	1.00	1.00	1.00	1.00	1.24	Ratio
										SP GR AC	1.046
											0.88

AMOUNT OF AGED RCY AC **2.7**  
 AC REPLACEMENT (ABR) **46.1**  
 VIRGIN AC **2.8**

**SUMMARY OF SUPERPAVE GYRATORY DESIGN DATA** BITUMINOUS MIXTURE AGED **1** HOURS @ **295**

DATA for N-int.		8									
	AC, %MIX	(Gmb)	(Gmm)	(Pa)	VMA	VFA	Vbe	Pbe	Pba		
MIX 1	4.5	2.173	2.539	14.4	21.2	32.0	6.76	3.24	1.22		
MIX 2	5.0	2.177	2.518	13.5	21.4	36.9	7.80	3.77	1.29		
MIX 3	5.5	2.201	2.489	11.9	21.0	43.2	9.09	4.29	1.28		
MIX 4	6.0	2.292	2.478	11.2	21.4	47.8	10.23	4.83	1.24		

DATA for N-dns.		50									
	(Gmb)	(Gmm)	(Pa)	VMA	VFA	Vbe	Pbe	Geo	Pba		
MIX 1	4.5	2.387	2.539	6.0	13.4	55.4	7.43	3.24	2.724	1.32	
MIX 2	5.0	2.406	2.518	4.5	13.2	66.1	8.73	3.77	2.732	1.29	
MIX 3	5.5	2.424	2.489	3.0	13.0	77.0	10.61	4.29	2.721	1.28	
MIX 4	6.0	2.434	2.470	1.8	13.1	85.3	11.31	4.83	2.719	1.24	

OPTIMUM DESIGN DATA @Nds: →		50									
	NUMBER OF GYRATIONS	%AC	Gmb	Gmm	VMA (Pa)	VFA	Geo	Gsb	TSR		
	50	5.5	2.424	2.489	Target 3.0	13.6	76.9	2.721	2.633	0.94	

REMARKS LINE 1 Hamburg & TSR made with warm mix.  
 REMARKS LINE 2 Moisture Ratio M1 @ 6.4%

Tested by: [Signature] Verified by: \_\_\_\_\_  
 Reviewed by: [Signature] Final Approval: \_\_\_\_\_

RR12003

# Table 29 Plant Mix 9 (P9)

IDOT Lab Verification No.:  Ver. 9.01-06.15.12 DATE: **September 28 2012**

Producer Number & Name → **4066-06 Rock Road Rockford** ← Plant Location **RR12002**  
 Material Code Number → **19512R HMA N50 19.0 REC BIND**

Plant Bin #	#5	#4	#3	#2	#1	MF	FRAP #3	FRAP #2	RAS #1	ASPHALT
042CM11	032CM16				037FM01		017CM1204		017FM08	10122
Source (PRCO #)	06072-01	50072-01			52010-07		4086-06		6016-04	5027-13
(NAME)	WCC	WCC			WCC		Rock Road		Southwind	BIP Amore
(LOC)	Irene	Irene			Alport		Irene		So. Beloit	Bartlett
(ADD. INFO)							Category 2			46-34
Aggregate Blend:	29.5	14.5	0.0	0.0	8.0	0.0	42.0	0.0	28.7	< AC in RAP
									6.0	PG 55-28
										100.0

Lab Preparing Design **IL**  
 Designing Lab Mix **RR12002**  
 Designing Lab Name **S.T.A.T.E.**

Agg No.	#5	#4	#3	#2	#1	MF	FRAP #3	FRAP #2	RAS #1	Aggregate Blend	Mixture Comp Spec
1" (25.0mm)	100.0	100.0	100.0	100.0	100.0	100.0	100.0	100.0	100.0	100	100
3/4" (19.0mm)	80.0	100.0	100.0	100.0	100.0	100.0	100.0	100.0	100.0	97	82-100
1/2" (12.5mm)	34.0	100.0	100.0	100.0	100.0	100.0	100.0	100.0	100.0	81	50-85
3/8" (9.5mm)	7.0	94.0	100.0	100.0	100.0	100.0	96.5	100.0	100.0	70	
No.4 (4.75mm)	2.0	32.0	100.0	100.0	96.0	100.0	48.9	100.0	97.3	39	24-50
No.10 (2.0mm)	2.0	5.0	100.0	100.0	86.0	100.0	25.7	100.0	92.3	24	20-38
No.16 (1.18mm)	2.0	4.0	100.0	100.0	82.0	100.0	20.2	100.0	79.4	19	10-25
No.30 (600µm)	2.0	4.0	100.0	100.0	46.0	100.0	18.7	100.0	61.7	15	
No.50 (300µm)	2.0	4.0	100.0	100.0	11.0	100.0	13.0	100.0	52.3	11	4-12
No.100 (150µm)	2.0	4.0	100.0	100.0	1.0	100.0	6.3	100.0	44.7	8	3-9
No.200 (75µm)	1.7	3.2	100.0	100.0	0.3	100.0	6.1	100.0	34.6	6.6	3-8

Bulk Sp Gr	2.628	2.812	1.909	1.900	2.628	1.000	2.880	1.000	2.500	2.830	Dust/AC
Absorption, %	2.19	2.60	1.00	1.00	1.30	1.00	1.00	1.00	1.90	1.36	Ratio
									<b>SP GR AC</b>	<b>1.848</b>	<b>1.01</b>

AMOUNT OF AGED RCY AC **3.3**  
 AC REPLACEMENT (ARR) **59.1**  
 VIRGIN AC **2.2**

**SUMMARY OF SUPERPAVE GYRATORY DESIGN DATA** BITUMINOUS MIXTURE AGED **1** HOURS @ **286**

DATA for N-bit.	g	AC, %MIX	(Gmb)	(Gmm)	(Pa)	VMA	VFA	Vbe	Pbe	Pba
MIX 1	5.0	2.150	2.525	13.0	21.3	35.8	7.61	3.93	1.44	
MIX 2	5.5	2.191	2.509	12.4	21.3	41.5	8.82	4.24	1.34	
MIX 3	6.0	2.209	2.498	11.2	21.1	47.0	9.91	4.66	1.42	
MIX 4	6.5	2.215	2.498	10.2	21.3	51.7	11.00	5.18	1.43	

DATA for N-bit.	g0	(Gmb)	(Gmm)	(Pa)	VMA	VFA	Vbe	Pbe	Gse	Pba
MIX 1	5.0	2.404	2.525	4.8	13.2	62.7	8.39	3.93	2.709	1.44
MIX 2	5.5	2.423	2.509	3.1	13.0	76.3	9.87	4.24	2.722	1.34
MIX 3	6.0	2.436	2.498	2.0	12.9	84.4	10.92	4.66	2.728	1.42
MIX 4	6.5	2.445	2.498	0.9	13.1	82.8	12.14	5.18	2.729	1.43

OPTIMUM DESIGN DATA @Nbit: →	NUMBER OF GYRATIONS	%AC	Gmb	Gmm	VMA (Pa) Target	VFA	Gse	Gsb	TSR	
	50	5.5	2.424	2.499	5.0	13.0	76.6	2.723	2.638	0.86

REMARKS LINE 1 **Hamburg & TSR made with warm mix.**  
 REMARKS LINE 2 **MeadwestVaco M1 @ 0.4%**

Tested by: *[Signature]* Verified by: *[Signature]*  
 Reviewed by: *[Signature]* Final Approval: *[Signature]*

RR12002

# Table 30 Plant Mix 10 (P10)

IDOT Lab Verification No. →  Ver. 0.01-06.16.12 DATE: **October 18 2012**

Producer Number & Name → **4066-06 Rock Road Rockford** ← Plant Location **RR12006**

Material Code Number → **19524R HMA N70 D REC SURF 9.5mm**

Plant Bin #	#5	#4	#3	#2	#1	MF	FRAP #3	FRAP #2	RAS #1	ASPHALT
Size		032CM16			037FM01	004MF02	017CM1204	017FM0400		1012B
Source (PROD #)		50072-01			02010-07	4066-06	4066-06	4066-06		6220-61
(NAME)		WCC			WCC	Rock Road	Rock Road	Rock Road		Flint Hills
(LOC)		Irwin			Airport	Rockford	Rockford	Rockford		Dubuque, IA
(ADD. INFO)										PG 58-28
Aggregate Blend:							3.7	6.0	6.0	< AC in RAP
	0.0	58.0	0.0	0.0	12.5	0.5	12.0	17.0	0.0	PG 58-28
										100.0

Lab Preparing Design   
 Designing Lab Mix  RR12006  
 Designing Lab Name  S.T.A.T.E.

Agg No.	#5	#4	#3	#2	#1	MF	FRAP #3	FRAP #2	RAS #1	Aggregate Blend	Mixture Comp Spec
1" (25.0mm)	100.0	100.0	100.0	100.0	100.0	100.0	100.0	100.0	100.0	100	
3/4" (19.0mm)	100.0	100.0	100.0	100.0	100.0	100.0	100.0	100.0	100.0	100	
1/2" (12.5mm)	100.0	100.0	100.0	100.0	100.0	100.0	100.0	100.0	100.0	100	100
3/8" (9.5mm)	100.0	94.0	100.0	100.0	100.0	100.0	96.5	100.0	100.0	96	90-100
No.4 (4.75mm)	100.0	32.0	100.0	100.0	96.0	100.0	48.9	98.5	100.0	54	28-65
No.8 (2.36mm)	100.0	5.0	100.0	100.0	80.0	100.0	25.7	74.2	100.0	20	20-48
No.16 (1.18mm)	100.0	4.0	100.0	100.0	62.0	100.0	20.2	61.2	100.0	22	10-32
No.30 (60µm)	100.0	4.0	100.0	100.0	40.0	100.0	16.7	36.8	100.0	16	
No.60 (300µm)	100.0	4.0	100.0	100.0	11.0	100.0	13.0	23.9	100.0	10	4-15
No.100 (150µm)	100.0	4.0	100.0	100.0	1.0	95.0	8.3	17.4	100.0	7	3-10
No.200 (75µm)	100.0	3.2	100.0	100.0	0.5	90.0	6.1	10.9	100.0	4.9	4-6

Bulk Sp Gr	#5	#4	#3	#2	#1	MF	FRAP #3	FRAP #2	RAS #1	Aggregate Blend	Dust/AC Ratio
	1.000	2.612	1.000	1.000	2.626	2.999	2.600	2.600	1.000	2.626	1.63
Absorption, %	1.00	2.66	1.00	1.00	1.30	1.60	1.00	1.00	1.00	1.63	6.83
										SP GR AC	1.246

AMOUNT OF AGED RCY AC  1.5

AC REPLACEMENT (ABR) 24.6

VIROIN AC  4.5

**SUMMARY OF SUPERPAVE GYRATORY DESIGN DATA** BITUMINOUS MIXTURE AGED  1 HOURS @  235

DATA for N-int. 7										
	AC, % MIX	(Gmb)	(Gmm)	(Pa)	VMA	VFA	Vbo	Pbe	Pba	
MIX 1	5.0	2.110	2.523	16.4	23.8	31.1	7.30	3.64	1.43	
MIX 2	5.5	2.122	2.593	16.2	23.7	35.8	8.49	4.16	1.42	
MIX 3	6.0	2.126	2.487	14.1	23.6	40.3	9.53	4.64	1.45	
MIX 4	6.5	2.142	2.484	13.1	23.8	45.1	10.75	5.22	1.37	

DATA for N-des. 70										
	(Gmb)	(Gmm)	(Pa)	VMA	VFA	Vbo	Pbe	Gse	Pba	
MIX 1	5.0	2.384	2.523	8.3	14.6	56.0	8.28	3.64	2.727	1.43
MIX 2	5.5	2.375	2.503	6.1	14.6	64.9	9.50	4.16	2.727	1.42
MIX 3	6.0	2.391	2.487	3.8	14.5	73.5	10.66	4.64	2.729	1.45
MIX 4	6.5	2.398	2.484	2.7	14.7	81.7	12.63	5.22	2.723	1.37

Hamburg Wheel Information	
Sample No. Passes	29000
Sample Wheel Depth	8.62

TSR Information	
Conditioned	81.2
Unconditioned	84.5
TSR	8.96
CA Strip Rating	1
FA Strip Rating	1
Additive Prod #	
Additive Product Name	
Additive %	

OPTIMUM DESIGN DATA @Ndes: →	NUMBER OF GYRATIONS	%AC	Gmb	Gmm	%WOODS (Pa) Target	VMA	VFA	Gse	Gsb	TSR
	70	5.9	2.389	2.489	4.0	14.5	72.5	2.726	2.629	8.96

REMARKS LINE 1: Hamburgs & TSR Made With Warm Mix  
 REMARKS LINE 2: MidwestVaso M1 @ 0.4%

Tested by: Verified by: \_\_\_\_\_

Reviewed by: Final Approval: \_\_\_\_\_

RR12006

# Table 31 Plant Mix 11 (P11)

IDOT Lab Verification No. →  Ver. 9.01-06.15.12 DATE: **October 3 2012**

Producer Number & Name → **4066-06 Rock Road Rockford** ← Plant Location **RRRO12002**

Material Code Number → **19524R HMA N70 D REC SURF 9.5mm**

Plant Dis #	#5	#4	#3	#2	#1	MF	FRAP #3	FRAP #2	RA5 #1	ASPHALT
Size		032CM10			037FM01		D17CM104	D17FM100	017FM03	10126
Source (PRDD #)		5072-01			52010-07		4066-06	4066-06	0119-04	0220-01
(NAME)		WCC			WCC		Rock Road	Rock Road	Southwind	Fibrel Hills
(LOC)		Irene			Airport		Rockford	Rockford	So. Belet	Dubuque, IA
(ADD. INFO)							Category 2	Category 2		PG 58-28
Aggregate Blend:	0.0	57.0	0.0	0.0	0.0	0.0	10.0	14.0	28.7	PG 58-28 ← AC in RAP
									5.0	100.0

Lab Preparing Design  Designing Lab Mix# **RRRO12002** Designing Lab Name **S.T.A.T.E.**

Agg No. Sieve Size	#5	#4	#3	#2	#1	MF	FRAP #3	FRAP #2	RA5 #1	Aggregate Blend	Mixture Comp Spec
1" (25.0mm)	100.0	100.0	100.0	100.0	100.0	100.0	100.0	100.0	100.0	100	
3/4" (19.0mm)	100.0	100.0	100.0	100.0	100.0	100.0	100.0	100.0	100.0	100	
1/2" (12.5mm)	100.0	100.0	100.0	100.0	100.0	100.0	100.0	100.0	100.0	100	100
3/8" (9.5mm)	100.0	94.0	100.0	100.0	100.0	100.0	96.5	100.0	100.0	96	90-100
No.4 (4.75mm)	100.0	32.0	100.0	100.0	98.0	100.0	48.9	98.6	97.3	92	28-65
No.8 (2.36mm)	100.0	5.0	100.0	100.0	90.0	100.0	25.7	74.2	92.3	28	28-48
No.16 (1.18mm)	100.0	4.0	100.0	100.0	82.0	100.0	20.2	51.2	78.4	22	16-32
No.30 (600um)	100.0	4.0	100.0	100.0	40.0	100.0	18.7	38.8	61.7	16	
No.50 (300um)	100.0	4.0	100.0	100.0	11.0	100.0	13.8	25.9	52.3	11	4-15
No.100 (150um)	100.0	4.0	100.0	100.0	1.0	100.0	9.3	17.4	44.7	9	3-10
No.200 (75um)	100.0	3.2	100.0	100.0	0.3	100.0	6.1	10.9	34.8	6.1	4-6

Bulk Sp Gr	1.020	2.612	1.000	1.000	2.628	1.600	2.860	2.660	2.500	2.821	Dust/AC
Absorption, %	1.00	2.80	1.00	1.00	1.30	1.00	1.00	1.00	1.00	1.50	Ratio
										SP GR AC	1.040
											1.62

AMOUNT OF AGED RCY AC  2.8  
AC REPLACEMENT (ABR)  48.3  
VIRGIN AC  3.1

### SUMMARY OF SUPERPAVE GYRATORY DESIGN DATA

BITUMINOUS MIXTURE AGED  1 HOURS @  285

DATA for N-des.	7	AC, %MIX	(Gmb)	(Gmm)	(Pa)	VMA	VFA	Vbe	Pbe	Pba
MIX 1	5.0	2.192	2.522	15.9	23.1	31.4	7.25	3.55	1.52	
MIX 2	5.5	2.126	2.591	15.0	23.3	35.9	8.37	4.09	1.49	
MIX 3	6.0	2.138	2.480	13.8	23.3	40.9	9.55	4.65	1.44	
MIX 4	6.5	2.146	2.464	12.9	23.4	48.9	10.55	5.11	1.48	

DATA for N-des.	70	AC, %MIX	(Gmb)	(Gmm)	(Pa)	VMA	VFA	Vbe	Pbe	Gse	Pba
MIX 1	5.0	2.355	2.922	6.6	14.7	55.9	8.04	3.55	2.726	1.52	
MIX 2	5.5	2.270	2.591	5.2	14.8	64.1	9.33	4.09	2.724	1.46	
MIX 3	6.0	2.285	2.480	3.8	14.5	73.6	10.88	4.65	2.720	1.44	
MIX 4	6.5	2.292	2.464	2.9	14.7	80.1	11.79	5.11	2.723	1.48	

OPTIMUM DESIGN DATA @Ndes: ---->	NUMBER OF GYRATIONS	%AC	Gmb	Gmm	VOIDS (Pa)	VMA	VFA	Gse	Gsb	TSR
	70	5.9	2.382	2.482	4.0	14.5	72.4	2.721	2.621	0.97

REMARKS LINE 1  Hamburg & TSR Made With Warm Mix  
REMARKS LINE 2  Maschwies Vaso M1 @ 5.4%

Tested by: *[Signature]* Verified by: \_\_\_\_\_  
Reviewed by: *[Signature]* Final Approval: \_\_\_\_\_

RRRO12002



# Table 32 Plant Mix 12 (P12)

DOT Lab Verification No. →  Ver. 9.01-05.15.12 DATE:

Producer Number & Name →    ← Plant Location

Material Code Number →

Plant Bin #	#5	#4	#3	#2	#1	MF	FRAP #3	FRAP #2	RAS #1	ASPHALT
Size	031CM14	031CM13		038FM20	#1	04MFP92	017CM1204		017FM88	10130
Source (PROD #)	52400-29	52400-29		50072-01		4399-09	4066-06		0619-04	1757-05
(NAME)	Rock Road	Rock Road		WCC		Rock Road	Rock Road		Southwind	Seneca
(LOC)	Lathers	Lathers		Ine		Rockford	Rockford		So. Beloit	Lemont
(ADD. INFO)										
Aggregate Blend:	50.0	24.5	0.0	8.0	0.0	5.0	3.5	0.0	28.7	SBS PG 79-28
							8.0	0.0	28.7	K AC in RAP
										PG 79-28
										100.0

Lab Preparing Design  Designing Lab Misc  Designing Lab Name

Agg No.	#5	#4	#3	#2	#1	MF	FRAP #3	FRAP #2	RAS #1	Aggregate Blend	Mixture Comp Spec
1" (25.0mm)	100.0	100.0	100.0	100.0	100.0	100.0	100.0	100.0	100.0	100	100
3/4" (19.0mm)	100.0	100.0	100.0	100.0	100.0	100.0	100.0	100.0	100.0	100	82-100
1/2" (12.5mm)	87.1	98.6	100.0	100.0	100.0	100.0	100.0	100.0	100.0	93	65 max
3/8" (9.5mm)	33.0	73.2	100.0	100.0	100.0	100.0	44.3	100.0	100.0	60	20-30
No.4 (4.75mm)	1.3	25.0	100.0	100.0	100.0	100.0	95.9	100.0	100.0	28	18-24
No.8 (2.36mm)	1.2	1.9	100.0	68.0	100.0	100.0	21.8	100.0	92.3	19	10-15
No.16 (1.18mm)	1.1	1.7	100.0	63.0	100.0	100.0	15.1	100.0	79.4	15	12-16
No.30 (600µm)	1.1	1.6	100.0	30.0	100.0	100.0	12.0	100.0	61.7	12	10-15
No.50 (300µm)	1.1	1.6	100.0	15.0	100.0	100.0	9.6	100.0	52.3	9	8-10
No.100 (150µm)	1.0	1.5	100.0	7.0	100.0	95.0	7.0	100.0	44.7	7.6	
No.200 (75µm)	1.0	1.3	100.0	4.3	100.0	90.0	5.3	100.0	34.0	7.6	

Bulk Sp Gr	2.710	2.696	1.000	2.641	1.000	2.900	2.686	1.000	2.590	2.696	Dust/AC Ratio
Absorption, %	1.36	1.50	1.00	1.90	1.00	1.00	1.00	1.00	1.00	1.31	1.28
										1.446	1.28

AMOUNT OF AGED RCY AC

AC REPLACEMENT (ARR)

VIRGIN AC

SUMMARY OF SUPERPAVE GYRATORY DESIGN DATA BITUMINOUS MIXTURE AGED  HOURS @

DATA for N-int. <input type="text" value="7"/>									
	AC, %MIX	(Gmb)	(Gmm)	(Pa)	VMA	VFA	Vbe	Pbe	Pba
MX 1	5.5	2.090	2.512	16.8	28.7	37.1	9.93	4.94	0.50
MX 2	6.0	2.104	2.494	15.6	28.6	41.3	11.00	5.44	0.60
MX 3	6.5	2.114	2.474	14.5	28.7	45.5	12.13	5.97	0.57
MX 4	7.0	2.116	2.455	13.8	27.0	48.8	13.18	6.48	0.56

DATA for N-des. <input type="text" value="80"/>									
	(Gmb)	(Gmm)	(Pa)	VMA	VFA	Vbe	Pbe	Gse	Pba
MX 1	5.5	2.383	2.512	5.1	18.5	68.0	11.33	4.94	2.737
MX 2	6.0	2.405	2.494	3.6	16.1	77.8	12.87	5.44	2.738
MX 3	6.5	2.413	2.474	2.5	16.3	84.8	13.94	5.97	2.736
MX 4	7.0	2.421	2.455	1.4	16.5	91.6	15.09	6.48	2.735

Hamburg Wheel Information

Sample No. Passes

Sample Wheel Depth

TSR Information

Conditioned

Unconditioned

TSR

CA Strip Rating

FA Strip Rating

Additive Prod #

Additive Product Name

Additive %

	NUMBER OF GYRATIONS	%AC	Gmb	Gmm	%VOIDS (Pa)	VMA	VFA	Gse	Gsb	TSR
OPTIMUM DESIGN DATA @Ndes: →	<input type="text" value="89"/>	6.03	2.446	2.483	Target <input type="text" value="3.5"/>	16.1	78.3	2.738	2.696	0.00

REMARKS LINE 1:

REMARKS LINE 2:

Tested by:

Verified by:

Revised by:

Final Approval:

RRR12007

# Table 33 Plant Mix 13 (P13)

IDOT Lab Verification No. →  Ver. 9.01-06.15.12 DATE:

Producer Number & Name →  ← Plant Location

Material Code Number →

Plant Bin #	#5	#4	#3	#2	#1	MF	FRAP #3	FRAP #2	RAS #1	ASPHALT
Size	031CM14	031CM13				044MF02	017CM1204	017FM400	017FM08	10120
Source (PRCD #)	52400-20	52400-20				4066-06	4066-06	4066-06	6615-04	1757-05
(NAME)	Rock Road	Rock Road				Rock Road	Rock Road	Rock Road	Southwind	Seneca
(LOG)	Lathers	Lathers				Rockford	Rockford	Rockford	So.Beloit	Lemont
(ADD. INFO)										
Aggregate Blend:	49.0	22.5	0.0	0.0	0.0	3.0	3.5	6.2	28.7	100.0
							10.0	8.0	7.5	Plan PG Grade > PG 70-28

Lab Preparing Design   
 Designing Lab Name

Agg No.	#5	#4	#3	#2	#1	MF	FRAP #3	FRAP #2	RAS #1	Aggregate Blend	Mixture Comp Spec
1" (25.0mm)	100.0	100.0	100.0	100.0	100.0	100.0	100.0	100.0	100.0	100.0	100
3/4" (19.0mm)	100.0	100.0	100.0	100.0	100.0	100.0	100.0	100.0	100.0	100.0	100
1/2" (12.5mm)	87.1	96.8	100.0	100.0	100.0	100.0	100.0	100.0	100.0	100.0	82-100
3/8" (9.5mm)	33.0	73.2	100.0	100.0	100.0	100.0	100.0	96.8	100.0	100.0	65 max
No.4 (4.75mm)	1.3	25.0	100.0	100.0	100.0	100.0	100.0	44.3	97.9	97.3	20-30
No.6 (2.36mm)	1.2	1.9	100.0	100.0	100.0	100.0	100.0	21.6	69.0	92.3	10-24
No.10 (1.18mm)	1.1	1.7	100.0	100.0	100.0	100.0	100.0	16.1	46.5	78.4	15
No.30 (600µm)	1.1	1.6	100.0	100.0	100.0	100.0	100.0	9.5	24.4	62.3	10-15
No.50 (300µm)	1.1	1.6	100.0	100.0	100.0	100.0	100.0	7.0	15.7	44.7	9
No.100 (150µm)	1.0	1.5	100.0	100.0	100.0	100.0	100.0	5.0	11.4	34.0	8-10
No.200 (75µm)	1.0	1.3	100.0	100.0	100.0	100.0	100.0	5.3	11.4	34.0	8-10

Bulk Sp Gr	#5	#4	#3	#2	#1	MF	FRAP #3	FRAP #2	RAS #1	Aggregate Blend	Dust/AC Ratio
2.710	2.686	1.000	1.000	1.000	1.000	2.900	2.660	2.660	2.660	2.686	1.25
Absorption, %	1.30	1.59	1.00	1.00	1.00	1.00	1.00	1.00	1.00	1.00	1.25
										SP GR AC	1.040

AMOUNT OF AGED RCY AC   
 AC REPLACEMENT (ABR)   
 VIRGIN AC

### SUMMARY OF SUPERPAVE GYRATORY DESIGN DATA

BITUMINOUS MIXTURE AGED  HOURS @

DATA for N-des. 7										
	AC, %MIX	(Gmb)	(Gmm)	(Pa)	VMA	VFA	Vbe	Fbe	Gse	Pba
MX1	5.5	2.092	2.507	16.6	26.4	37.3	0.95	4.90	0.64	
MX2	6.0	2.108	2.492	15.4	29.2	41.3	10.83	5.34	0.70	
MX3	6.5	2.115	2.471	14.4	29.4	45.4	11.88	5.80	0.85	
MX4	7.0	2.134	2.454	13.1	25.1	50.0	13.05	6.37	0.88	

DATA for N-des. 80										
	(Gmb)	(Gmm)	(Pa)	VMA	VFA	Vbe	Fbe	Gse	Pba	
MX1	5.5	2.379	2.507	5.1	15.3	88.6	11.20	4.90	2.731	0.64
MX2	6.0	2.405	2.492	3.5	15.8	78.1	12.36	5.34	2.735	0.70
MX3	6.5	2.418	2.471	2.1	15.8	86.6	13.49	5.80	2.732	0.85
MX4	7.0	2.430	2.454	1.0	15.8	93.7	14.87	6.37	2.734	0.88

Hamburg Wheel Information	
Sample No. Passes	20000
Sample Wheel Depth	3.61

TSR Information	
Conditioned	121.3
Unconditioned	135.0
TSR	0.90
CA Strip Rating	2
FA Strip Rating	1
Additive Prod #	
Additive Product Name	
Additive %	

OPTIMUM DESIGN DATA @Ndes: --->	NUMBER OF CYRATIONS		%AC	Gmb	Gmm	VOIDS (Pa)	VMA	VFA	Gse	Gsb	TSR
	80	599									
	80	599	6.0	2.405	2.462	3.5	15.8	77.0	2.735	2.686	0.80

REMARKS LINE 1 Hamburgs & TSR Made With Warm Mix  
 REMARKS LINE 2 MeadowsVaco M1 @ 0.5%

Tested by: *M. J. [Signature]* Verified by: \_\_\_\_\_  
 Reviewed by: *M. J. [Signature]* Final Approval: \_\_\_\_\_

RRR12004

### Table 34 Plant Mix 14 (P14) (Joliet)

Excel Ver. 11.01.05.09.13

QC Test Strip Results



ASSIGNMENT INFORMATION				/FOR DTY03305 & DTY03000		
Inspector #: 910000000	Date: 102513	Seq #: 000		Contract / Section No.	Job No.	Quantity
Bit Mix Plant: 6509-01	Mix Code: 19514R	Quantity: 299.4		60P70	C9160611	299.4
Resp Loc: 91	Lab: PP	Dist Mix #: 81BIT138Z4				
Type Insp: PRO	Lab Name: Joliet Asphalt	Mix Name: HMA N50 D REC SURF				

**/FOR DTY03309**

Sub Lot: <input type="text" value="1"/>	Type: <input type="text" value="S"/>	Washed: <input type="text" value="Y"/>	Lot: <input type="text"/>						
Virgin Aggs	BIN7	BIN6	BIN5	BIN4	BIN3	BIN2	BIN1	MF	NEW AB%
MIX%						43.0	22.7	0.5	3.5
AGG%						45.5	24.0	0.5	

Producer	Material	%
Binder	1757-05	10126
Additive		3.5

RCY Aggs	RCY 4	RCY 3	RCY 2	RCY 1	Remarks:
MIX%			5.9	24.4	
AGG%			6.0	24.0	
RCY AB			3.7	6.9	

Sub Lot: <input type="text" value="1"/>	% PASS	AJMF	Sub Lot: <input type="text"/>	% PASS	AJMF
1.5	100	100	1.5		
1	100	100	1		
3/4	100	100	3/4		
1/2	100	100	1/2		
3/8	94	93	3/8		
#4	53	53	#4		
#8	32	32	#8		
#16	21	21	#16		
#30	15	16	#30		
#50	10	11	#50		
#100	7	7	#100		
#200	5.2	5.5	#200		
AB	5.4	5.4	AB		

Sub Lot: <input type="text"/>	Type: <input type="text"/>	Washed: <input type="text"/>	Lot: <input type="text"/>						
Virgin Aggs	BIN7	BIN6	BIN5	BIN4	BIN3	BIN2	BIN1	MF	NEW AB%
MIX%						43.0	22.7	0.5	
AGG%						45.5	24.0	0.5	

RCY Aggs	RCY 4	RCY 3	RCY 2	RCY 1	Remarks:
MIX%			5.9	24.4	
AGG%			6.0	24.0	
RCY AB			3.7	6.9	

**/FOR DTY03000 / TRANS 308**

Sub Lot: <input type="text" value="1"/>	Type: <input type="text" value="1"/>	Wash: <input type="text" value="Y"/>	Sub Lot: <input type="text" value="2"/>	Type: <input type="text" value="1"/>	Wash: <input type="text" value="Y"/>
Corr.	% PASS	AJMF	Corr.	% PASS	AJMF
1.5	100	100	1.5	100	100
1	100	100	1	100	100
3/4	100	100	3/4	100	100
1/2	100	100	1/2	100	100
3/8	93	93	3/8	97	93
#4	53	53	#4	58	53
#8	34	32	#8	32	32
#16	25	21	#16	21	21
#30	20	16	#30	14	16
#50	14	11	#50	8	11
#100	10	7	#100	5	7
#200	6.3	5.5	#200	4.1	5.5
AB	0.59	5.3	AB	0.62	5.4

Sub Lot: <input type="text"/>	Type: <input type="text"/>	AB%: <input type="text"/>	Target AB: <input type="text"/>	Sub Lot: <input type="text"/>	Type: <input type="text"/>	AB%: <input type="text"/>	Target AB: <input type="text"/>	Dust/AB 1: <input type="text" value="1.2"/>	Dust/AB 2: <input type="text" value="0.7"/>	AB Replmnt 1: <input type="text" value="36.2"/>	AB Replmnt 2: <input type="text" value="33.5"/>
-------------------------------	----------------------------	---------------------------	---------------------------------	-------------------------------	----------------------------	---------------------------	---------------------------------	---------------------------------------------	---------------------------------------------	-------------------------------------------------	-------------------------------------------------

Remarks: \_\_\_\_\_  
Remarks: \_\_\_\_\_

Sub Lot: <input type="text" value="1"/>	Gsb: <input type="text" value="3.086"/>			
Gyratory Results:				
Nd	Gmb	Gmm	Voids	FVMA
50	2.763	2.903	4.8	15.2

COPIES:  
District Office  
Inspector  
JOLIET ASPHALT  
RE:  
Jeff Ogrodnik

Sub Lot: <input type="text" value="2"/>	Gsb: <input type="text" value="3.086"/>			
Gyratory Results:				
Nd	Gmb	Gmm	Voids	FVMA
50	2.772	2.902	4.5	15.3

QC Manager:	Phone:
Rick Rahn	815-726-1090
Tested By:	Email:
Dan Donegan	ddonegan@jolietasphalt

Remarks: \_\_\_\_\_  
Remarks: \_\_\_\_\_





## Appendix C: IL-SCB Results

**Table 37 Plant Mixtures**

**Table C-1.1 P1-P15 IL-SCB (25°C at 50 mm/min)**

Mix ID	Mix Name	Energy (LLD) (J/m <sup>2</sup> )	Avg	Std Dev	COV	Flexibility Index	Avg	Std Dev	COV	Peak Load (KN)	Avg	Std Dev	COV
P1	TOL MIX 1	1510.4	1558.9	168.3	10.8	2.6	2.4	0.4	15.4	3.7	3.7	0.1	3.2
		1784.9				2.7				3.9			
		1381.4				1.9				3.6			
P2	TOL MIX 2	1648.6	1752.6	103.9	5.9	2.8	3.3	0.5	14.4	4.1	4.0	0.0	0.9
		1856.5				3.7				4.0			
		1391.4				1.6				3.9			
P3	TOL MIX 3	1276.3	1277.5	203.3	15.9	2.1	1.7	0.4	23.8	3.6	3.6	0.2	5.7
		1029.1				1.2				3.4			
		1527.2				1.7				3.9			
P4	TOL MIX 4	1484.7	1337.5	33.3	2.5	2.9	1.3	0.2	13.9	3.5	4.1	0.1	2.9
		1304.2				1.1				4.2			
		1370.8				1.4				4.0			

**Table 37 (cont.)**

P5	TOL MIX 5		1040.8	54.2	5.2		0.3	0.0	7.1		4.9	0.1	1.5
		1095.0				0.3				4.9			
		986.6				0.3				4.8			
P6	TOL MIX 6	2089.7	1957.4	153.1	7.8		2.7	0.5	18.7	5.1	4.8	0.3	5.2
		1742.8				2.0				4.6			
		2039.7				3.2				4.6			
P7	TOL MIX 7	2120.5	2015.8	125.3	6.2		5.3	0.6	11.8	9.7	3.6	0.1	3.2
		2141.1				5.9				3.8			
		1890.6				4.7				3.5			
P8	N50-50	1040.4	1184.6	121.5	10.3		1.8	0.5	26.3	1.5	3.6	0.3	9.3
		1337.6				2.5				3.4			
		1175.8				1.5				4.1			
P9	N50-60	1059.7	967.2	92.4	9.6		1.6	0.6	37.1	2.2	2.8	0.2	7.3
		874.8				1.0				2.6			
P10	N70-25	2024.1	1969.4	127.7	6.5		8.9	1.7	19.2	9.1	3.0	0.1	4.3
		2091.1				10.9				2.8			
		1793.0				6.8				3.0			
P11	N70-50	1141.6	1366.7	159.2	11.7		2.0	0.6	28.3	1.2	4.3	0.4	8.6
		1473.9				2.5				3.9			
		1484.7				2.4				4.1			
		1145.4				1.1				3.8			
P12	N80-25	1581.3	1828.9	271.8	14.9		8.2	1.4	17.6	2.6	2.8	0.1	4.6
		1119.5				1.5				3.5			
		1557.1				6.8				2.7			
		2100.7				9.7				3.0			

**Table 37 (cont.)**

P13	N80-50	1603.4	1338.5	270.5	20.2	1.9	2.8	1.4	49.2	4.6	3.6	0.7	19.2
		1444.9				4.7				3.0			
		556.8				0.3				3.5			
		646.2				0.4				3.9			
		967.1				1.7				3.3			
P14	TR-JOLIET	2161.3	2225.5	131.7	5.9	5.2	6.9	1.1	16.7	3.8	3.8	0.1	2.3
2441.7	8.4	3.8											
2208.3	7.2	4.0											
2090.6	6.7	3.7											
P15	TR-SANDENO	1537.1	1444.8	61.5	4.3	2.6	2.1	0.3	14.5	4.0	3.8	0.2	5.8
		1434.3				1.9				4.0			
		1443.5				1.8				3.6			
		1364.1				2.2				3.5			
P12	N80-25	1581.3	1828.9	271.8	14.9	2.6	8.2	1.4	17.6	3.6	2.8	0.1	4.6
		1119.5				1.5				3.5			
		1557.1				6.8				2.7			
		2100.7				9.7				3.0			
P13	N80-50	1603.4	1338.5	270.5	20.2	1.9	2.8	1.4	49.2	4.6	3.6	0.7	19.2
		1444.9				4.7				3.0			
		556.8				0.3				3.5			
		646.2				0.4				3.9			
		967.1				1.7				3.3			
P14	TR-JOLIET	2161.3	2225.5	131.7	5.9	5.2	6.9	1.1	16.7	3.8	3.8	0.1	2.3
		2441.7				8.4				3.8			
		2208.3				7.2				4.0			
		2090.6				6.7				3.7			
P15	TR-SANDENO	1537.1	1444.8	61.5	4.3	2.6	2.1	0.3	14.5	4.0	3.8	0.2	5.8
		1434.3				1.9				4.0			
		1443.5				1.8				3.6			
		1364.1				2.2				3.5			



**Table 38 P17-P22 IL-SCB (25°C at 50 mm/min)**

Mix	Replicate ID	Energy (LLD) (J/m <sup>2</sup> )	Average	Std Dev	COV	Peak Load (kN)	Average Peak Load	Std Dev	COV	FI	Average	Std Dev	COV
P17	147M-B1.dat	2110.8	2167.9	53.0	2.4	4.2	4.1	0.1	1.3	4.3	4.5	0.2	5.4
	147M-B2.dat	2215.5				4.0				4.8			
	147M-T2.dat	2177.3				4.1				4.6			
P18	156M-B2.dat	2024.8	2048.7	126.9	6.2	4.0	4.0	0.1	2.2	4.4	4.5	0.2	4.2
	156M-T1.dat	2185.8				4.0				4.7			
	156M-T2.dat	1935.4				4.1				4.4			
P19	157M-B1.dat	1687.6	1884.7	159.5	8.5	4.1	4.2	0.1	2.6	3.2	3.5	0.4	10.9
	157M-B2.dat	1942.5				4.2				4.0			
	157M-T1.dat	2065.0				4.4				3.7			
	157M-T2.dat	1843.9				4.1				3.2			
P20	141M-B1.dat	2095.5	2015.7	98.5	4.9	3.7	3.8	0.1	3.2	5.3	5.1	0.3	6.4
	141M-B2.dat	2093.1				3.7				5.3			
	141M-T1.dat	1983.8				3.9				5.3			
	141M-T2.dat	1890.3				3.8				4.6			
P21	140M-B1.dat	1779.4	1817.9	125.5	6.9	3.1	3.0	0.1	4.7	6.7	6.9	0.3	4.6
	140M-B2.dat	1958.1				3.2				6.6			
	140M-T2.dat	1716.2				2.9				7.2			
P22	159M-B1.dat	2008.9	1963.6	98.4	5.0	3.0	3.1	0.1	4.0	9.0	8.8	1.9	21.3
	159M-B2.dat	2031.3				3.1				10.5			
	159M-T1.dat	1850.7				3.3				6.8			

**Table 39 P1-P15 IL-SCB (25°C at 25 mm/min)**

Mix	Replicate ID	Energy (LLD) (J/m <sup>2</sup> )	Average	Std Dev	COV	Peak Load (kN)	Average Peak Load	Std Dev	COV
P1	MIX1-SCB-3-T-1.dat	1291.3	1296.6	15.6	1.2	3.2	3.1	0.1	4.3
	MIX1-SCB-4-B-1.dat	1314.1				2.9			
	MIX1-SCB-3-T-1.dat	1284.4				3.2			
P2	MIX2-SCB-3-B-1.dat	1349.0	1383.6	31.1	2.2	4.5	4.5	0.1	2.4
	MIX2-SCB-3-B-2.dat	1393.1				4.6			
	MIX2-SCB-3-T-2.dat	1408.9				4.4			
P3	MIX3-SCB-4-B-1.dat	1043.6	1073.8	44.5	4.1	4.1	4.0	0.1	3.4
	MIX3-SCB-4-B-2.dat	1124.9				3.9			
	MIX3-SCB-4-T-1.dat	1053.0				4.1			
P4	MIX4-SCB-3-B-2.dat	1054.6	1112.2	64.4	5.8	4.3	4.2	0.2	4.3
	MIX4-SCB-3-T-1.dat	1181.7				4.0			
	MIX4-SCB-4-B-1.dat	1100.2				4.4			
P5	MIX5-SCB-3-B-1.dat	1194.9	1203.5	12.1	1.0	4.4	4.7	0.4	7.9
	MIX5-SCB-3-T-1.dat	1212.0				5.0			
P6	MIX6-SCB-4-B-1.dat	1738.1	1879.7	149.5	8.0	4.8	4.8	0.3	5.3
	MIX6-SCB-4-B-2.dat	1865.1				4.5			
	MIX6-SCB-4-T-1.dat	2035.9				5.0			
P7	MIX7-SCB-3-B-1.dat	1839.1	2040.0	204.1	10.0	3.0	3.0	0.1	4.7
	MIX7-SCB-3-T-1.dat	2247.1				3.2			
	MIX7-SCB-3-T-2.dat	2033.8				2.9			
P8	N50-50-SCBII-1-T-2 HI.dat	1392.8	1161.9	229.4	19.7	2.4	3.3	0.9	26.4

**Table 39 (cont.)**

	N50-50-SCBIII-B-1-1 HI.dat	934.1				3.5			
	N50-50-SCBIII-T-2-2 HI.dat	1158.8				4.1			
P9	N50-60-SCB4-B-1 HI.dat	548.5	644.0	82.8	12.9	3.2	3.1	0.3	10.4
	N50-60-SCB4-T-2 HI.dat	690.6				3.4			
	N50-60-SCBII-2-B-2 HI.dat	693.0				2.8			
P10	N70-25-SCBII-3-2 HI.dat	1224.1	1269.9	64.8	5.1	2.1	2.2	0.1	5.2
	N70-25-SCBIII-T-2-2 HI.dat	1315.7				2.3			
P11	N70-50-SCBII-2-T-1 HI.dat	1115.4	1260.4	126.7	10.1	3.5	3.4	0.1	3.9
	N70-50-SCBIII-T-2-1 HI.dat	1350.0				3.3			
	N70-50-SCBIII-T-2-1 HI.dat	1315.8				3.4			
P12	N80-25-SCBII-2-B-1 HI.dat	1100.4	1316.6	226.1	17.2	2.3	2.5	0.2	7.6
	N80-25-SCBIII-T-2-1 HI.dat	1297.9				2.5			
	N80-25-SCBIII-T-3-1 HI.dat	1551.5				2.7			
P13	N80-50-SCBII-2-B-2 HI.dat	705.6	745.2	141.6	19.0	3.5	3.3	0.2	5.5
	N80-50-SCBIII-B-1-1 HI.dat	902.5				3.1			
	N80-50-SCBIII-T-2-1 HI.dat	627.6				3.3			
P14	TR-J-4-B-1.dat	1388.5	1387.0	57.3	4.1	2.0	2.2	0.2	7.3
	TR-J-4-T-1.dat	1434.3				2.1			
	TR-J-6-B-2.dat	1419.1				2.4			
	TR-J-6-T-1.dat	1305.9				2.3			
P15	TR-S-3-B-2.dat	970.2	1039.1	89.0	8.6	2.7	2.6	0.2	5.9
	TR-S-3-T-2.dat	960.1				2.7			
	TR-S-5-B-2.dat	1082.7				2.4			
	TR-S-5-T-2.dat	1143.3				2.5			

**Table 40 P1-P15 IL-SCB (25°C at 6.25 mm/min)**

Mix	Replicate ID	Energy (LLD) (J/m <sup>2</sup> )	Average	Std Dev	COV	Peak Load (kN)	Average Peak Load	Std Dev	COV
P1	MIX1-SCB-1-B-1.dat	1145.3	1073.3	65.1	6.1	1.9	2.1	0.2	8.2
	MIX1-SCB-1-B-2.dat	1055.7				2.2			
	MIX1-SCB-2-T-2.dat	1018.8				2.3			
P2	MIX2-SCB-1-B-2.dat	1071.5	1131.4	208.7	18.4	2.1	2.2	0.4	16.8
	MIX2-SCB-1-T-1.dat	1363.5				2.6			
	MIX2-SCB-1-T-2.dat	959.3				1.9			
P3	MIX3-SCB-2-B-2.dat	855.9	827.3	165.9	20.0	1.6	1.5	0.2	14.8
	MIX3-SCB-2-T-1.dat	977.1				1.6			
	MIX3-SCB-2-T-2.dat	649.0				1.2			
P4	MIX4-SCB-1-B-1.dat	976.1	946.4	133.6	14.1	2.5	2.4	0.1	4.3
	MIX4-SCB-1-B-2.dat	855.2				2.3			
	MIX4-SCB-1-T-1.dat	1007.9				2.5			
P5	MIX5-SCB-1-B-2.dat	879.9	933.4	80.6	8.6	1.4	1.5	0.1	6.7
	MIX5-SCB-2-B-1.dat	933.2				1.5			
	MIX5-SCB-2-T-2.dat	987.1				1.6			
P6	MIX6-SCB-1-B-1.dat	879.9	933.4	53.6	5.7	2.2	2.1	0.1	3.4
	MIX-6-SCB-1-T-1.dat	933.2				2.0			
	MIX6-SCB-1-T-2.dat	987.1				2.1			
P7	MIX7-SCB-1-T-2.dat	1369.1	1358.9	212.4	15.6	2.8	3.1	0.4	11.2
	MIX7-SCB-2-B-1.dat	1141.5				3.1			
	MIX7-SCB-2-B-2.dat	1565.9				3.5			
P12	N80-25-5-B.dat	680.3	786.9	133.3	16.9	1.7	1.7	0.0	0.7
	N80-25-9-B.dat	744.0				1.7			
	N80-25-9-T.dat	936.3				1.7			
P13	N80-50-8-T.dat	724.0	729.4	95.9	13.1	2.2	2.3	0.1	5.6

**Table 40 (cont.)**

	N80-50-9-B.dat	827.8				2.5			
	N80-50-9-T.dat	636.3				2.3			
P14	JOLIET-12-T-2.dat	1286.2	1201.9	108.8	9.0	2.0	2.2	0.2	8.0
	JOLIET-13-T-1.dat	1079.1				2.2			
	JOLIET-16-T-2.dat	1240.3				2.4			
P15	SANDENO 13-T-1.dat	867.4	904.0	51.7	5.7	1.6	1.7	0.1	4.6
	SANDENO 17-B-1.dat	940.5				1.7			

**Table C-2 Laboratory Mixtures**

**Table 41 L3-L13**

Mix ID	Mix Name	Energy				SCB Strength				FI	Avg	Std Dev	COV
		(LLD)	Avg	Std Dev	COV	(MPa)	Avg	Std Dev	COV				
L3	L3 N90-0 (PG 70-22)	2273.7	2306.9	72.5	3.1	0.36	0.37	0.01	1.79	16.1	15.7	0.77	4.9
		2407.6				0.38				16.4			
		2239.6				0.37				14.6			
L4	L4 N90-0 (PG 64-22)	1715.2	1943.5	161.9	8.3	0.45	0.37	0.06	16.4	10.9	12.8	1.75	13.7
		2043.9				0.31				12.2			
		2071.5				0.34				15.1			
L5	L5 N90-30 (PG 70-22)	1450.6	1417.6	54.4	3.8	0.53	0.48	0.03	7.2	2.1	2.3	0.26	11.5
		1462.0				0.47				2.6			
		1341.3				0.45				2.0			
L6	L6 N90-30 (PG 58-28)	1391.0	1503.5	71.24	4.7	0.42	0.51	0.10	18.9	4.4	4.6	0.94	20.3
		1588.0				0.46				4.6			
		1510.0				0.64				3.5			
		1525.0								6.1			
L7	L7 N90-20 (PG 58-28)	1747.4	1718.2	75.9	4.4	0.37	0.36	0.02	4.6	9.0	9.2	0.39	4.27
		1793.1				0.36				9.7			
		1614.2				0.33				8.9			
L8	L8 N90-10 (PG 64-22)	1964.8	2019.4	111.1	5.5	0.5	0.50	0.01	1.4	4.8	5.9	1.14	19.6
		2174.3				0.5				7.5			
		1919.1				0.49				5.3			
L9	L9 N90-30 (PG 58-28)- AS	1643.3	1642.1	58.2	3.6	0.45	0.44	0.02	4.3	3.5	4.0	0.59	15.0
		1570.3				0.42				4.8			
		1712.9				0.46				3.6			

**Table 41 (cont.)**

L10	L10 N90-60 (PG 58-28)- AS	1140.3	1374.1	218.4	15.9	0.50	0.56	0.07	12.0	1.3	1.8	0.32	18.1
		1235.1				0.52				1.7			
		1408.6				0.56				2.1			
		1714.0				0.67				2.0			
L11	L11 N90-0 (PG 64-22)- AS		1464.9	164.9	11.2	0.46	0.33	0.09	27.3		12.9	0.61	4.8
		1651.5				0.34				13.8			
		1490.3				0.31				12.4			
		1250.7				0.21				12.5			
L12	L12 N90- 30-7% IDOT (PG 58-28)- AS	1510.4	1442.5	67.9	4.7	0.38	0.39	0.01	3.9	5.7	4.7	0.58	12.4
		1444.8				0.42				4.8			
		1322.2				0.40				4.3			
		1430.4				0.38				4.6			
		1504.5				0.39				3.9			
L13	L13 N90- 30-7% SW (PG 58-28)- AS	1631.6	1540.8	232.3	15.1	0.55	0.50	0.04	7.6	2.6	2.6	0.20	7.6
		1833.8				0.47				2.7			
		1604.4				0.55				2.8			
		1506.3				0.49				2.5			
		1127.8				0.46				2.2			